

**RSM-BASED OPTIMIZATION STUDY ON
POLYSACCHARIDE PRODUCTION BY WILD-SERBIAN
Ganoderma applanatum STRAIN (BGS6Ap) IN A BATCH
FERMENTATION**

JOSHINI PILLAI BALAMURUGAN

**FACULTY OF SCIENCE
UNIVERSITY MALAYA
KUALA LUMPUR**

2021

**RSM-BASED OPTIMIZATION STUDY ON
POLYSACCHARIDE PRODUCTION BY WILD-
SERBIAN *Ganoderma applanatum* STRAIN (BGS6Ap)
IN A BATCH FERMENTATION**

JOSHINI PILLAI BALAMURUGAN

**DISSERTATION SUBMITTED IN FULFILMENT OF
THE REQUIREMENTS FOR THE DEGREE OF
MASTER OF SCIENCE**

**INSTITUTE OF BIOLOGICAL SCIENCES
UNIVERSITY OF MALAYA
KUALA LUMPUR**

2021

**UNIVERSITY OF MALAYA
ORIGINAL LITERARY WORK DECLARATION**

Name of Candidate: **JOSHINI PILLAI BALAMURUGAN**

Matric No: **17197966/SMA180037**

Name of Degree: **MASTER OF SCIENCE**

Title of Dissertation (“this Work”):

**RSM-BASED OPTIMIZATION STUDY ON POLYSACCHARIDE
PRODUCTION BY WILD-SERBIAN *Ganoderma applanatum* STRAIN
(BGS6Ap) IN A BATCH FERMENTATION**

Field of Study:

BIOTECHNOLOGY

I do solemnly and sincerely declare that:

- (1) I am the sole author/writer of this Work;
- (2) This Work is original;
- (3) Any use of any work in which copyright exists was done by way of fair dealing and for permitted purposes and any excerpt or extract from, or reference to or reproduction of any copyright work has been disclosed expressly and sufficiently and the title of the Work and its authorship have been acknowledged in this Work;
- (4) I do not have any actual knowledge nor do I ought reasonably to know that the making of this work constitutes an infringement of any copyright work;
- (5) I hereby assign all and every rights in the copyright to this Work to the University of Malaya (“UM”), who henceforth shall be owner of the copyright in this Work and that any reproduction or use in any form or by any means whatsoever is prohibited without the written consent of UM having been first had and obtained;
- (6) I am fully aware that if in the course of making this Work I have infringed any copyright whether intentionally or otherwise, I may be subject to legal action or any other action as may be determined by UM.

Candidate’s Signature

Date:

Subscribed and solemnly declared before,

Witness’s Signature

Date:

Name:

Designation:

**RSM-BASED OPTIMIZATION STUDY ON POLYSACCHARIDE
PRODUCTION BY WILD-SERBIAN *Ganoderma applanatum* STRAIN (BGS6Ap)
IN A BATCH FERMENTATION**

ABSTRACT

A wild-Serbian *Ganoderma applanatum* strain BGS6Ap (GASB) from Mount Kosmaj, Serbia was successfully isolated and molecularly identified. Molecularly, GASB generated 651 base pairs that were sequenced and found to be a different strain of *G. applanatum* strain ATCC and *Ganoderma sp.* strain GPS 047 in the same clade using NCBI-BLAST. One factor at a time (OFAAT) method was implemented for growth curve and morphological analysis to study the temperature effect of the mycelium growth. Reflecting on to its natural cold habitat in Eastern Europe, GASB favoured the temperature of 25°C for biomass, exopolysaccharide (EPS) and endopolysaccharide (ENS) production followed by 20°C and 30°C. Morphologically verified, large dense mycelia pellets exhibited high (biomass-ENS) and hairy starburst pellets (EPS). Growth curve analysis using liquid fermentation was conducted and differentiated based on the pellet formation that contributed to biomass (5.04 g/L), ENS (0.51 g/L), EPS (1.46 g/L) at temperature of 25°C (biomass, ENS) and 20°C (EPS). In response surface methodology, the applied central composite design proved that the experimental results were found to be significant for biomass and ENS production. The results gave the optimized biomass (17.51 g/L), EPS (2.59 g/L) and ENS (3.47 g/L) production at day 15 (10g /L of glucose), initial pH 6, 24°C and 153 rpm. Extracted EPS, ENS and glucan sulphate (GS) gave a confirmation spectral linkage in FTIR (between 2928 cm⁻¹ and 889cm⁻¹) and NMR (δ 4.30 and 5.20 ppm) as exo- β -D-glucan and endo- β -D-glucan when compared with β -D-glucan standard of *Laminarin*. This blueprint could be employed to achieve high biomass, EPS and ENS when subjected to high scale bioreactor system for other temperate medicinal mushrooms.

Keywords: *Ganoderma applanatum*; wild-Serbian mushroom; biomass; exopolysaccharide; endopolysaccharide; optimization.

Universiti Malaya

**OPTIMISASI PENGHASILAN POLISAKARIDA MENGGUNAKAN RSM
DARIPADA SERBIA *Ganoderma applanatum* STRAIN (BGS6Ap) YANG LIAR
MENGGUNAKAN FERMENTASI CECAIR TERENDAM**

ABSTRAK

Fungi tumbesaran lambat, cendawan liar-Serbia bernama *G. applanatum* BGS6Ap (GASB) telah dikenal pasti dari Gunung Kosmaj, Serbia. Cendawan GASB telah dikenalpasti dari segi morfologi dan molekul berdasarkan ciri-ciri morfologi. Dari segi pengenalan molekul, GASB menghasilkan 651 pasangan asas yang didapati serupa dengan *G. applanatum* dalam klade A yang sama yang dibandingkan menggunakan NCBI Blast (Alat Pencari Alignment Asas) diguna untuk bina pokok filogenetik. Berikutnya, kajian awal menggunakan kaedah satu faktor pada satu masa (OFAAT) dilaksanakan untuk mengetahui lebih lanjut kajian pertumbuhan dan analisis morfologi bagi mengkaji kesan suhu terhadap pertumbuhan GASB. Secara morfologi disahkan bahawa pelet miselium besar dan padat menunjukkan biojisim dan ENS tinggi sementara pelet berbulu bentuk bintang menyumbang dalam produktiviti EPS. Graf analisis tumbesaran GASB menggunakan SLF dilakukan serta dibezakan berdasarkan pembentukan pellet (analisis morfologi) menyumbang kepada biojisim (5.04 g/L), ENS (0.51 g/L), EPS (1.46 g/L) pada suhu 25°C (biojisim, ENS) dan 20°C (EPS). Selepas itu, SLF dilakukan menggunakan metodologi gerak tindak balas permukaan RSM dengan menggunakan CCD yang menunjukkan bahawa semua modal dalam hasil kajian disignifikan. Hasil kajian menunjukkan pengeluaran biojisim maksimum (17.51 g/L), EPS (2.59 g/L) and ENS (3.47 g/L) pada hari ke-15 meggunakan komposisi media optimum dengan glukosa (10g /L), pH 6, suhu (24°C) dan kadar pergolakan (153 rpm). EPS, ENS dan GS yang diekstrak memberikan spektrum pengesahan dalam FTIR antara (2928 cm⁻¹ dan 889cm⁻¹) dan NMR (δ 4.30 dan 5.20 ppm) sebagai exo- β -D-glukan dan endo- β -D-glukan ketika berbanding dengan β -D-glukan *Laminarin*. Keadaan yang

diptimumkan boleh diguna untuk mencapai biojisim, EPS dan ENS tinggi ketika ditingkatkan ke bioreactor.

Kata kunci: *G. applanatum*; biojisim; endopolisakarida; eksopolisakarida; pengoptimum

Universiti Malaya

ACKNOWLEDGEMENTS

First, I would like to thank God for the wisdom that He has bestowed upon me, the strength and good health to complete my research. Next, I would like to express my highest appreciation to my supervisor Dr Wan Abd Al Qadr Imad Wan Mohtar, to whom I owe my sincerest gratitude as for none of this would be possible without his help and he has never failed to encourage and motivate me throughout completing my project. I am grateful for his expertise, guidance, and support, which has made the completion of this project easier for me. I owe my sincere gratitude to my co-supervisor Dr Rahayu Ahmad, who taught me about fermentation during my undergraduate studies and to Dr Kusaira, who helped me when I needed to use equipment in other labs.

Moreover, I would like to extend my appreciation to the laboratory staffs, Ms Rusidah, Ms Sarah, Ms Asyikin and Mr Nadzrul as I am highly indebted to them as they have been a great help throughout my project, to guide me whenever I encounter problems related to conducting my projects like booking equipment and alternative resources around University Malaya. I would also like to thank my family especially my parents and siblings for the endless moral support, love and care they have provided me throughout my entire life and during this research that drove me to complete it successfully.

Lastly but not least I would like to thank my laboratory partners from Functional Omics and Bioprocessing Laboratory, Mr Sugunendran Supramani, Ms Faizah, Mr Azzimi, Ms Raihan, and others for their endless encouragement, kindness, support, helpful input, and assistance throughout this entire research. Soon, I hope that upon the knowledge I have gained I would be able to make a valuable contribution towards this industry.

TABLE OF CONTENTS

ABSTRACT.....	iii
ABSTRAK	v
ACKNOWLEDGMENTS.....	vi
TABLE OF CONTENTS.....	vii
LIST OF FIGURES.....	xiii
LIST OF TABLES.....	xvi
LIST OF SYMBOLS AND ABBREVIATION.....	xviii
LIST OF APENDICES.....	xx
CHAPTER 1: INTRODUCTION.....	2
1.1 Research background	2
1.2 Research Objectives.....	4
1.3 Problem Statement.....	4
1.4 Scope of Work.....	6
1.5 Dissertation Outline.....	6
CHAPTER 2: LITERATURE REVIEW	7
2.1 Fungi.....	7
2.2 Mushroom.....	7
2.3 Mycelium.....	8
2.4 Spore germination.....	9
2.5 Lifecycle of Phylum Basidiomycota.....	10
2.6 Structure of <i>Ganoderma</i> sp. Basidiospores.....	11

2.7	Taxonomy of <i>Ganoderma</i> sp.....	12
2.8	<i>Ganoderma</i> sp.....	13
2.9	<i>Ganoderma applanatum</i> from temperate habitat.....	14
2.10	Polysaccharides of <i>Ganoderma</i> sp.....	16
2.11	Wild-Serbian <i>Ganoderma applanatum</i> strain (BGS6Ap).....	16
2.12	Submerged liquid fermentation (SLF).....	18
2.13	Biological Growth Models.....	19
2.14	Response Surface Methodology (RSM).....	20
 CHAPTER 3: MATERIALS AND METHODS.....		21
3.1	Cultivation of wild-Serbian <i>Ganoderma applanatum</i> strain BGS6Ap.....	22
3.2	Identification of wild-Serbian <i>Ganoderma applanatum</i> strain BGS6Ap.....	22
3.2.1	Preparation of mycelium for DNA extraction.....	22
3.2.2	PCR amplification.....	28
3.2.3	PCR-amplified product purification and sequencing.....	23
3.2.4	Gel Electrophoresis & Data analysis.....	24
3.2.5	Phylogenetic analysis.....	24
3.2.6	Verification of species.....	24
3.3	Submerged liquid fermentation of wild-Serbian <i>Ganoderma applanatum</i> strain BGS6Ap.....	24
3.3.1	Dry Cell Weight.....	25
3.3.2	Exopolysaccharide (EPS) extraction.....	25
3.3.3	Endopolysaccharide (ENS) extraction.....	26
3.3.4	Morphology analysis.....	26
3.3.5	Microscopic Analysis.....	26

3.3.6	Statistical analysis.....	26
3.4	Optimisation of growth parameters (initial pH, agitation rate, temperature, glucose concentration) of wild-Serbian <i>Ganoderma applanatum</i> BGS6Ap using response surface methodology (RSM).....	27
3.4.1	Optimisation of growth parameters using RSM.....	27
3.5	Characterization of exo-endopolysaccharides from the mycelium of wild-Serbian <i>G.applanatum</i> strain BGS6Ap using Fourier-transform infrared spectroscopy (FTIR) and nuclear magnetic resonance spectroscopy (NMR).....	28
3.5.1	Fourier-transform infrared spectroscopy (FTIR).....	28
3.5.2	Nuclear magnetic resonance spectroscopy (NMR).....	28
CHAPTER 4: RESULTS AND DISCUSSION.....		29
4.1	Cultivation and Identification of wild-Serbian <i>Ganoderma applanatum</i> strain BGS6Ap.....	29
4.2	Identification of wild-Serbian <i>Ganoderma applanatum</i> strain BGS6Ap.....	32
4.2.1	Gel electrophoresis.....	32
4.2.2	Standard curve.....	33
4.2.3	Phylogenetic Tree.....	36
4.2.4	Verification of species wild-Serbian <i>Ganoderma applanatum</i> BGS6Ap...37	
4.3	Growth curve study.....	39

4.3.1	Effect of temperature on biomass, EPS and ENS production of wild-Serbian <i>Ganoderma applanatum</i> strain BGS6Ap in submerged liquid fermentation.....	39
4.3.2	Effect of temperature on pellet morphology of wild-Serbian <i>Ganoderma applanatum</i> strain BGS6Ap in submerged liquid fermentation.....	49
4.4	Optimisation of growth parameters (initial pH, glucose concentration, agitation rate, temperature) using response surface methodology.....	61
4.4.1	Optimisation of mycelium biomass at day 10	63
4.4.2	Optimisation of Exopolysaccharide (EPS) production at day 10.....	67
4.4.3	Optimisation of Endopolysaccharide (ENS) production at day 10.....	71
4.4.4	Validation of the optimised media composition.....	75
4.4.5	Optimisation of mycelia biomass production at day 15.....	78
4.4.6	Optimisation of EPS production at day 15.....	82
4.4.7	Optimisation of ENS production at day 15.....	86
4.4.8	Validation of the optimised media composition at day 15.....	90
4.4.9	Comparison with other literature.....	91
4.5	Characterisation of exo-endopolysaccharides from the mycelium of wild-Serbian <i>G. applanatum</i> strain BGS6Ap using Fourier-transform infrared spectroscopy (FTIR) and nuclear magnetic resonance spectroscopy (NMR).....	93
4.5.1	Fourier-transform infrared spectroscopy (FTIR).....	93
4.5.2	Nuclear magnetic resonance spectroscopy (NMR).....	95

CHAPTER 5: CONCLUSION.....	97
REFERENCES.....	99
APPENDIX.....	107

Universiti Malaya

LIST OF FIGURES

Figure 1.1	: Graph obtained using Clarivate software to search for optimization of <i>Ganoderma applanatum</i> . Source was obtained using Thomson Reuters (Web of Science) with the keywords “ <i>Ganoderma applanatum</i> ” and “Fermentation”	4
Figure 2.1	: Basic morphology of a mushroom fruiting body (figure is by author)	8
Figure 2.2	: The basic life cycle of a Basidiomycota fungal mushroom sexual reproductive system (figure is by author).....	10
Figure 2.3	: Structure of <i>Ganoderma sp.</i> Basidiospores (figure is by author) ...	11
Figure 2.4	: Basic apparatus of a laboratory-scale submerged fermentation (figure by author)	16
Figure 3.1	: Summary of methodology for exopolysaccharide, endopolysaccharide, and biomass production from wild-Serbian <i>Ganoderma applanatum</i> strain BGS6Ap mycelium in submerged liquid fermentation.....	19
Figure 4.1	: (A) <i>G. applanatum</i> fruiting body. (B) Basidiospores of <i>G. applanatum</i> under a microscope. (C) Mycelium of <i>G. applanatum</i> on PDA plate (Day 7). (D) First seed culture of wild-Serbian <i>G. applanatum</i> in SLF (Day 10) and (E) wild-Serbian <i>G. applanatum</i> in SLF at day 20. (F) Depicts the mycelium after filtration from (E). (G) Depicts the extracted ENS and (H) macroscopic morphology of dried biomass	27
Figure 4.2	: The locality of wild-Serbian <i>G. applanatum</i> strain BGS6Ap found at the mountain of Kosmaj (yellow bar indicates the 147-m distance at the coordinates 44°27'57''N 20°33'52''E). Source: Google, 2020.....	28
Figure 4.3	: Agarose gel electrophoresis of DNA isolated from wild-Serbian <i>G. applanatum</i> strain BGS6Ap mycelium. Lane 1 resembles 10 kb DNA marker; lane 2 resembles positive control (+ve); lane 3 represents negative control (-ve) and lane 4 corresponds to the sample GASB.....	30
Figure 4.4	: Standard curve log ₁₀ (size of base pairs) against distance migrated of wild-Serbian <i>G. applanatum</i> strain BGS6Ap.....	32
Figure 4.5	: Phylogenetic tree of wild-Serbian <i>G. applanatum</i> strain BGS6Ap generated by neighbouring-joining with evolutionary distance. Bar = 0.00010.....	34

Figure 4.6	: Species verification of wild-Serbian <i>G. applanatum</i> strain BGS6Ap using A plasmid Editor (ApE) software.....	35
Figure 4.7	: Time profile of wild-Serbian <i>G. applanatum</i> strain BGS6Ap mycelia during shake flask batch-fermentation and effect of temperature (20°C, 25°C,30°C) on the production of biomass, exopolysaccharide and endopolysaccharide for 35 days.....	38
Figure 4.8	: Microscopic (A) and macroscopic (B) observation of wild-Serbian <i>G. applanatum</i> strain BGS6Ap at temperature (20°C) for biomass, exopolysaccharide and endopolysaccharide production in liquid fermentation. Details of pellet detachment from protruding hyphal tips (yellow arrow). Images (A) and (B) were taken at 4-fold magnification and bar = 100µm.....	41
Figure 4.9	: Microscopic (A) and macroscopic (B) observations of wild-Serbian <i>G. applanatum</i> strain BGS6Ap at temperature (25°C) for biomass, exopolysaccharide and endopolysaccharide production in liquid fermentation. Details of pellet detachment from protruding hyphal tips (yellow arrow). Images (A) and (B) were taken at 4-fold magnification and bar = 100µm.....	43
Figure 4.10	: Microscopic (A) and macroscopic (B) observation of wild-Serbian <i>G. applanatum</i> strain BGS6Ap at temperature (30°C) for biomass, exopolysaccharide and endopolysaccharide production in liquid fermentation. Details of pellet detachment from protruding hyphal tips (yellow arrow). Images (A) and (B) were taken at 4-fold magnification and bar = 100µm.....	45
Figure 4.11	: Microscopic (A) and macroscopic (B) variations in mycelia during batch-fermentation of wild-Serbian <i>G. applanatum</i> strain BGS6Ap at temperature 20°C. Details of pellet detachments from protruding hyphal tips is in red arrow. Images (A) and (B) were taken at 4-fold magnification and bar = 100µm.....	48
Figure 4.12	: Microscopic (A) and macroscopic (B) variations in mycelia during batch-fermentation of wild-Serbian <i>G. applanatum</i> strain BGS6Ap at temperature 25°C. Details pellet detachments from protruding hyphal tips is in red arrow. Images (A) and (B) were taken at 4-fold magnification and bar = 100µm.....	52
Figure 4.13	: Microscopic (A) and macroscopic (B) variations in mycelia during batch-fermentation of wild-Serbian <i>G. applanatum</i> strain BGS6Ap at temperature 25°C. Details pellet detachments from protruding hyphal tips is in red arrow. Images (A) and (B) were taken at 4-fold magnification and bar = 100µm.....	55
Figure 4.14	: Response surface profile (3D plot) of biomass production from wild-Serbian <i>G. applanatum</i> strain BGS6Ap (D10) displaying the interaction between (A) temperature and agitation, (B) agitation and pH, (C) glucose and agitation, (D) temperature and pH, (E) temperature and glucose and (F) glucose and pH.....	64

Figure 4.15	: Response surface profile (3D plot) of exopolysaccharide production from wild-Serbian <i>G. applanatum</i> strain BGS6Ap (D10) displaying the interaction between (A) temperature and agitation, (B) agitation and pH, (C) glucose and agitation, (D) temperature and pH, (E) temperature and glucose and (F) glucose and pH.....	68
Figure 4.16	: Response surface profile (3D plot) of endopolysaccharide production from GASB (D10) displaying the interaction between (A) temperature and agitation, (B) agitation and pH, (C) glucose and agitation, (D) temperature and pH, (E) temperature and glucose and (F) glucose and pH.....	72
Figure 4.17	: Response surface profile (3D plot) of biomass production from wild-Serbian <i>G. applanatum</i> strain BGS6Ap (D15) displaying the interaction between (A) temperature and agitation, (B) agitation and pH, (C) glucose and agitation, (D) temperature and pH, (E) temperature and glucose and (F) glucose and pH.....	78
Figure 4.18	: Response surface profile (3D plot) of exopolysaccharide production from wild-Serbian <i>G. applanatum</i> strain BGS6Ap (D15) displaying the interaction between (A) temperature and agitation, (B) agitation and pH, (C) glucose and agitation, (D) temperature and pH, (E) temperature and glucose and (F) glucose and pH.....	82
Figure 4.19	: Response surface profile (3D plot) of endopolysaccharide production from wild-Serbian <i>G. applanatum</i> strain BGS6Ap (D15) displaying the interaction between (A) temperature and agitation, (B) agitation and pH, (C) glucose and agitation, (D) temperature and pH, (E) temperature and glucose and (F) glucose and pH.....	86
Figure 4.20	: Comparison of β -glucan IR spectra. A: glucan standard <i>Laminarin</i> ; B: exopolysaccharide; C: endopolysaccharide; D: glucan sulphated glucan derived from batch fermentation of wild-Serbian <i>G. applanatum</i> strain BGS6Ap.....	91
Figure 4.21	: Comparison of β -glucan ^1H NMR spectra of β -D-glucan derived from batch cultures of wild-Serbian <i>G. applanatum</i> strain BGS6Ap and <i>Laminaria digitate</i> standard in $\text{D}_2\text{O}-d_6$	93

LIST OF TABLES

Table 2.1	: Scientific classification of <i>Ganoderma</i>	12
Table 2.2	: Comparison of Serbian <i>Ganoderma</i> sp. cultivation method and research summary.....	14
Table 2.3	: Identification of Wild-Serbian <i>Ganoderma applanatum</i> strain BGS6Ap.....	15
Table 3.1	: Experimental range and levels of independent variables.....	25
Table 4.1	: Standard curve to identify the unknown size for wild-Serbian <i>G. applanatum</i> strain BGS6Ap.....	31
Table 4.2	: Production of maximum yield of biomass, exopolysaccharide, endopolysaccharide by wild Serbian <i>G. applanatum</i> strain BGS6Ap when cultivated on different temperatures.....	58
Table 4.3	: Experimental design matrix using response surface methodology through central composite design with variables and responses for the biomass, exopolysaccharide and endopolysaccharide for day 10 of wild-Serbian <i>G. applanatum</i> strain BGS6Ap.....	61
Table 4.4	: Analysis of variance for the experimental results of the central composite design quadratic model for biomass from wild-Serbian <i>G. applanatum</i> strain BGS6Ap at day 10.....	63
Table 4.5	: Analysis of variance for the experimental results of the central composite design quadratic model for exopolysaccharide production from wild-Serbian <i>G. applanatum</i> strain BGS6Ap at day 10.....	67
Table 4.6	: Analysis of variance for the experimental results of the central composite design quadratic model for endopolysaccharide production from wild-Serbian <i>G. applanatum</i> strain BGS6Ap at day 10.....	71
Table 4.7	: Validation of the model with the optimised media composition in 250 mL shake flasks at day 10.....	74
Table 4.8	: Experimental design matrix using response surface methodology through central composite design with variables and responses for the biomass, exopolysaccharide and endopolysaccharide for day 15 of wild-Serbian <i>G. applanatum</i> strain BGS6Ap.....	75
Table 4.9	: Analysis of variance for the experimental results of the central composite design quadratic model for biomass production from wild-Serbian <i>G. applanatum</i> strain BGS6Ap at day 15.....	77

Table 4.10	: Analysis of variance for the experimental results of the central composite design quadratic model for exopolysaccharide production from wild-Serbian <i>G. applanatum</i> strain BGS6Ap at day 15.....	81
Table 4.11	: Analysis of variance for the experimental results of the central composite design quadratic model for endopolysaccharide production from wild-Serbian <i>G. applanatum</i> strain BGS6Ap at day 15.....	85
Table 4.12	: Validation of the model with the optimised media composition in 250 mL shake flasks at day 15.....	88
Table 4.13	: Comparison of <i>Ganoderma</i> sp. statistical optimisation using submerged-liquid fermentation with the literature.....	89

Universiti Malaysia

LIST OF SYMBOLS AND ABBREVIATION

°C	:	Degree Celsius
<i>Knuc</i>	:	Evolutionary distance
μm	:	Micrometre
<i>cm-</i>	:	Wavelength per distance
ANOVA	:	Analysis of Variance
bp	:	Base pairs
cm	:	Centimetre
CCD	:	Central composite design
g	:	Grams
dNTPs	:	Deoxyribonucleotide triphosphate
DCW	:	Dry Cell Weight
ENS	:	Endopolysaccharide
EPS	:	Exopolysaccharide
FTIR	:	Fourier-Transform Infrared Spectroscopy
kb	:	Kilobase
gDNA	:	Genomic deoxyribonucleic acid
GF/C	:	Glass microfiber filter paper
GS	:	Glucan Sulphate
GASB	:	Wild-Serbian <i>Ganoderma applanatum</i> strain BGS6Ap
ITS	:	Internal Transcribed Spacer Regions
L	:	Litres
mg	:	Milligrams
mm	:	Millimetres
min	:	Minutes

MW	:	Molecular Weight
MSA	:	Multiple Sequence Alignment
MHz	:	Megahertz
NA	:	Nutrient Agar
NMR	:	Nuclear Magnetic Resonance
PCR	:	Polymerase Chain Reaction
PDA	:	Potato Dextrose Agar
pH	:	Potential hydrogen
RSM	:	Response surface methodology
s	:	Seconds
SD	:	Standard deviation
SSF	:	Solid Substrate Fermentation
SLF	:	Submerged Liquid Fermentation
TE	:	Tris-EDTA buffer
TBE	:	Tris-Borate-EDTA buffer
YE	:	Yeast Extract

LIST OF APENDICES

Appendix A	: Solubility test conducted on (A) EPS dissolved in 1% NaOH, (B) EPS dissolved NaCl, (C) EPS dissolved in 50% DMSO and 50%methanol.....	104
Appendix B	: Zone of inhibition by glucan-sulfated exopolysaccharide.....	104
Appendix C	: Zone of inhibition by glucan sulphate against common pathogenic bacteria which are (A, E) <i>Serratia marcescens</i> , (B,F) <i>Escherichia coli</i> , (C, G) <i>Staphylococcus aureus</i> (D, H) <i>Staphylococcus epidermis</i> . The strength measured by the absence or presence of a zone of inhibition at varying concentrations of exhibiting antibacterial activity. (+) control used was Gentamycin and (-) control used was 99% Ethanol. The diameter of a sterile blank disc is 6mm.....	105
Appendix D	: Scanning electron microscope (SEM).....	106

CHAPTER 1: INTRODUCTION

1.1 Research background

The fruiting body of mushrooms is a reproductive part of fungus whose growing substrate can be soil or decaying logs, tree barks, stumps, and wood. (Ogbe et al., 2009). *Ganoderma applanatum* (GA) is commonly known as shelf fungus used in malades for people suffering from a wide range of diseases such as diabetes, renal failure, and constipation (Acharya, K. et al., 2005). Fruiting bodies of GA are widely used as an alternative to modern-day medicine (Adotey et al., 2011). Bioactive polysaccharides obtained from medicinal mushrooms exhibit a wide range of biological activities such as antifungal, antibacterial and antitumor activities (Sun et al., 2015). Polysaccharides can be acquired through two distinctive methods identified as solid substrate fermentation (SSF) and submerged liquid fermentation (SLF) (Wan-Mohtar et al., 2016). Submerged liquid fermentation SLF is the modern technique used to harvest polysaccharides economically within 15 days or less while SSF is the conventional technique used to collect polysaccharide from its fruiting body which takes months (Wan-Mohtar et al., 2016)

Submerged liquid fermentation (SLF) provides swifter production of biomass and polysaccharides in a shorter time within a reduced space and minimal chances of contamination (Ahmad et al., 2013b). The mycelium grows as a tightly packed mass in liquid medium containing essential nutrients that will develop into ovoid-shaped pellets (Supramani et al., 2019). The difference in pellet morphology correlates with the production of polysaccharides on whether biomass, EPS or ENS produced are high or low (Wan- Mohtar et al., 2016 & Supramani et al., 2019). Mushroom polysaccharide exists in binary forms that constitute of exopolysaccharides (EPS), produced outside of the mycelium and endopolysaccharide (ENS), formed within the mycelium (Supramani et al., 2019)

Optimization of the vital SLF parameters (temperature, glucose concentration, agitation speed, pH) is essential as it affects the biomass, EPS and ENS (Ahmad et al., 2013b). However only minimal interest has been given to the optimization of media elements hence Response surface methodology (RSM) is the best suitable means that can be used to boost the cultivation of polysaccharides (Wan-Mohtar et al., 2016c). RSM is a valuable statistical tool which simulates the interaction between multiple factors in contrast to one-factor-at-a-time (OFAAT) (Wan-Mohtar et al., 2016c).

In this study, the therapeutic mushroom GASB was subjected to molecular characterization before SLF. Then, a preliminary investigation was conducted using the OFAAT method to obtain baseline information. Based on the baseline data, RSM was used to correlate between a set of experimented variables to provide optimized conditions for maximum yield of polysaccharides (ENS and EPS). The selected parameters used in RSM were initial pH, glucose concentration, agitation rate, and temperature.

1.1 Research Objective

1. To identify the wild-Serbian *G. applanatum* strain BGS6Ap using morphological and molecular techniques.
2. To determine the effect of temperature on pellet morphology for biomass, EPS and ENS production in submerged liquid fermentation of the wild-Serbian *G. applanatum* strain BGS6Ap.
3. To optimize biomass, EPS, and ENS production of wild-Serbian *G. applanatum* strain BGS6Ap in batch fermentation using RSM.
4. To characterize extracted mycelial EPS and ENS using spectral analysis.

1.2 Problem Statement

Most commercial mushroom products developed from old fruiting bodies via conventionally cultivated methods are time-consuming, where it takes several months to years (especially with *Ganoderma applanatum*) and the whole production is prone to contamination. Past studies of *Ganoderma sp.* from the Serbian region focused only on the fruiting bodies and bioactive composition and not on polysaccharide (EPS and ENS) production (Rašeta, M. J. et al., 2017; Stojković et al., 2014). The previous study proved that locally cultivated *Ganoderma sp.* and European *Ganoderma sp.* have different properties and characteristics due the different environmental conditions, eg. substrate (Hennicke et al., 2016). Moreover, the conventional method of cultivating fruiting bodies involves a tedious and long incubation period. Therefore, submerged liquid fermentation can serve as an alternative to producing vital effective bioactive compounds such as EPS and ENS.

On the other hand, submerged fermentation of therapeutic mushrooms is expanding extensively throughout the world and seems to be a promising and powerful tool to produce exopolysaccharides (Wan-Mohtar et al., 2016c). Mushroom has been well-

known to have nutritional and healing properties, but they were only consumed wholesomely or by cooking to obtain its nutritional value. Thus, using submerged fermentation, EPS-ENS can be extracted, and the known amount of antifungal and antimicrobial attributes can be identified in a shorter time, limited space and with less risk of contamination. Figure 1.1 shows the graph obtained from Clarivate software from the years 1970's to 2020 displaying only four publications related to *G. applanatum* and submerged liquid fermentation. The most recent study was conducted in 2018. To date no studies showed the attempt to optimise media for GA mycelium growth and production of EPS-ENS in liquid fermentation.

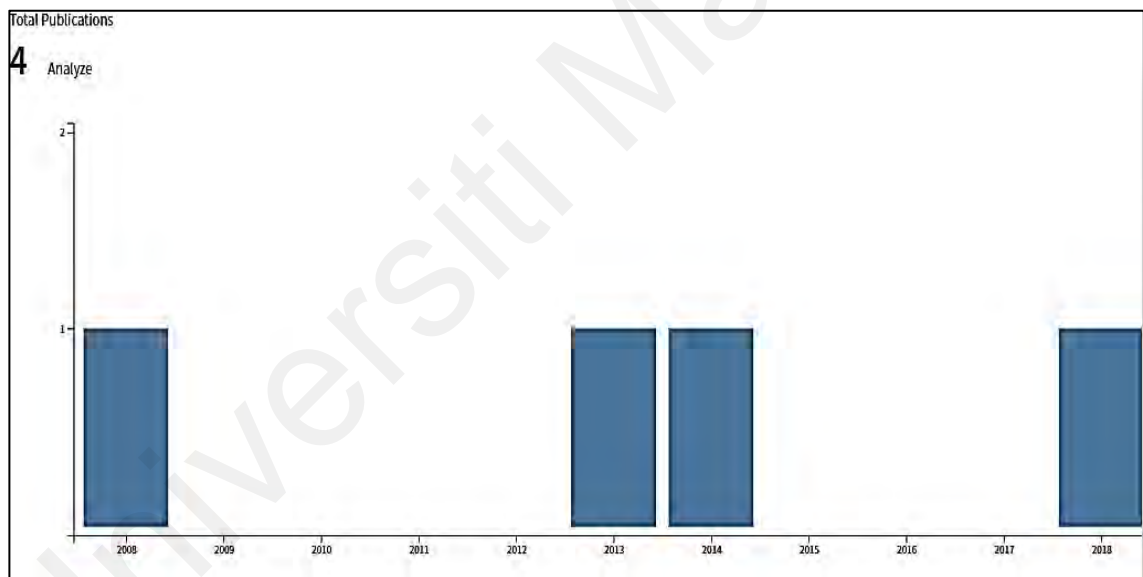


Figure 1.1: Graph obtained using Clarivate software to search for cultivation optimization of *Ganoderma applanatum*. Source was obtained using Thomson Reuters (Web of Science from years 1970's to 2020) with the keywords "*Ganoderma applanatum*" and "Fermentation".

1.3 Scope of Work

This research concentrates on the cultivation and development of a therapeutic mushroom, wild Serbian *G. applanatum* in liquid fermentation to produce biomass, EPS and ENS. A preliminary investigation was conducted using temperature as the critical parameter that was optimized. Next, RSM was used to study the correlation between four essential physical and chemical factors (agitation rate, temperature, initial pH, and glucose concentration) and its effect on the production of polysaccharides.

1.4 Dissertation outline

This dissertation comprises of six chapters: Chapter One depicts the introduction for the study; Chapter two summarises the literature review of the current research. Chapter Three explains the material and methods used in the analysis; Chapter Four details the results and discussion and Chapter Five sums up the conclusions of the research. Lastly, Chapter Six proposes future work.

CHAPTER 2: LITERATURE REVIEW

2.1 Fungi

Fungi are split into macrofungi and microfungi. Mushrooms fall in the class of macrofungi that is visible and can be seen by the naked eye without using any scientific aid like microscopes. Fungi are eukaryotic, heterotrophic and reproduce using spores (Rosemary Kinge et al., 2017). One part of the kingdom of fungi are saprophytes due to their nature of obtaining nutrients by feeding off dead or decaying organic matter. The basic mushroom cell is hyphae, while the densely connected hyphae represent mycelium. (Nie et al., 2013).

Fungi are divided into four significant phyla: Ascomycota, Basidiomycota, Zygomycota, and Chytridiomycota. Most edible mushrooms come from the phylum Basidiomycota and are recognized by its club-shaped fruiting bodies known as basidia which form at the swollen end of the hypha (Adl et al., 2012). Basidia is the reproductive organ of mushrooms that produces Basidiomycetes are also referred as gill fungi due to its serrated margin or gill-like structure found on the under part of the club. These gills-like structures are nothing but compacted hypha. GA belongs to the Phylum Basidiomycota (Wang et al., 2016).

2.2 Mushrooms

For the past thousands of years, humankind has valued mushroom as an essential and edible medical source of food (Synytsya et al., 2009). Mushroom fruiting bodies are rich with vitamins such as B1 (thiamine), B2 (riboflavin), C (ascorbic acid) and D (fat-soluble secosteroids) together with some significant elements such as K (potassium) and P (phosphorus) (Synytsya et al., 2009). Mushrooms seem to have very little fat content (around 15% and below) whereas protein content is higher, about 19% to 35% (Synytsya et al., 2009). Carbohydrates are found in abundant and mostly present

in forms of glycoproteins or polysaccharides (Zhang et al., 2011). Examples of polysaccharides are chitin, α - and β -glucans, and hemicelluloses such as xylans or galactans. Most of the polysaccharides are present as glucans with varying glycosidic linkages such as (1, 3), (1, 4), (1, 6), it can be branched or linear or even consists of heteroglycans (Synytsya et al., 2009).

“Elixir of Life” has proved to be the terminology used to describe mushrooms since ancient history by Chinese (Valverde et al., 2015). Mushrooms are incredibly nutritive and most commonly renowned for their therapeutic qualities that are a source for creating physiologically beneficial and non-toxic remedies (Jo et al., 2014). Mushrooms are a kind of macrofungi referred to as the spore-bearing fruiting body of a fungus that is fleshy and mostly discovered on the dirt growing on its food resource (Zhang et al., 2014). Edible mushrooms like the *G. lucidum* has been used in Chinese pharmaceutical products as quick wound-healing agents which are now being explored by scientist and researchers (Cheng et al., 2013). Non-edible mushrooms are noxious and sometimes lethal to a living organism (Jo et al., 2014).

2.3 Mycelium

In nature mushrooms “grow” much like blooms do and like flowers, mushrooms grow amid conditions of the year when the conditions are appropriate and suitable. Figure 2.1 shows the basic morphology of the mushroom fruiting body and its parts. The significant component of fungus is its mycelia which lives inside substrate such as decaying wood and rot (Yang et al., 2003).

Mushrooms do not impersonate by seed or collect imperativeness by photosynthesis as plants do. They replicate by using strategies like asexual spores. These spores duplicate to make a mass that is known as hyphae and aggregately a group of hyphae perceived as mycelium (Yang et al., 2003). Mushrooms ingest supplements from its

environment like wood using mycelium in a two-stage process. The initial step is the release of catalyst or substances by mycelium on its substrate or environment to breakdown proteins into smaller units to use as nutrients. Next, the mycelium ingests or takes up these simple units using a mix of both facilitated diffusion and active transport (Yang et al., 2003)

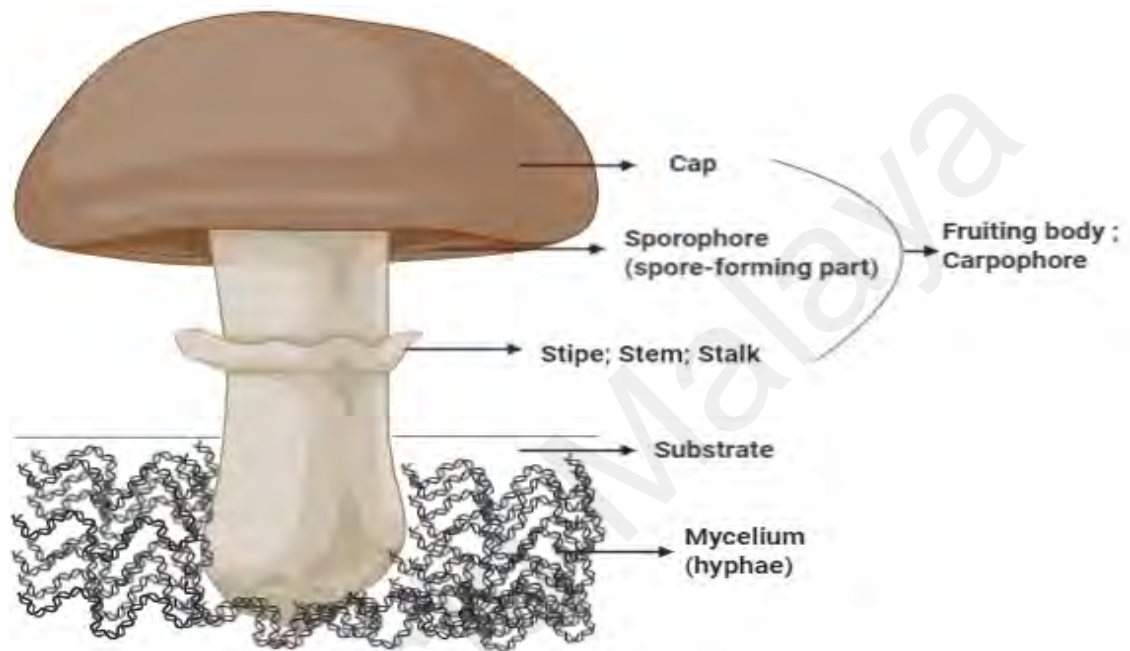


Figure 2.1: Basic morphology of a mushroom fruiting body (figure is by author).

2.4 Spore Germination

Kingdom fungi's primary mode of growth is through apical extension forming the hyphal structure. A fungal spore subjected to advantageous conditions transits from a dormant to an actively metabolizing cell, which result in the formation of a visible mycelium (Gougouli et al., 2013). Germination of a spore is the conversion of the dormant spore into an active spore that occurs because of a time interval of gradual swelling of the spore, therefore, increase in both diameter and weight (Gougouli et al., 2013). After incubation, a germ tube will arise from the enlarged spore and grow to a certain length and is considered as germinated (Gougouli et al., 2013). In a recent study,

its shown that each mycelium has varying germination time and lag time depending on its physiological state (Gougouli et al., 2013).

2.5 Lifecycle of Phylum Basidiomycota

Most edible fungi originate from Phylum Basidiomycota that distinguished based on its standard club-shaped fruiting bodies known as basidia which form the swollen end of the hyphae (Niemelä et al., 2008). As evident from the Figure 2.2. basidiospores are created, basidiospores created through sexual reproduction and usually two mating strains found in basidia will fuse to form a diploid zygote. The diploid zygote will move forward to undergo meiosis and mating of these two different strains is known as karyogamy (Pegler, D., 1996). After meiosis, haploid nuclei will migrate into basidiospores and propagate to form homokaryotic hyphae and primary mycelium (Adl et al., 2012). In the dikaryotic stage, mycelia from different strains may mate to form secondary mycelium with haploid nuclei. Secondary mycelium will form basidiocarp known as the fruiting body that bulges from the ground. The basidiocarp shall form abundant basidium detected under the cap of the mushroom fruiting body (Gottlieb et al., 1999).

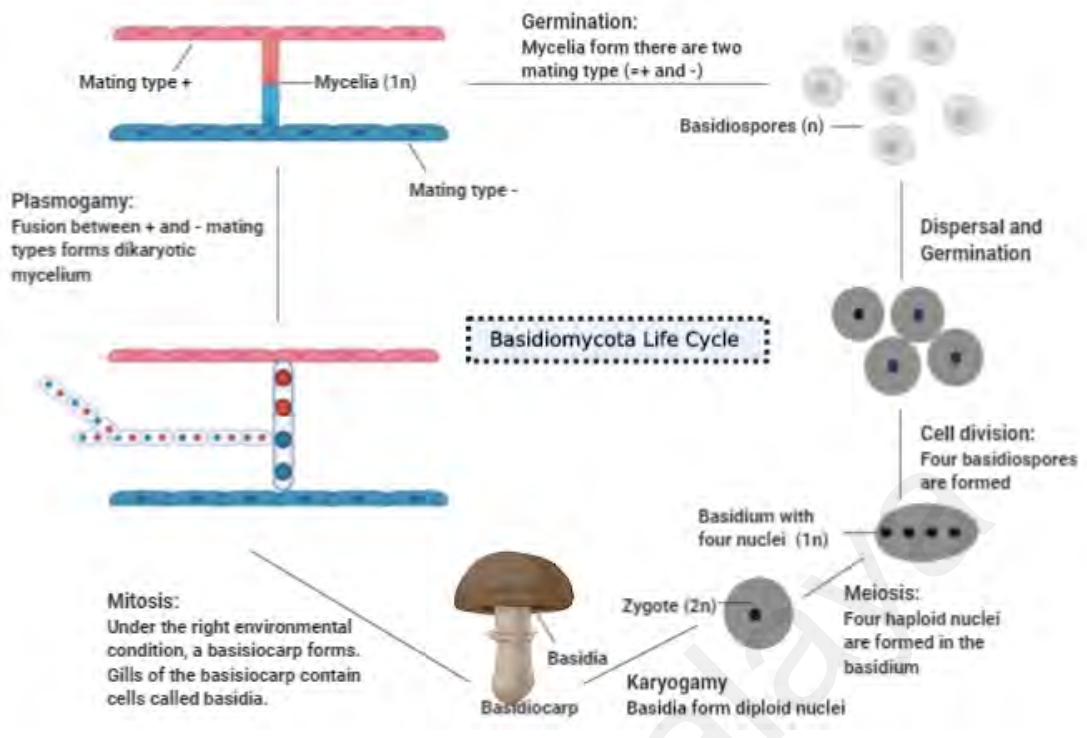


Figure 2.2: The basic life cycle of a Basidiomycota fungal mushroom sexual reproductive system (figure is by author).

2.6 Structure of *Ganoderma* sp. Basidiospores

Basidiospores of *Ganoderma* sp. are incredibly distinctive and can be used to differentiate between the genus from specific macroscopically similar species (Adaskaveg et al., 1986; Banerjee et al., 1959) Microscopically the fundamental structure of basidiospores vary among the interspecies and differ depending on their environmental factors and place of growth (Adaskaveg et al., 1986; Banerjee et al., 1959; Pegler, D., 1996).

Basidiospores are ovoid-shaped, with a projecting apex referred to as hyaline episporium (Banerjee et al., 1959). The projecting apex will collapse at maturity forming a truncated appearance (Banerjee et al., 1959). An endospore is yellowish-brown in colour, and exospore possess a smooth texture when it is young, although during maturity roughened up (Banerjee et al., 1959). *G. applanatum* has significantly smaller

spores as compared to other species that are ovoid-shaped (Pegler, D. N. et al., 1973). The young spores of *G. applanatum* are deposited in the perispore membrane (Pegler, D. N. et al., 1973). Previous studies (Banerjee et al., 1959) shown that *G. lucidum* and *G. applanatum* are capable of forming secondary spores usually produced by hyphae found in sporophores.

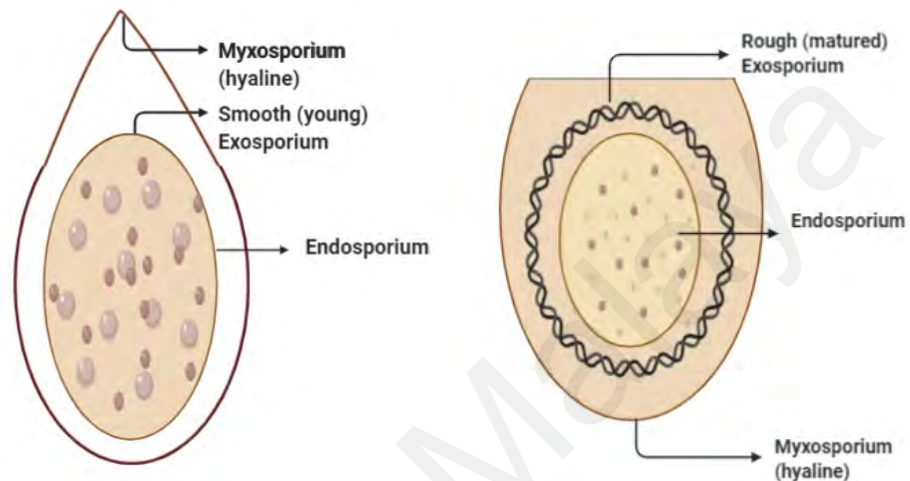


Figure 2.3: Structure of *Ganoderma* sp. Basidiospores (figure is by author).

2.7 Taxonomy of *Ganoderma* sp.

In 1881, Karsten established *Ganoderma* based on *G. lucidum* (Curtis: Fr) P. Karst Donk that was found in 1948 (Gottlieb et al., 1999). Discovery of *G. lucidum* created Ganodermataceae family based on certain criteria such as spore irregularities, geographical distribution, basidiome macromorphology, host specificity, and cutis anatomy (Gottlieb et al., 1999). Polypore mushrooms are most frequently cultivated on wood and the genus *Ganoderma* falls in this order.

There are approximately 80 known species which falls in the following order, and several are from tropical forest. These *Ganoderma* species are a vital variety due to their extensive usage in Asia as medicinal properties and their bioremediation potential. *Ganoderma* can be separated from different polypore's since they have a twofold walled basidiospore. They prominently indicated as shelf mushrooms or bracket fungi (Gottlieb

et al., 1999). Table 2.1 shows the scientific classification for the slow-growing *G. applanatum*.

Table 2.1 Scientific classification of *Ganoderma applanatum*

Kingdom	Fungi
Phylum	Basidiomycota
Class	Agaricomycetes
Order	Polyporales
Family	Ganodermataceae
Genus	Ganoderma
Species	Applanatum

2.8 *Ganoderma* sp.

The Ganodermataceae family, the phrase invented by “Gano” implying shiny or bright and “derma” signifying skin (Benkeblia, 2015). Ganodermataceae is a saprophytic fungus devouring on wood and having a bright or shiny skin covering the fruiting body (Benkeblia, 2015; Gottlieb et al., 1999). For many years, mushrooms from this family are known to have medicinal properties and been used to treat various health problems and diseases. Some of the most prominent species are *G. lucidum*, *G. applanatum*, *G. tsugae* and many more (Wan-Mohtar et al., 2017). *Ganoderma* sp. is generally known as a therapeutic fungal biofactory due to its positive effects. Chemical constituents such as polysaccharides, proteins, adenosine, sterols, lectins and triterpenoids are some of its biologically active constituents. (Zhang et al., 2012).

Ganoderma sp. is used against, liver diseases, lung problems, diabetes, cancer, heart disease, HIV, antiherpetic activities, and many other illnesses (Benkeblia, 2015; Zhang et al., 2012). Additional defensive impacts of *Ganoderma* sp. have been reported; for instance DNA protection against the strand breakage caused by hydroxyl radicals, UV irradiation, boosting the immune system and antifibrotic effects (Benkeblia, 2015).

Primeval Chinese medical researchers believe that “Lingzhi” also known as *G. lucidum* could boost the body’s resistance and enhance the health of the patient using one of the major and oldest techniques called “Fuzheng Guben” (Zhang, H. et al., 2012).

2.9 *Ganoderma applanatum* from temperate habitat

G. applanatum (Pers.) Karst, belongs to Polyporaceae and originates from the Basidiomycota phylum, also called as “*Elfvigia applanate*” (Jeong et al., 2008). *G. applanatum* (GA) is one of the traditional Chinese medical fungi known to grow primarily on decaying forest or park trees (Niemelä et al., 2008). *G. lucidum* (GL) or Lingzhi is one of the earliest mushrooms studied for its medicinal properties and GA considered to have similar properties as GL like having antioxidant, anticancer properties and more (Jeong et al., 2008). GA has observed to form semicircular carpophores on decaying branches such as beech tree. GA thought to have tumorigenic attributes, antibacterial, antiviral actions, and modulation of immunes responses (Jo et al., 2014).

GA found in the north of Iran possess medical attributes with the potential to inhibit the growth of melanoma used to treat esophageal cancer (Moradali et al., 2006). Previous studies demonstrated that GA was used in Chinese medicine to treat rheumatic tuberculosis (Moradali et al., 2006). Earlier studies show that the polysaccharides of GA contain hydroxyl radicals and superoxide anion used to improve diabetes, cardiovascular disease, inflammation, etc. (Acharya, Krishnendu et al., 2005; Zhou et al., 2018). According to Moradali et al., (2006) and Nie et al., (2013), GA had the potential to resolve indigestion, relieve pain, reduce phlegm and hemostasis owing to the isolation of steroids and fatty acids such as ganoderic acid and applanoxidic acid.

Species	Herbarium Ref.	Origin	Temperature Range	Place of Isolation	Cultivation	Research Summary	Reference
<i>G. applanatum</i>	BGS6Ap	Serbia	18°C-24°C	Mount Kosmaj	SLF	Morphological analysis and optimization in liquid fermentation	<i>Current study</i>
<i>G. lucidum</i>	BGF4A1	Serbia	17°C-25°C	Mount Avala	SLF	Optimization of polysaccharides	(Hassan et al., 2019)
<i>G. lucidum</i>	GLK-12	Serbia	18°C-24°C	Košutnjak park	Fruiting body	Cosmeceutical analysis	(Kozarski et al., 2019)
<i>G. applanatum</i>	12-00714	Serbia	18°C-24°C	Morović woods	Fruiting body	Cytotoxicity analysis	(Rašeta et al., 2017)
<i>G. lucidum</i>	12-00715						
<i>G. applanatum</i>	-	Serbia	15°C-25°C	Košutnjak park	Fruiting body	Antibacterial and antifungal analysis	(Klaus et al., 2016)
<i>G. lucidum</i>	-	Serbia	18°C-25°C	Bojčinska forest	Fruiting body	Chemical and bioactive property analysis	(Stojković et al., 2014)
<i>G. applanatum</i>	-	Serbia	16°C-26°C	Obedska lake	Fruiting body	Chemical characterization of polysaccharides	(Kozarski et al., 2012)
<i>G. lucidum</i>	-	Serbia	16°C-25°C	Bella Crkva	Fruiting body	Anticancer analysis	(Harhaji Trajković et al., 2009)
<i>G. lucidum</i>	G1-I	Serbia	15°C-22°C	Serbian woods	Fruiting body	Antimicrobial analysis	(Klaus et al., 2007)
<i>G. lucidum</i>	K1						

Table 2.2: Comparison of Serbian *Ganoderma* sp. cultivation method and published findings.

2.10 Polysaccharides of *Ganoderma* sp.

Ganoderma sp. is widely known as a therapeutic fungal bio-factory because of its capability to produce novel myco-chemicals (Yuan, 2012). The fungal species contains biochemical properties such as terpenes and polysaccharides that are beneficial for the prevention of diseases such as hypertension, cancers, diabetes, AIDS and more. This mushroom is widely used as health supplement and in preparation of traditional herbal medicine all over the world such as China, Japan and more (Paterson, 2006). Polysaccharides are a structurally diverse class of macromolecules that contains a wide variety therapeutic chemical property. Major bioactive compounds commonly found in *Ganoderma* sp. are β -1-3 and β -1-6-D glucans. Polysaccharides can be divided into two types which are water soluble polysaccharide (ganoderans, glycoprotein and heteropolysaccharides) water insoluble polysaccharides (crude glucan extracts). Both the types of polysaccharides exhibited antitumor, antioxidative and immunomodulating activities (Paterson, 2006).

2.11 Wild-Serbian *Ganoderma applanatum* strain BGS6Ap

Wild-Serbian *G. applanatum* strain (BGS6Ap) was isolated from Mount Kosmaj where the name originates from the Celtic word “cos” which means forest and the pre-Indian word “May” that means mountain. However, the Romans adapted the name Kosmaj to mythology because it gained the meaning of the Mayan habitat. The fruiting body of this strain was isolated from a dead beech tree. After collection, carpophores were identified according to the methods of classical herbarium taxonomy to confirm the correct species (Phillips, 1981). The representative voucher specimens and their mycelial cultures were deposited at the herbarium of the Department of Industrial Microbiology (University of Belgrade – Faculty of Agriculture in the culture collection for mushrooms).

According to Karthikeyan et al., (2009) and Stojković et al., (2014), the differences in the chemical constituents of *Ganoderma* sp. have been assigned to different locations of collection. Other than that, past studies of *Ganoderma* sp. from the Serbian region focused only on the fruiting bodies and bioactive composition after the EPS production (Rašeta et al., 2017; Stojković et al., 2014).

Mushroom name	<i>Ganoderma applanatum</i>
Country	Republic of Serbia
Mushroom type	Wild
Coordinate	44° 27' 57" N, 20° 33'52" E
Isolation Place	Mountain Kosmaj
Temperature Range	18°C-24°C

Table 2.3 Identification of Wild-Serbian *G. applanatum* strain BGS6Ap

2.12 Submerged liquid fermentation (SLF)

Submerged fermentation referred to as liquid fermentation is an alternative method used for mushroom cultivation because the conventional approach is costly and time-consuming usually taking several months for the first fruiting body to appear (Ahmad et al., 2013a). Other than that, it is an effective and efficient method that provides speedy growth of mycelium biomass and production of crude intracellular and extracellular polysaccharides within a confined space with very minimal chances of contamination (Ahmad et al., 2013a). This liquid media that is either broth or molasses contains essential substrates needed for the growth of mushroom mycelium (Subramaniyam et al., 2012). Besides, submerged fermentation may need the frequent or constant supplement of substrates as it will be rapidly used up by the microorganism. This technique is also one of the easiest ways used to purify products with the help of assays (Subramaniyam et al., 2012). Figure 2.4 illustrates the media composition and setup on an incubator shaker. First seed culture, typically done using a 250 mL Erlenmeyer flask with a working volume of 100 mL. Then it is upscaled to second seed culture done in 500 mL Erlenmeyer flask with a working volume of 200 mL.



Figure 2.4: Basic apparatus of a laboratory-scale submerged fermentation (figure by author)

2.13 Biological Growth Models

Growth models could be used to describe the behavior of fungal mycelium under various physical and chemical conditions such as temperature, water activity, pH, agitation, and concentration of carbon source (Zwietering et al., 1990). Growth curves are significantly used to analyze the fundamental characteristics of a given organism or cellular pattern (Kahm et al., 2010). Growth modes are used to distinguish the relationship between the concentration of a compound of a substrate and its effect on the cell and after the link has been established the shelf life as well as the microbial safety of the mycelium can be predicted (Kahm et al., 2010; Zwietering et al., 1990).

A primary growth curve will describe cells from an old culture inoculated into a freshly prepared culture medium and for a while there will be no growth as the culture is adapting to the surrounding environment and this is known as the initial stationary phase (Bayne-Jones et al., 1929; Buchanan, 1918). Then next, the multiplication of culture begins causing the number of organisms to gradually increase with time and well-known as the positive growth acceleration phase (lag phase) (Buchanan, 1918; Pamment et al., 1978). The logarithmic phase shows the consistent rate of increase in organism followed by a stationary phase in which there is no increase or decrease in organism growth. Lastly, is the death phase in which the number of organisms decreases gradually (Bayne-Jones et al., 1929; Buchanan, 1918).

2.14 Response Surface Methodology (RSM)

Optimization defines as enhancing the performance of a system or a process to receive the full advantage from it. The word optimization has frequently been used in analytical chemistry as a method of determining the circumstances at which to utilize a procedure that creates the best possible response (Bezerra et al., 2008). RSM established in the early 1950s that comprised of fundamental experimental design for linear response models, including the depiction of techniques for the determination of optimum operating conditions (Khuri et al., 2010). In the 1970s, more modeling techniques were introduced that covered Taguchi's parameter design and its response surface alternate method (Khuri et al., 2010). Finally, in early 2000, modern RSM appeared. It included additional extensions like advanced graphical techniques, linear models, and improved response surface models. (Khuri et al., 2010). RSM entails of a cluster of mathematical and statistical methods applied during the development of an adequate functional connection between a response of interest, y , and several related control variables designated by x_1, x_2, \dots, x_k (Khuri et al., 2010).

CHAPTER 3: MATERIALS AND METHODS

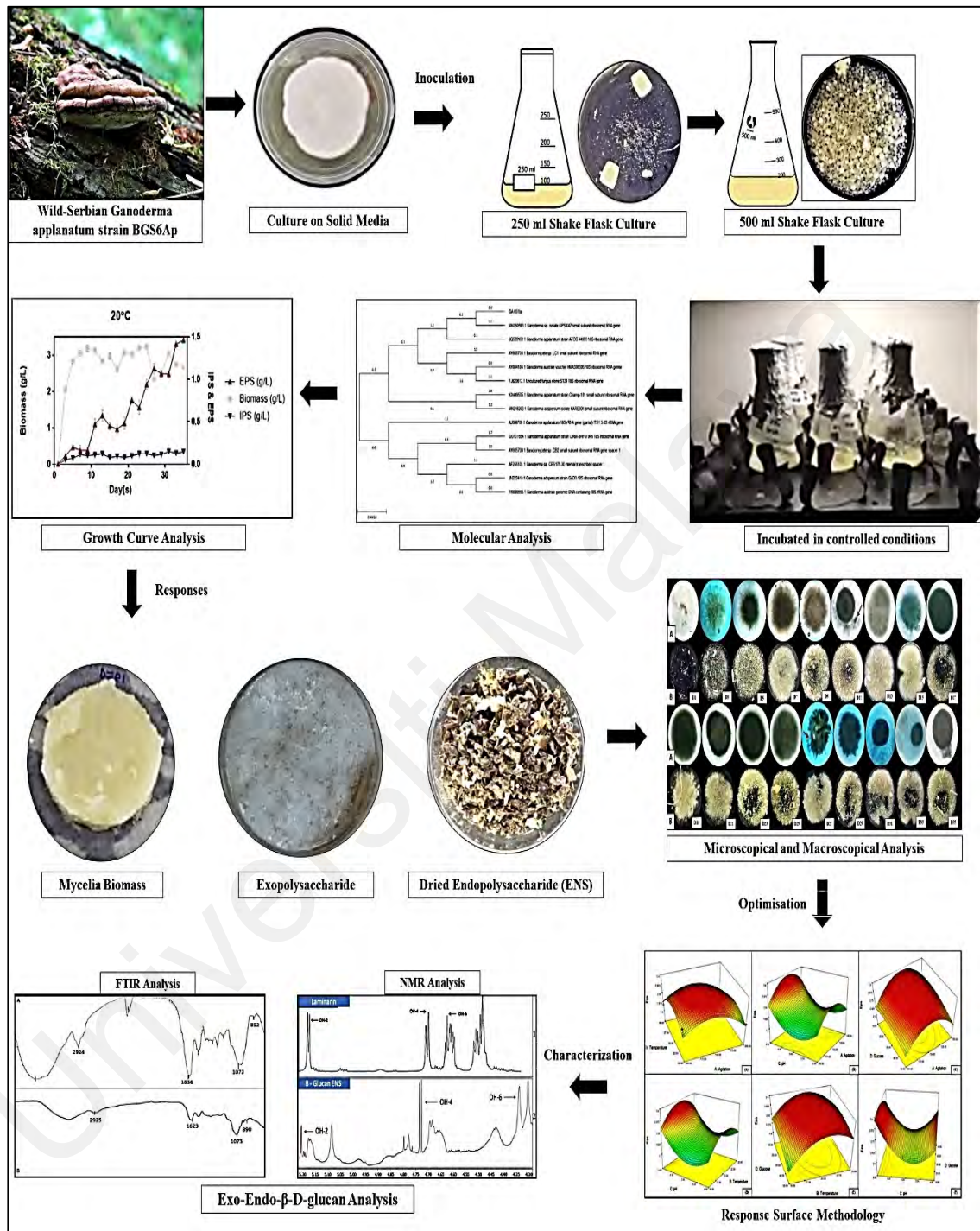


Figure 3.1: Summary of methodology for exopolysaccharide, endopolysaccharide, and biomass production from wild-Serbian *Ganoderma applanatum* strain BGS6Ap mycelium in submerged liquid fermentation (figure by author).

3.1 Cultivation of organism

The GASB was screened and isolated from Mount Kosmaj, Serbia by Prof. Dr. Anita Klaus from the University of Belgrade. The fungus was sub-cultured onto potato dextrose agar (PDA) upon receiving and incubated at 30°C until the mycelium covers the entire PDA plate. Plates were then stored at 4°C and preserved on PDA slants. The medium composition for seed culture and batch fermentation was maintained at the same metrics (g/L): Glucose 30, Yeast Extract 1, KH₂PO₄ 0.5, MgSO₄ 0.5, and NH₄Cl 8 (Wan-Mohtar et al., 2016a).

3.2 Identification

3.2.1 Preparation of mycelium for DNA extraction

GASB mycelium was prepared on a PDA plate and freeze-dried. Selected parts of the mycelium were removed from the agar with a sterile scalp. The mycelium was ensured to be liberated from traces of agar and suspended in 1ml of pure water. The solution and mycelium were both placed in an Eppendorf tube and fragmented by robust pipetting. 0.1 g of Caesium Chloride (CsCl) was added into the tube and centrifuged at 13000 rpm for 10 min. Next, the bulk mycelium was removed from the surface of the solution, hence leaving behind the agar at the bottom of the tube and mycelial strands dispersed in the solution. Distilled water was used to wash the mycelium twice and subjected to freeze-drying and stored at – 20°C (Liao et al., 2015).

Then, RNase was added, and the mixture was incubated (5 min, 37°C). Next, NaCl (165 µl, 5 mol/l) solution was added, and the tube was inverted multiple times before being subjected to centrifugation (14000 × g, 20 min, 4°C). The supernatant was transferred to a fresh tube. Chloroform and phenol (400 µl each) were added to the tube with supernatant and gently inverted multiple times until the solution became cloudy. Next,

the solution was subjected to centrifugation ($14000 \times g$, 20 min, 4°C). Then, the aqueous phase was removed and extracted using equal volumes of chloroform. 95% ethanol (2 volumes), to precipitate the DNA.

Finally, to purify the DNA, lysis buffer (500 μl) was added and mixed by pipetted gently. NaCl was added and lightly mixed by inverting the tubes several times. Purified DNA was extracted by adding two volumes of chloroform and subjected to centrifugation ($14000 \times g$, 20 min, 4°C). 95% ethanol was used to precipitate, and 70% ice-cold ethanol was used to wash the DNA. The washed DNA was dried and dissolved in TE buffer (50 μl) and kept at -20°C (Hennicke et al., 2016)

3.2.2 PCR Amplification

The subsequent DNA pellet was dissolved in $1 \times$ Tris – EDTA (50 μL) to form purified fungal DNA. Fungal identification was made using two internal transcribed spacer (ITS) primers which are universal primers (ITS1 and ITS4). 500 μl of the solution was inserted into PCR tubes, then 0.5 pmol of primers were put in together with deoxynucleotides triphosphates (dNTPs, 200 μM each), 0.5 U DNA polymerase and PCR buffer with water. PCR was done as follow: 1 cycle (98°C for 2 min) for initial denaturation; 25 cycles (98°C for 15 secs; 60°C for 30 secs; 72°C for 30 secs) for annealing and extension, followed by one cycle (72°C for 10 min) for a final extension of amplified DNA (Usuldin et al., 2020)

3.2.3 PCR-amplified product purification and sequencing

16-capillary 3100 Genetic analysers (Applied Biosystems) were used to purify and precisely sequence the PCR products. BigDye® Terminator v3.1 Cycle Sequencing Kit (Applied Biosystems) was used in conjunction with the protocols supplied by the manufacturer (Usuldin et al., 2020)

3.2.4 Gel Electrophoresis and Data analysis

The PCR products were analysed on an agarose gel (1%) at 80 V for 1 h using TBE buffer. The standard curve was made by interpolating the size of the unidentified DNA fragments. The standard curve was performed by measuring distance of every fragment migrating on the gel. The sequence of gDNA acquired submitted to Blast, and NCBI Nucleotide Collection database was chosen, and the query was submitted. The sequences that produced significant arrangement was produced, and the top 10 hit blast was chosen for Multiple Sequencing Alignment (MSA). MSA was obtained using Clustal Omega (Usuldin et al., 2020).

3.2.5 Phylogenetic analysis

Neighboring joining (NJ) used in Molecular Evolutionary Genetics Analysis (MEGA-X) were the exact fungal species computed using evolutionary distance (*Knuc*). Then the phylogenetic tree was generated, and any known species closest to the *Knuc* are considered the same species.

3.2.6 Verification of species

Verification of species was done by comparing the mismatches using A plasmid Editor (ApE) software between the sequence of the gDNA and sequence closest to the *Knuc* species.

3.3 Submerged liquid fermentation (SLF)

The inoculum preparation of GASB consists of two seed culture stage (first seed and second seed) that was cultivated for 20 days at 20 C – 30°C, 100 rpm, 30g/L glucose concentration and pH 4 (preliminary study). In media optimisation study (RSM), the conditions are as follows; 20°C – 30°C, 100-200 rpm agitation, 10 g/L–50 g/L glucose concentration and initial pH 4 – 6 by following conditions given in Table 2. First seed

culture: Two square mycelia plug (5 mm x 5 mm: cut using a sterile scalpel) from 14 days old plate were inoculated into an Erlenmeyer flask (250 mL) which already contained fermentation medium (100 mL). Second seed culture: on the 20th day, first seed culture was homogenised using a sterile hand blender for 20 second. Then, 20% this homogenised mixture was used as inoculum for the second seed culture and allowed to ferment another 20 days before analysis. The medium composition for seed culture and SLF was maintained at same metrics (g/L): Yeast Extract 1, K₂HPO₄ 0.5, KH₂PO₄ 0.5, MgSO₄ 0.5, and NH₄Cl 8. Each experiment was conducted in triplicates(Wan-Mohtar et al., 2016a).

3.3.1 Dry cell weight (DCW)

DCW of the GASB produced by SLF was estimated by filtering a 200-mL sample through a pre-dried and weighed GF/C filter (Whatman Ltd., U.K.) using a Buchner funnel filter set attached to a water pump, followed by repeated washing (three times) of the mycelial biomass with distilled water. The mycelial or pellets filter cake was dried overnight in the dryer and cooled in a desiccator for 24h before weighing. Calculation of the DCW was done by subtraction of pre-weighed filter mass from the mass with the filtrate and multiplied by the dilution factor to get DCW in g/L. All values were taken based on averages of at least three independent trials (Wan-Mohtar et al., 2016a; Wan-Mohtar et al., 2016b)

3.3.2 Exopolysaccharide (EPS) extraction

EPS was obtained from filtered supernatants of the harvested fermentation broth. Then, the crude EPS was precipitated by the addition of four volumes of 99.9% (v/v) ethanol and left overnight at 4 °C. The precipitate was separated by centrifugation at 9,000 rpm for 10 min, this was repeated twice. The precipitate was filtered through a pre-dried and weighted GF/ C filter paper and washed twice with 5mL of 95% (v/v) ethanol. It was reassigned to desiccators, left to dry to constant weight, and the weight of EPS was then

estimated (Wan-Mohtar et al., 2016a; Wan-Mohtar et al., 2016b)

3.3.3 Endopolysaccharide (ENS) extraction

The ENS of GASB was extracted using the mycelium. ENS was obtained from the filtrate (washed mycelium). The mycelium (1g) was mixed with 20 mL distilled water, then sterilised at 121°C for 30 minutes. After sterilizing, the mixture was filtered to obtain the supernatant. Crude ENS was precipitated by the addition of 1: 4 ratios of 99.9% (v/v) ethanol and left overnight at 4 °C to one volume of cell-free filtrate. The precipitate was then separated by centrifugation at 9,000 rpm for 10 min and the process was repeated twice. Furthermore, the precipitate was filtered through a pre-dried and weighted GF/ C filter paper and washed twice with 5mL of 95% (v/v) ethanol. It was reassigned to desiccators, left to dry to constant weight, and the weight of ENS was then estimated (Ubaidillah et al., 2015).

3.3.4 Morphology analysis

The morphology details of the samples collected were assessed using a light microscope (Leica) through a camera (8-megapixel camera (Apple Inc., Cupertino, CA, USA) with 1.5 μ pixels. The camera captured images of 640 x 1136 pixels, 8.5-mm focal distance, and f/2.2 aperture.

3.3.5 Microscopic Analysis

The mycelia sample was stained using methylene blue stain. Moreover, the mycelia sample was poured with media and sealed with parafilm. This step enabled the observation of the mycelia as it is in the media. The plate was observed under an inverted microscope (Leica M165 C) (Wan-Mohtar et al., 2016a).

3.3.6 Statistical analysis

The analysis was carried out in a triplicate manner, and the mean (\pm SD) was determined with GraphPad Prism 7 software (Version 7.00) and an error bar was made as mean. The absence of an error bar indicates that the size of the symbol is more

significant than the error value (Wan- Mohtar et al., 2016a)

3.4 Optimisation of growth parameters (initial pH, agitation rate, temperature, glucose concentration) of wild-Serbian *Ganoderma applanatum* strain BGS6Ap using response surface methodology.

3.4.1 Optimisation of growth parameters using RSM

Based on the findings obtained from the preliminary study, temperature showed the highest significance for the responses (biomass, EPS production and ENS production). Media composition that was kept constant in shake flask (g/L) was as follows: NH_4Cl_2 4, Yeast Extract 1, KH_2PO_4 0.5, K_2HPO_4 0.5, MgSO_4 0.5. Central Composite Design (CCD) was used to optimise the production of biomass, EPS and ENS. Table 3.1 illustrates the levels and range of variables used for this study.

Independent variables	Range and levels		
	-1	0	1
Glucose (g L^{-1})	10.0	30.0	50.0
pH	4.0	5.0	6.0
Temperature ($^{\circ}\text{C}$)	20	25	30
Agitation (rpm)	100	150	200

Table 3.1: Experimental range and levels of independent variables

3.5 Characterisation of exo-endopolysaccharides from the mycelium of wild-Serbian *G. applanatum* strain BGS6Ap using Fourier-transform infrared spectroscopy (FTIR) and nuclear magnetic resonance spectroscopy (NMR)

3.5.1 Characterization of exo-endopolysaccharide using NMR spectroscopy

The analysis was performed using a 700 MHz NMR spectrometer (Ascend™ 700, Bruker, Germany). Crude ENS (10mg) was mixed with 500 µL of deuterium oxide (D₂O) at room temperature. The mixture was vortexed and sonicated for 15 minutes until crude polysaccharide completely dissolved. Next, the mixture was subjected to centrifugation at 10000 x g for 10 min. The supernatant was transferred to a 5 mm NMR tube (Norvell, 211 Sigma Aldrich, Canada) for analysis (Supramani et al., 2019; Usuldin et al., 2020).

3.5.2 Fourier-transform infrared spectroscopy (FTIR)

FTIR of crude ENS and EPS (0.5 g each) was obtained using the laboratory equipment Agilent Cary 630 equipped with diamond ATR (Attenuated Total Reflectance). The frequency range used to measure as wave numbers was 4000 -650 cm⁻¹. The crude ENS were subjected to analysis using real-time Micro-Lab software (Usuldin et al., 2020).

CHAPTER 4: RESULTS AND DISCUSSION

4.1 Cultivation and Morphological Identification of wild-Serbian *Ganoderma applanatum* strain BGS6Ap (GASB)

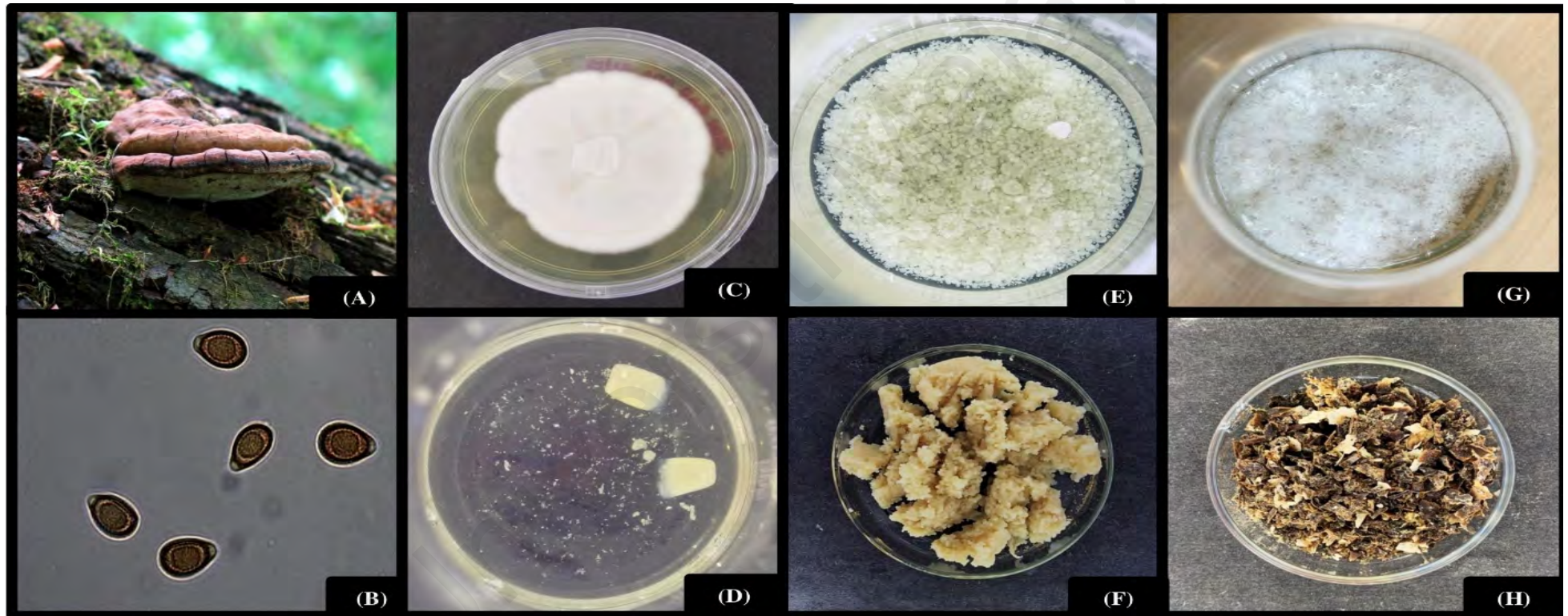


Figure 4.1: (A) *G. applanatum* fruiting body. (B) Basidiospores of *G. applanatum* under a microscope. (C) Mycelium of *G. applanatum* on PDA plate (Day 7). (D) First seed culture of wild-Serbian *G. applanatum* in SLF (Day 10) and (E) wild-Serbian *G. applanatum* in SLF at day 20. (F) Depicts the mycelium after filtration from (E). (G) Depicts the extracted ENS and (H) macroscopic morphology of dried biomass.

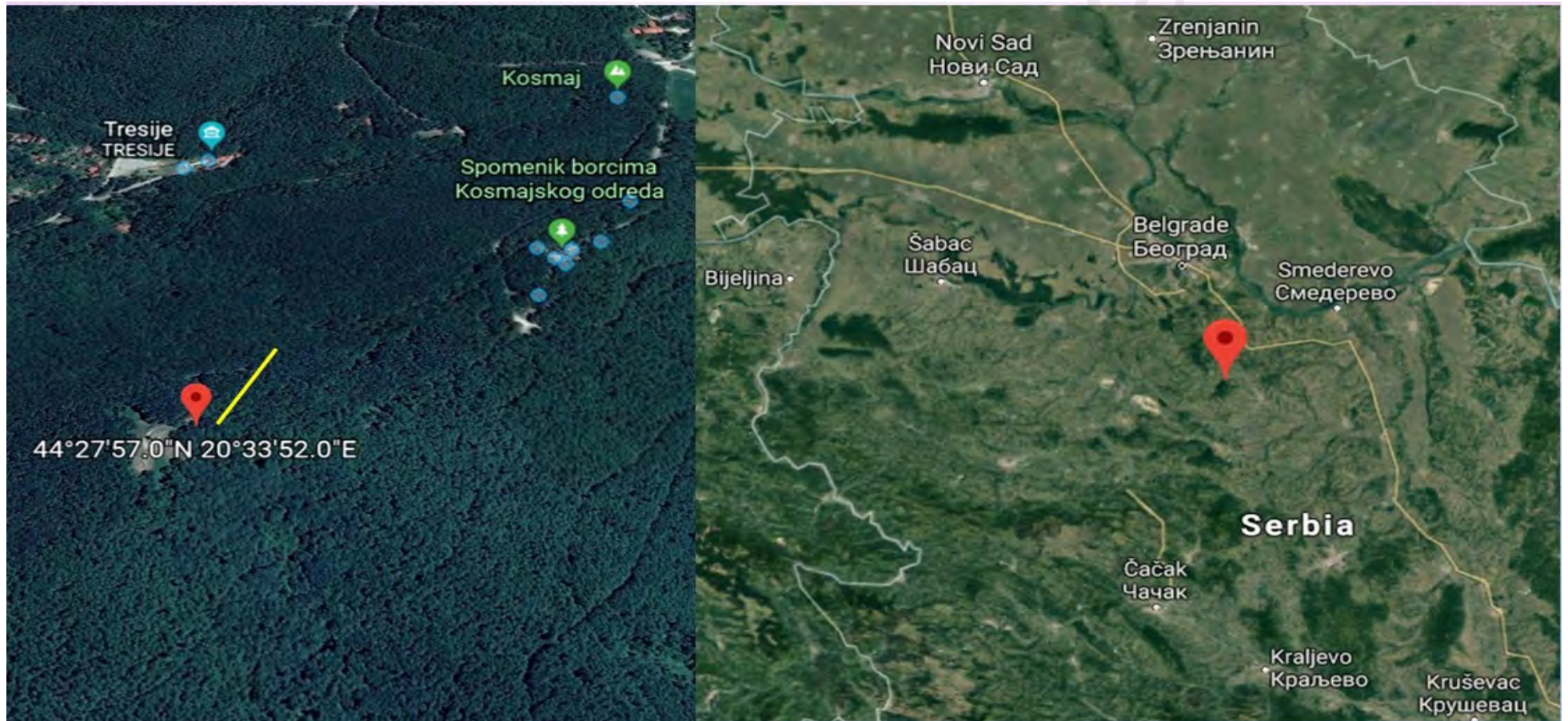


Figure 4.2: The locality of wild-Serbian *G. applanatum* strain BGS6Ap found at the mountain of Kosmaj (yellow bar indicates the 147-m distance at the coordinates 44°27'57''N 20°33'52''E). Source: Google, 2020.

Morphological identification was performed on the on the following GASB structures: basidiospores and mycelium (grown under different conditions). Firstly, the fruiting body was analyzed based on its colour and shape. From Figure 4.1 A, it was observed to have a brown-woody cap growing on the bark of a dead tree including the carpophores of the fruiting body. Figure 4.1 B shows, spores morphology observed under a microscope at 100x magnification, where the bulging hyaline structure, exosporium and endosporium were seen and compared to the study carried out by Banerjee (1959). Next Figure 4.1 C displays the mycelium morphology when grown on PDA plate on D7, was dense and distinctive. Fluffy and healthy mycelial growth was observed at the edges showing that the mycelium was still actively growing and continue growing until D10 to D12. Two seed culture stage was cultivated for maximum growth using SLF, as observed in Figure 4.1 D as the first seed culture (D10). The mycelium was displayed as a large pellet-ball and densely structured. Also, tiny pellets were dispersed in the liquid medium, probably separated from the primary pellet (Wan-Mohtar et al., 2016a; Wan-Mohtar et al., 2016b). Figure 4.1E shows the second seed culture stage (D10) where more mycelia hyphal tips were produced after homogenisation of the pellets in Figure 4.1D was used as inoculum. The observation above illustrates that ovoid shape pellets dispersed equally throughout the liquid medium (Wan-Mohtar et al., 2016a). Figure 4.2 revealed the location of GASB discovered at the mountain of Kosmaj and yellow bar indicates the 147-m distance at the coordinates shown in Figure 4.

4.2 Molecular Identification of wild-Serbian *G. applanatum* strain BGS6Ap

4.2.1 Gel electrophoresis

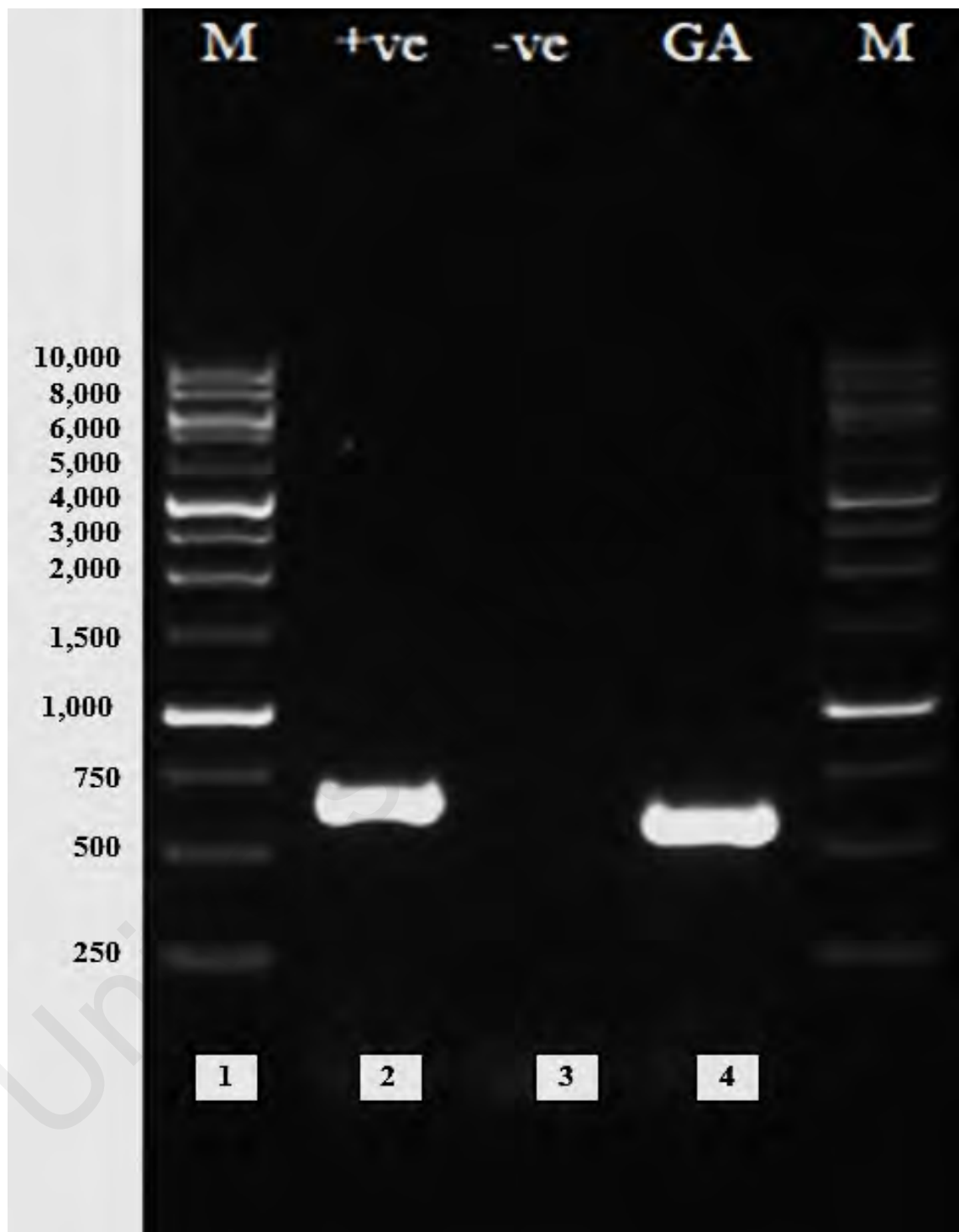


Figure 4.3: Agarose gel electrophoresis of DNA isolated from wild-Serbian *G. applanatum* strain BGS6Ap mycelium. Lane 1 resembles 10 kb DNA marker; lane 2 resembles positive control (+ve); lane 3 represents negative control (-ve) and lane 4 corresponds to the sample GA

4.2.2 Standard Curve

Standard Curve			
Strain	X (distance migrated) cm	Size of Ladder Fragment in BP	Y (Log 10 Size)
	4.93	10000	4.00
	5.22	8000	3.903089987
	5.75	6000	3.77815125
	6.05	5000	3.698970004
	6.41	4000	3.602059991
	6.99	3000	3.477121255
	7.35	2500	3.397940009
	7.84	2000	3.301029996
	8.55	1500	3.176091259
	9.58	1000	3.
	10.30	750	2.875061263
	11.20	500	2.698970004
	12.64	250	2.397940009
BGS6Ap	10.49	650.5879273 = 651 bp	2.813306

Table 4.1: Standard curve to identify the unknown DNA base pair (b0) size for wild-Serbian *G. applanatum* strain BGS6Ap.

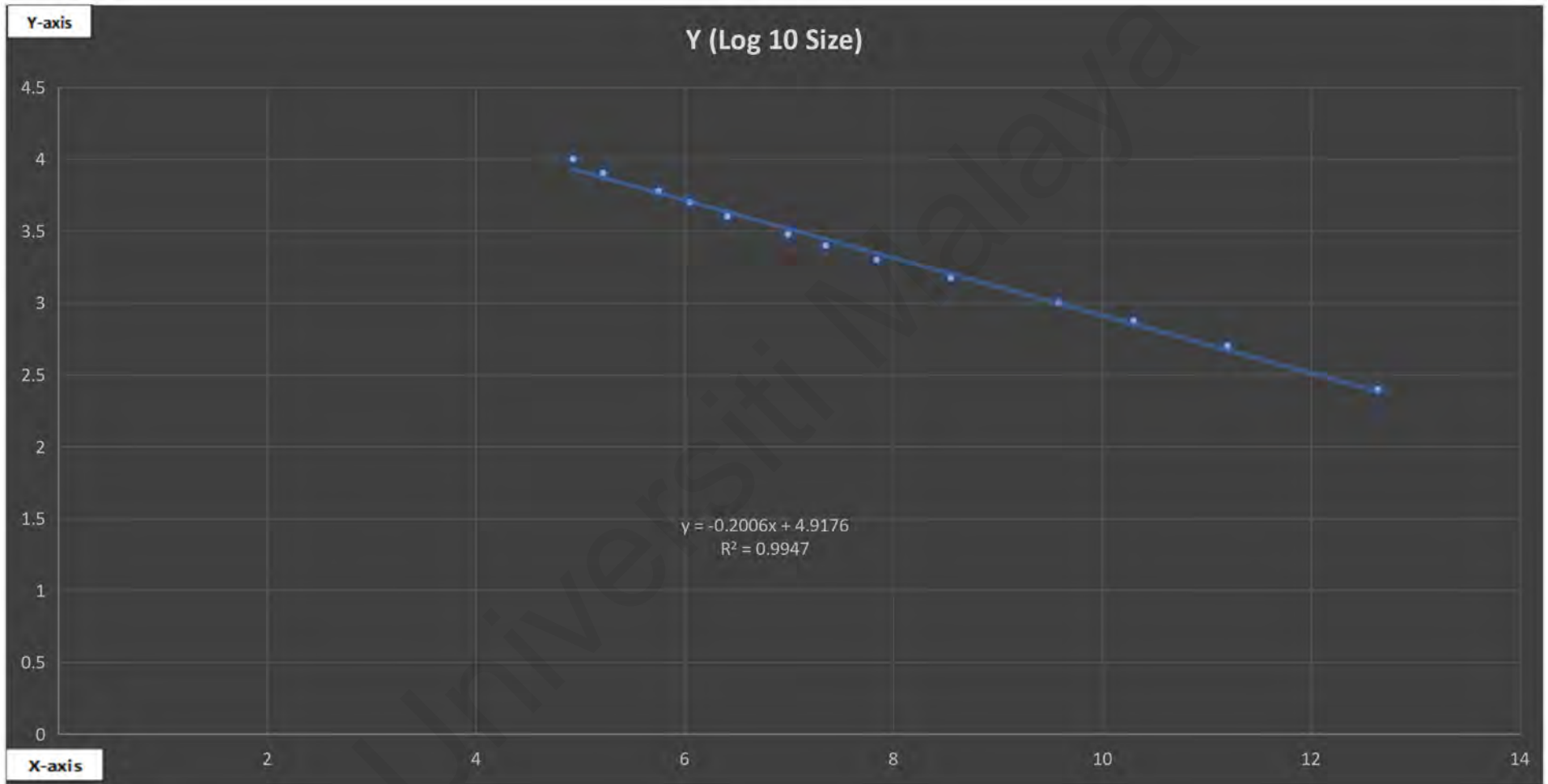
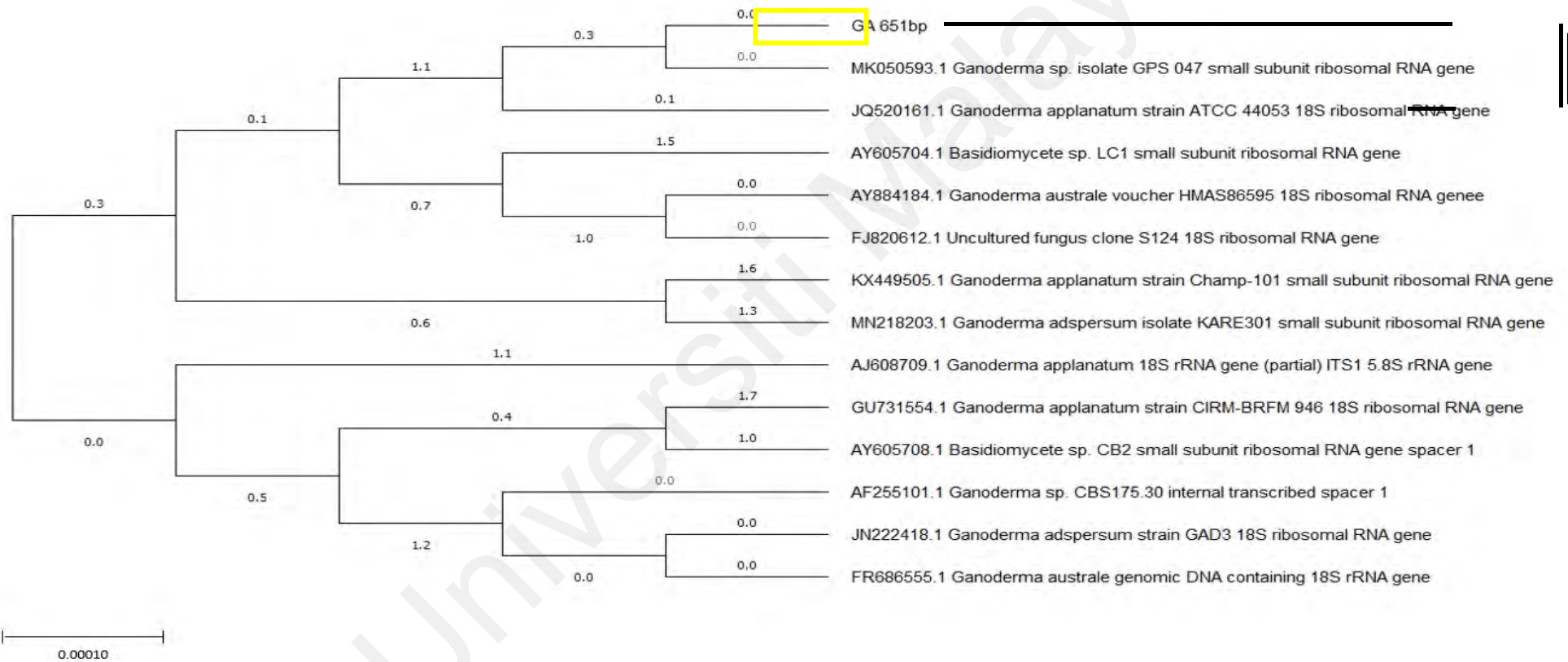


Figure 4.4: Standard curve of log₁₀ (size of base pairs) against distance migrated of wild-Serbian *G. applanatum* strain BGS6Ap

The traditional taxonomic distinction between Ganodermataceae is by basidium traits. Size of basidiospores and morphology of the basidium (hyphal features) could be used to identify a particular species. However, under various growing conditions diagnostic characteristics can mislead can or overlap between the species taxonomy and as a result lead to misidentification of *Ganoderma sp.* (Utomo et al., 2005). Molecular identification of a wild fungal sample is significant because it can differentiate and precisely identify the species of the wild fungal sample in advance of research; hence molecular identification was made on the GASB. Figure 4.2 shows the agarose gel under UV light, DNA fragments of GASB were estimated. The marker (M) serves as a guide to generate the standard curve, and the lane tagged GA shows that the wild fungal species GASB falls between the 500-750 DNA ladder same as the positive control.

Table 4.1 denotes the distance migrated by the DNA fragments (Adl et al., 2012), size of ladder fragment and \log_{10} size. The standard curve is vital to determine the number of base pairs in a DNA fragment and it is usually build based on regression analysis (Prichard et al., 2003). Regression analysis follows the concept of $y = MX + C$ and is made based on the “best fit” line (Prichard et al., 2003). Data from table was used to estimate base pairs of GASB to 651 bp and data used to plot the standard curve, as shown in Figure 4.3 with r^2 of 0.9947. R^2 is the correlation coefficient that indicates the strength of correlation between x and y, and it should be between -1 and 1, the closer it is to 1 the more robust the correlation (Prichard et al.,2003).

4.2.3 Phylogenetic Tree



CLADE
A

Figure 4.5: Phylogenetic tree of wild-Serbian *G. applanatum* strain BGS6Ap generated by neighbouring-joining with evolutionary distance.

Bar = 0.00010 μ m

4.2.4 Verification of species wild-Serbian *G. applanatum* strain BGS6Ap

```
Wild-Serbian Ganoderma applanatum strain BGS6Ap.ape from 1 to 651
Alignment to
JQ520161.1 Ganoderma applanatum strain ATCC 44053 18S ribosomal RNA gene.ape from 1 to 652

Matches():650
Mismatches(#):1
Gaps():1
Unattempted(.):0

      *      *      *      *      *      *      *      *      *      *
1 TTCCGTAGGTGAACCTGCGGAAGGATCAITATCGAGTTTGGACTGGGTGTAGCTGGCCTTACGAGGCATGTGCACGCCCTGCTCATCCGCTCCTACACC 100
|
|
|
1 TTCCGTAGGTGAACCTGCGGAAGGATCAITATCGAGTTTGGACTGGGTGTAGCTGGCCTTACGAGGCATGTGCACGCCCTGCTCATCCGCTCCTACACC 100
      *      *      *      *      *      *      *      *      *      *

      *      *      *      *      *      *      *      *      *      *
101 TGTGCACCTACTGTGGGTTTACGAGTCGCGAAACAGGCCCGTTTCATTGCGGCTTGTGGAGCGCACTTGTTCGCTGCGTTTATCACAACTCTATAAAGTA 200
|
|
|
101 TGTGCACCTACTGTGGGTTTACGAGTCGCGAAACAGGCCCGTTTCATTGCGGCTTGTGGAGCGCACTTGTTCGCTGCGTTTATCACAACTCTATAAAGTA 200
      *      *      *      *      *      *      *      *      *      *

      *      *      *      *      *      *      *      *      *      *
201 TTAGAATGTGTAATGCGATGTAACGCATCTATATACAACCTTCAGCAACGGATCTCTTGGCTCTCGCATCGATGAAGAACCAGCGAAATGCGATAAGTA 300
|
|
|
201 TTAGAATGTGTAATGCGATGTAACGCATCTATATACAACCTTCAGCAACGGATCTCTTGGCTCTCGCATCGATGAAGAACCAGCGAAATGCGATAAGTA 300
      *      *      *      *      *      *      *      *      *      *

      *      *      *      *      *      *      *      *      *      *
301 ATGTGAATTCGAGAATTCAGTGAATCATCGAATCTTGAACGCACCTTGGCTCCTTGGTATTCGAGGAGCATGCCTGTTTGAAGTGCATGAAATCTTC 400
|
|
|
301 ATGTGAATTCGAGAATTCAGTGAATCATCGAATCTTGAACGCACCTTGGCTCCTTGGTATTCGAGGAGCATGCCTGTTTGAAGTGCATGAAATCTTC 400
      *      *      *      *      *      *      *      *      *      *

      *      *      *      *      *      *      *      *      *      *
401 AACTTACGAGCTTCTTGGAGGTTTGTAGGTTGGACTTGGAGGCTTGTGGCTTCTTAAAGGTCGGCTCCTCTTAAATGCATTAGCTTGGTTCCCTTGGCG 500
|
|
|
401 AACTTACGAGCTTCTTGGAGGTTTGTAGGTTGGACTTGGAGGCTTGTGGCTTCTTAAAGGTCGGCTCCTCTTAAATGCATTAGCTTGGTTCCCTTGGCG 500
      *      *      *      *      *      *      *      *      *      *

      *      *      *      *      *      *      *      *      *      *
501 ATCGGGTGTGCGGTGTGATAATGCTACGCCCGACCGTGAAGCGTTTGGCAAGCTTCTAACCGTCTCGGTATAGAGACAAGTTTATGACCTCTGACCT 600
|
|
|
501 ATCGGGTGTGCGGTGTGATAATGCTACGCCCGACCGTGAAGCGTTTGGCAAGCTTCTAACCGTCTCGGTATAGAGACAAGTTTATGACCTCTGACCT 600
      *      *      *      *      *      *      *      *      *      *
```

Figure 4.6: Species verification of wild-Serbian *G. applanatum* strain BGS6Ap using A plasmid Editor (ApE) software

Once the product was sequenced, it aligned with the top-15 related species retrieved from NCBI GenBank to generate a phylogenetic tree, which was constructed based upon the maximum composite likelihood method. Figure 4. 3 shows the comprehensive phylogenetic analysis that displays the evolutionary distance (*K nuc*) values. Based on the reference databases, GASB was placed in the same clade (Clade A) with two other *Ganoderma sp.* strains (GPS047 and GA ATCC 44053) originating from Iran and Japan, which both are temperate continental countries. Results in Figure 4.6 shows A plasmid Editor (ApE) used for species verification between GASB (631 bp) and *G. applanatum* strain ATCC 44053 18s ribosomal RNA gene (632 bp). From the results, only one base pair was found mismatched at base pair 508 (GASB) and base pair 509 (GAATCC44053). Moreover, only one unknown base pair was found between the two species hence it can be concluded that GASB has 99% similarities with *G. applanatum* strain ATCC 44053 18s ribosomal RNA gene.

4.3 Growth Curve Study

4.3.1 Effect of temperature on biomass, exopolysaccharide and endopolysaccharide production of wild-Serbian *G. applanatum* strain BGS6Ap in submerged liquid fermentation.

Shake flask batch fermentation was conducted to explain the initial hyphal growing tips and the effect on biomass, EPS and ENS production prior to the implementation of RSM. The temperature as a prominent factor has been studied in a preliminary study because GASB originates from continental climate. During summer it is slightly warm and more humid while the winters are very cold and windy (Obratov-Petković et al., 2006). The temperature on the mountain is usually below 20°C, and occasionally the highest is 27°C and below (Obratov-Petković et al., 2006). The media component has been maintained as described in section 3.8, and the temperature was adjusted to 20°C, 25°C and 30°C.

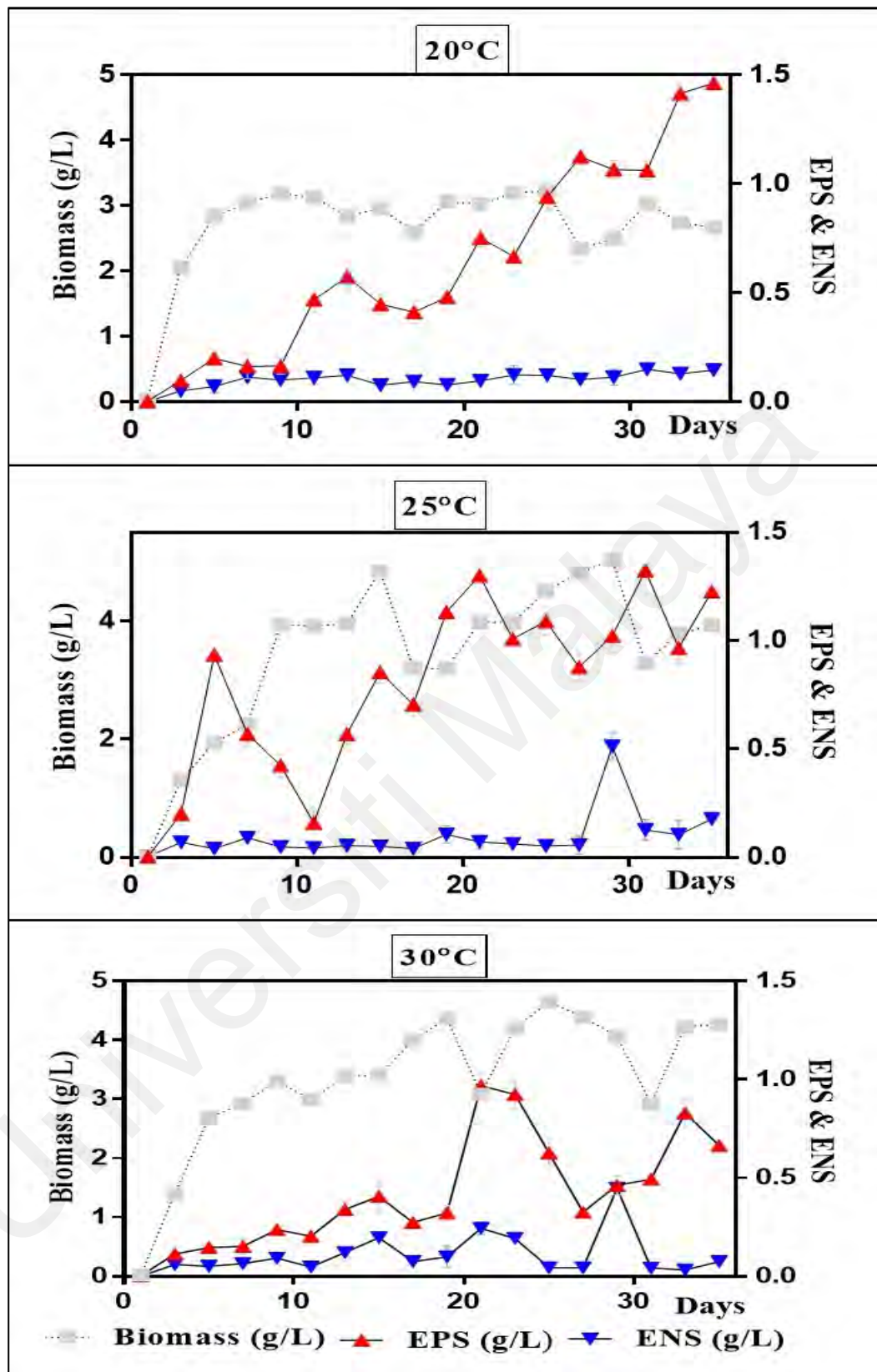


Figure 4.7: Time profile of wild-Serbian *G. applanatum* strain BGS6Ap mycelia during shake flask batch-fermentation and effect of temperature (20°C, 25°C, 30°C) on the production of biomass, exopolysaccharide and endopolysaccharide for 35 days.

Based upon the obtained growth curve for 20°C (Figure 4.7) the fermentation process had successfully followed the typical fungal growth curve pattern until D17 (2.06037 ± 0.07 g/l) where the biomass decreased but on D19 (3.0667 ± 0.04) an increase was observed, henceforth the study was conducted for 35 days until the stationary or death phase was established. However, GASB has proven to be an extremely slow-growing mushroom and the highest biomass was found to be on D25 (3.2307 g/l ± 0.04) and kept growing still after 35 days. The biomass started to increase at D3 (2.0597 g/l ± 0.01) and accelerated rapidly until D9 (3.1867 g/l). From D11 (3.1293 ± 0.05) to D17 (2.06037 ± 0.07 g/l), the fluctuation of the decrease in biomass was between ± 0.4 . On D19 (3.0667 ± 0.04), biomass consistently increased until D25 being the highest and lowest on D27, supported by the pellet morphology (Figure 4.8). After D27, biomass was found to increase until D31 (3.0387 g/l ± 0.02) and decrease until D35 (2.6677 g/l ± 0.04).

Meanwhile, EPS and ENS production was slow for the first ten days because GASB mycelium was still adapting to the surrounding environment and in the growth phase (Wagner et al., 2003; Wan-Mohtar et al., 2016a). After ten days, a rapid increase in both EPS and ENS was observed until D13. After that, a constant decrease and increase in ENS and EPS can simultaneously be observed until D35. The highest level of EPS was achieved on D35 (1.4633 g/l ± 0.02) and ENS achieved on D31 (0.1510 g/l ± 0.03).

As evident from the growth curve at 25 (Figure 4.7), the fermentation process, the fermentation process had successfully followed the regular fungal growth curve pattern and yielded the highest biomass, EPS and ENS concentration compared to the other temperature. The biomass was slow-growing until D13 had a lesser 1st generation time interval compared to 20°C on D17. Then, biomass peaked at D15 (4.8437 g/L ± 0.07) and transitioned into the 2nd generation pellet growth until it peaked at the highest

biomass produced on D29 ($5.0354 \text{ g/L} \pm 0.07$). In between, there was a slight drop in biomass yield on D17 ($3.1993 \text{ g/L} \pm 0.06$) and D31 ($3.2817 \text{ g/L} \pm 0.03$). The decrease in biomass is due to detached pellets from the 1st generation and 2nd generation parent pellets. Under this temperature, the ENS follows a similar trend as biomass on D29 ($0.5120 \text{ g/L} \pm 0.06$) achieving the highest ENS concentration. Meanwhile, the highest level of EPS was accumulated on D31 ($1.3237 \text{ g/L} \pm 0.03$) and follows a trend of increase on D5 ($0.9343 \text{ g/L} \pm 0.02$), 15 ($0.8540 \text{ g/L} \pm 0.05$), and D21 ($1.3100 \text{ g/L} \pm 0.08$).

Fermentation process at $30 \text{ }^\circ\text{C}$, had successfully followed the regular fungal growth curve pattern until D19 demonstrating the slowest to adapt to the environment because GASB was subjected to an environment outside of its range (30°C) and comfort zone considering that the highest temperature from its locality is 27°C . Biomass was observed to have peaked on D19 ($4.3653 \text{ g/L} \pm 0.08$) and highest on D25 ($4.6487 \text{ g/L} \pm 0.03$). A significant decrease in biomass was observed on D21 ($3.0843 \text{ g/L} \pm 0.07$) and D31 being the lowest ($2.9230 \text{ g/L} \pm 0.06$). Meanwhile, EPS and ENS production were highest respectively on D21 ($0.9683 \text{ g/L} \pm 0.06$) and 29 ($0.4474 \text{ g/L} \pm 0.03$).

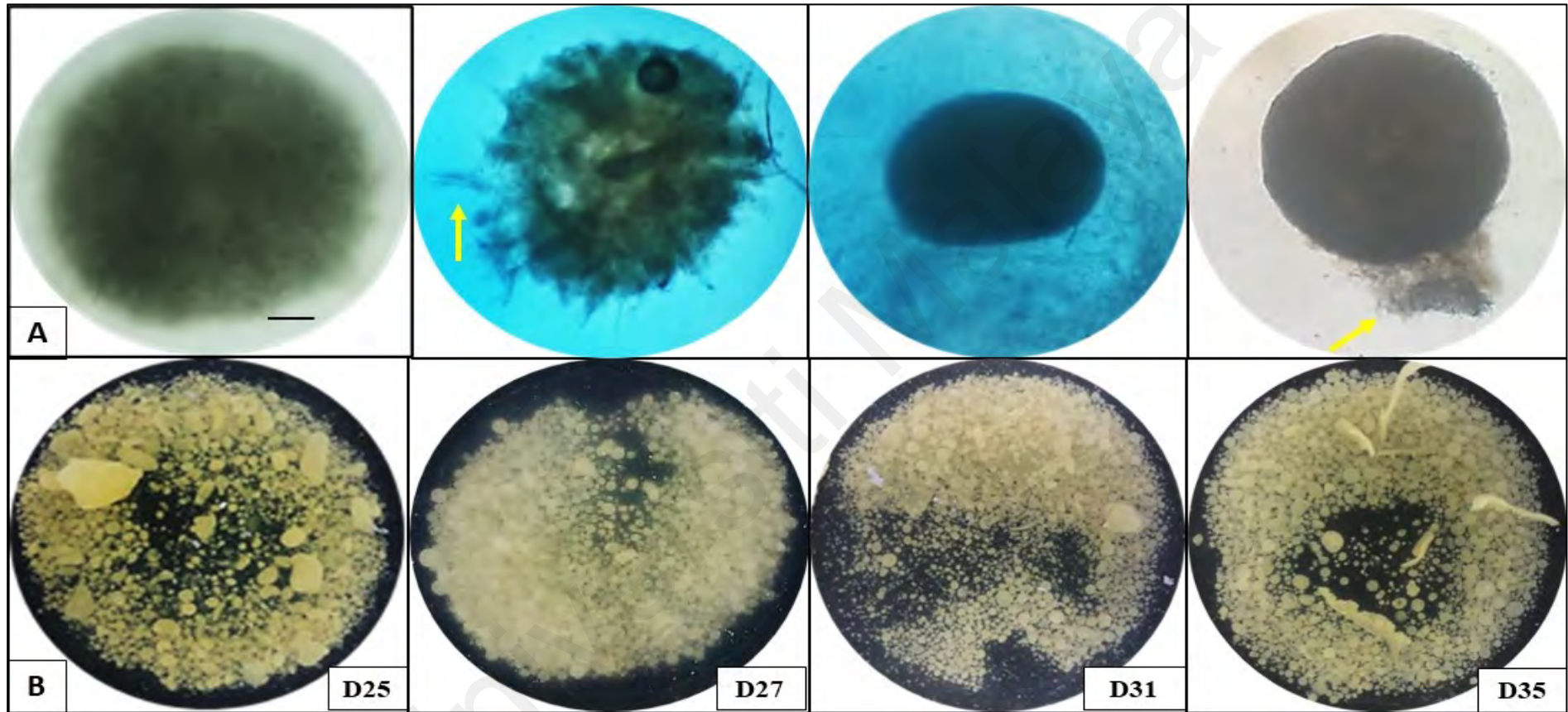


Figure 4.8: Microscopic (A) and macroscopic (B) observation of wild-Serbian *G. applanatum* strain BGS6Ap at temperature (20°C) for biomass, exopolysaccharide and endopolysaccharide production in liquid fermentation. Details of pellet detachment from protruding hyphal tips (yellow arrow). Images (A) and (B) were taken at 4-fold magnification and bar = 100µm.

GASB expressed macroscopic and microscopic changes that behave gradually over time. Figure 4.8 (D25) illustrates compact, dense-core pellets with hairy hyphal tips and macroscopically pellets are small because fragmentation has occurred due to continuous agitation for 25 days, therefore, correlates with the increase in EPS and ENS concentration (Wan-Mohtar et al., 2016a). The small pellets were consuming nutrients in the surrounding media to survive hence secreting EPS and yielded higher biomass compared to larger pellets which are in-line with increased oxygen diffusion and significant surface area (Supramani et al., 2019; Xu et al., 2015). In D27 (lowest biomass), the culture was macroscopically clumped together, irregular-shaped with small, dispersed pellets. Under the microscope, the presence of irregular hairy pellets with protuberances and a slightly hollow structure were observed. The clumping of pellets is a self-immobilization technique to protect against shear effects triggered by stress caused by continuous agitation and lack of nutrients after 27 days (Yang et al., 1998).

The EPS was highest on D35, macroscopically observed to have irregular globular shaped pellets while the media was viscous with gelatinous substance. Pellets were hairy and with short protruding hyphal tips. EPS concentration was the highest because pellets disintegrated from the 2nd generation parent pellet and liberated into the medium as 3rd generation pellets caused by pellet fragmentation starting from D25 (Wagner et al., 2003; Wagner et al., 2004). ENS showed the highest peak on D31, due to small, tiny, dispersed pellets which appeared without hairy protuberances and not densely packed. ENS was higher when the pellets were smaller because of dense growth and lower oxygen diffusion rate (Supramani et al., 2019).

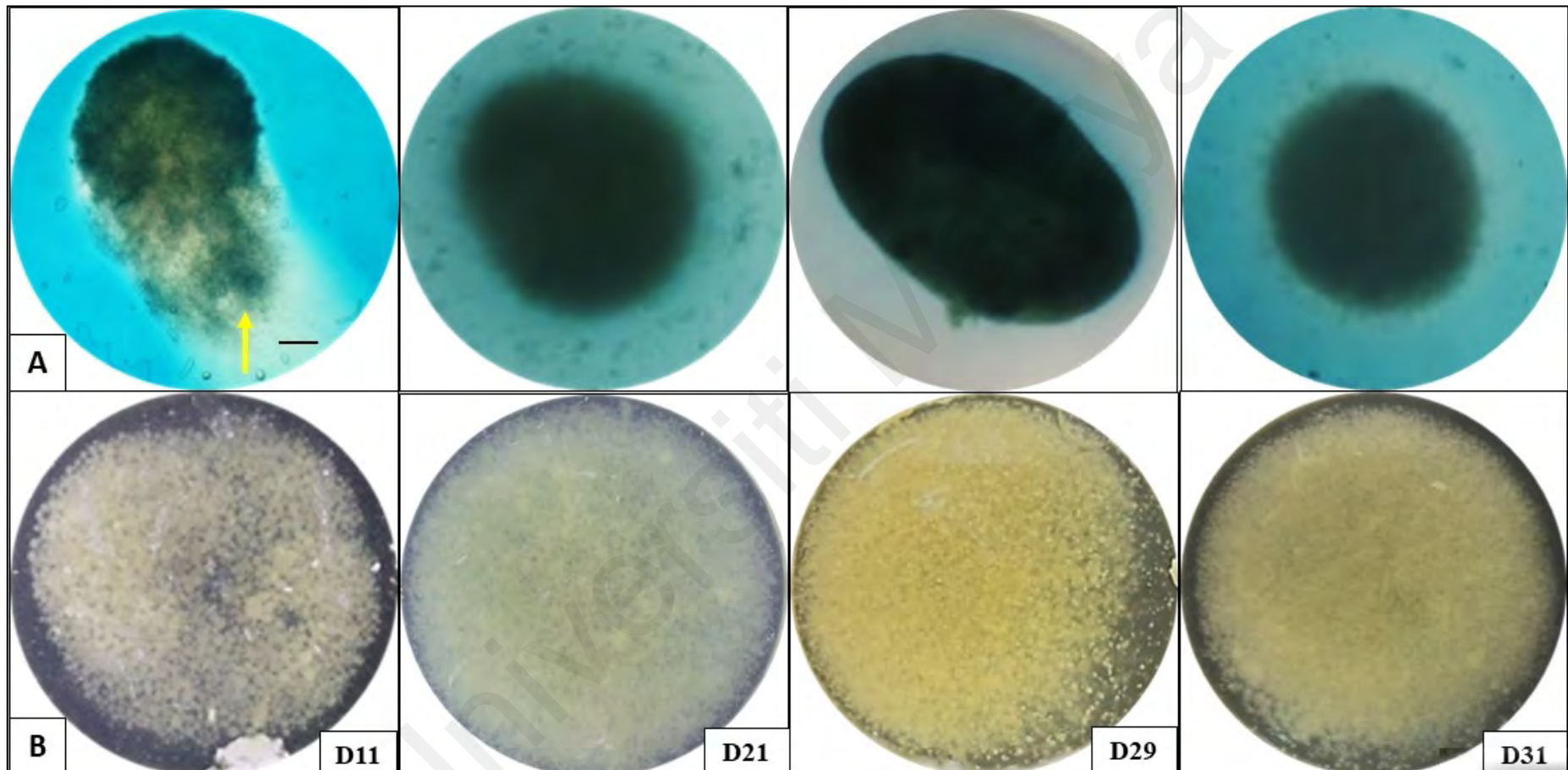


Figure 4.9: Microscopic (A) and macroscopic (B) observations of wild-Serbian *G. applanatum* strain BGS6Ap at temperature (25°C) for biomass, exopolysaccharide and endopolysaccharide production in liquid fermentation. Details of pellet detachment from protruding hyphal tips (yellow arrow). Images (A) and (B) were taken at 4-fold magnification and bar = 100µm.

From Figure 4.9, D11 demonstrates an accelerated increase for EPS, a gradual increase in biomass and a decrease in ENS. Macroscopically on D5, some pellets were clumped and had irregularly shaped pellets. Microscopy revealed a starburst-like pellets with long protruding hyphal tips. The media was viscous at an early stage throughout this temperature and moving into D11, illustrating detachment of 2nd generation pellets from the surface of 1st generation pellet. After some time, an interval of growth and complete detachment from the parent pellet, EPS increases again at D15 and the same trend followed for D21 and D29 except in the case of the 3rd and 4th generation pellets. The time interval between 1st generation to 4th generation decreases and 25°C is the only temperature to shows pellet morphology with multiple detachment progression.

Figure 4.9 shows the macroscopic morphology of EPS increment (D21, D31), with highly viscous media. EPS concentration was at its peak because the gelatinous substance is adhering on the pellets and surrounding media causing it to become highly viscous and this substance strongly reacts with 95% ethanol indicating the presence of polysaccharides in the media (Wagner et al., 2003; Wagner et al., 2004). Microscopically it can be observed that at both days the mycelium has protruding hyphal tips and compact core ovoid-shaped pellets. The pellets had fragmentized to tiny pellets due to the short time interval of multiple accelerated detachment progression.

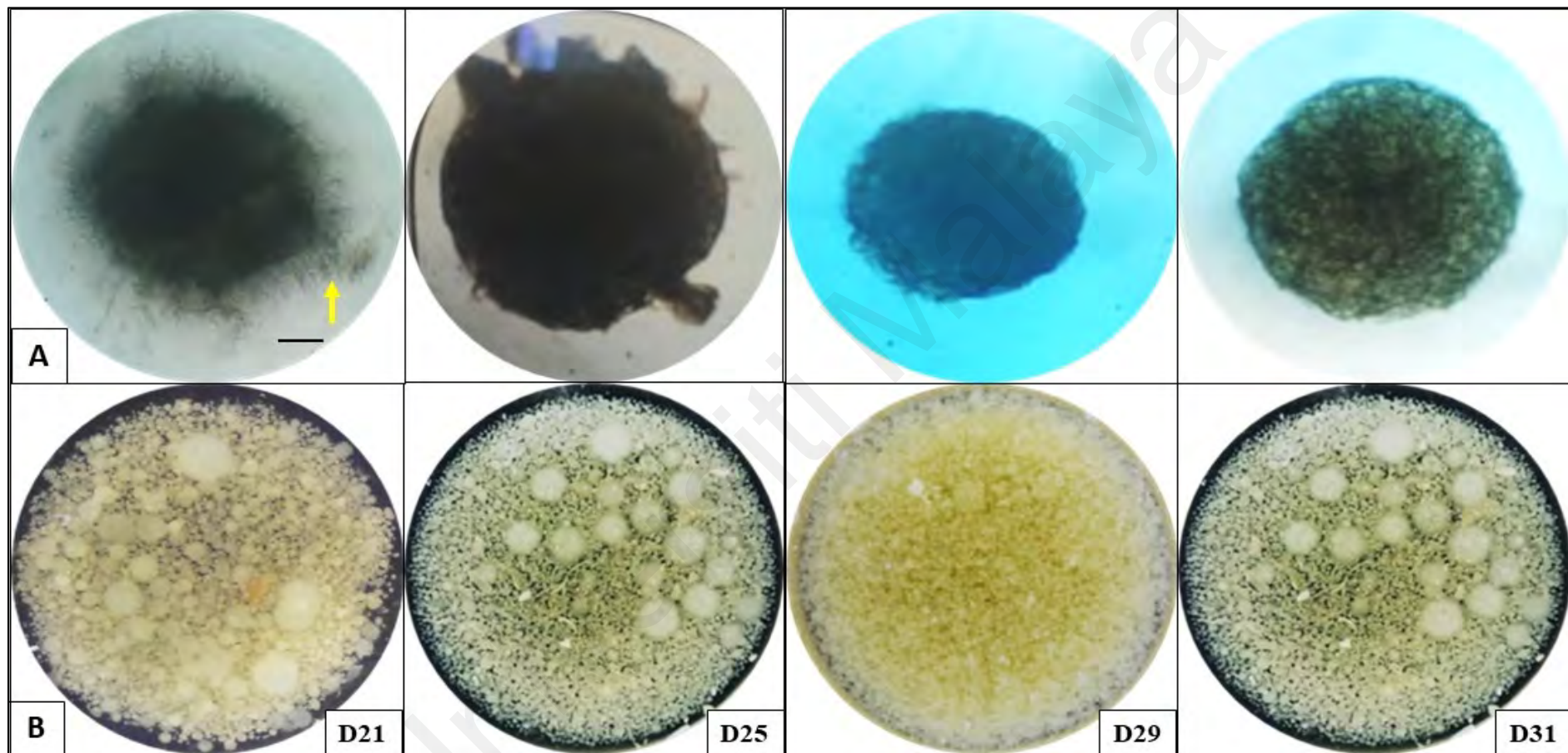


Figure 4.10: Microscopic (A) and macroscopic (B) observation of wild-Serbian *G. applanatum* strain BGS6Ap at temperature (30°C) for biomass, exopolysaccharide and endopolysaccharide production in liquid fermentation. Details of pellet detachment from protruding hyphal tips (yellow arrow). Images (A) and (B) were taken at 4-fold magnification and bar = 100µm.

Macro-view of the biomass on D25 revealed irregularly shaped, medium-sized ovoid of irregularly shaped, medium-sized ovoid, and clumped pellets with hairy morphology. On the other side, microscopy showed large dense-core with thick-branched pellets. The pellets were large, and compact hence yielded high biomass as previously reported by Wan-Mohtar et al., (2016a). In D31, the trend illustrates the lowest biomass concentration. In macro-view these pellets were similar to those from D25. However, microscopy showed more hollow globular pellets which yielded low biomass due to high diffusion of oxygen and sizeable surface area (Supramani et al., 2019). Macroscopically, EPS on D21 gave similar irregular shaped, medium-sized ovoid, and clumped pellets with hairy morphology while microscopically, it showed starburst hairy pellets with long hyphal tips. Previous findings stressed out that hairy protuberance of the 2nd generation pellets detaches from the parent pellet thus utilizing the surrounding media for the necessary metabolic process required for mycelium progression (Acharya et al., 2005; Supramani et al., 2019; Wagner et al., 2004; Wan-Mohtar, et al., 2016a).

ENS concentration was highest at D29, 24h prior to the lowest biomass production, indicating that the pellets on D29 were small. They were irregular in shape but uniformly dispersed throughout the media while under the microscope the pellets were compact and dense. As an agreement with Wagner et al., (2004), small dense pellets yield higher ENS than large pellets. At 30°C, pellets clumped together in comparison with 25°C and 20°C because of stress-induced factor subjected by temperature hence protecting itself using the self-immobilization method to prevent from shearing (Supramani et al., 2019; Wagner et al., 2004; Wan-Mohtar, et al., 2016a).

4.3.2 Effect of temperature on pellet morphology of wild-Serbian *G. applanatum* strain BGS6Ap in submerged liquid fermentation.

According to Wagner et al., (2003) and Wan- Mohtar et al., (2016), there are two significant types of pellet growth known as 1st generation and 2nd generation. According to Fazenda et al., (2010) and Wan- Mohtar et al., (2016), the feather-like morphology during the slow-growing stage (1st generation) contributes to the growth of the 2nd generation pellets by detachment from the surface of the parent pellets. Formation of the first small pellets occurs during the 1st generation growth where a significant amount of protuberance of hairy growth is observed on the surface of mycelium pellets. The protuberance indicates the first break of mycelium into a small pellet. According to Wagner et al., (2003) and Fazenda et al., (2010), EPS production is usually low when 1st generation pellets were molded but reported that EPS production in 2nd generation pellets is higher due to actively growing hyphal tissue compared to newly inoculated mycelium that requires time to adapt and thrive in freshly cultured media (1st generation).

Other than that, the time profile analysis conducted was considered extensive and there was no addition of any media components to replenish the used nutrients, hence according to Wan- Mohtar et al., (2016) and Yang & Liao, (1998), due to accumulation of stress, EPS can attach to mycelia pellet thereby decreasing the excretion of EPS into the media. Based on time profile conducted by Supramani et al., (2019) and Wan- Mohtar et al., (2016), on Malaysian *G. lucidum* and European *G. lucidum* showed a death phase approximately around D15 differing from the GASB used in this study with a longer cultivation time.

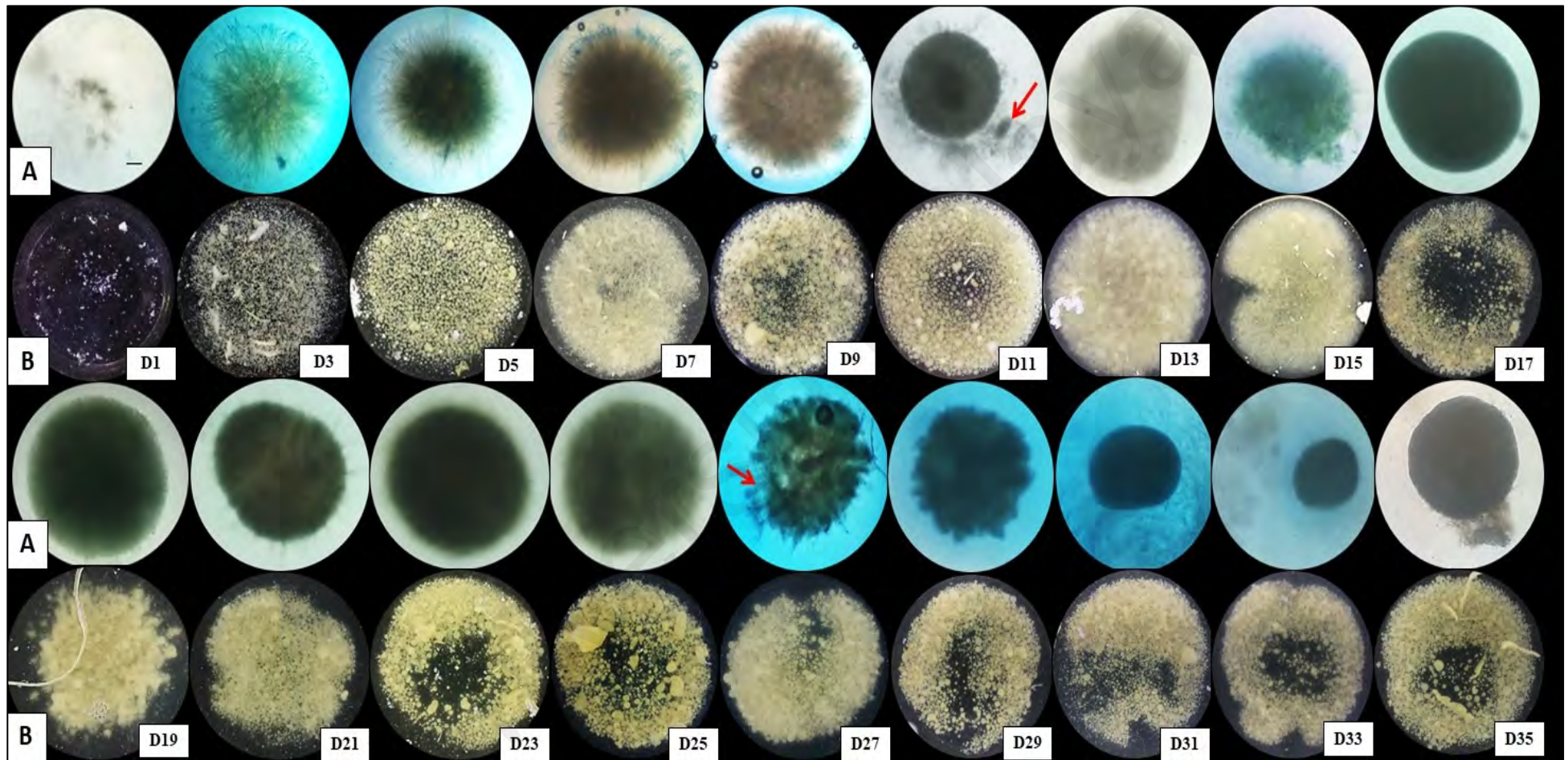


Figure 4.11: Microscopic (A) and macroscopic (B) variations in mycelia during batch-fermentation of wild-Serbian *G. applanatum* strain BGS6Ap at temperature 20°C. Details of pellet detachments from protruding hyphal tips is in red arrow. Images (A) and (B) were taken at 4-fold magnification and bar = 100µm.

GASB showed diverse morphological characteristics throughout the shake flask batch fermentation and the effect on EPS-ENS production before the implementation of RSM. Based on the time profile (Figure 4.11), GASB was subjected to second seed to improve the homogeneity of culture with a blender by removing agar from the mycelium in the previous seed for maximum amount of hyphal tips (Wagner et al., 2003; Wan-Mohtar, et al., 2016a). D1 shows the sheared mycelium particles and clumped hairy feathers dispersed in the media due to a high intensity of the shearing effect. The mycelial biomass increased from D1 to D9 with clumping structures increasing in size and pellets width. Clumped pellets are a self-immobilization technique used to protect the mycelium from any stress-induced condition that originated from shear stress or media viscosity build up (Supramani et al., 2019; Wagner et al., 2004). Moreover, long sparsely branched hyphal filaments were predominant progressively becoming short hyphal filaments (more branching) displayed at D1 to D9. According to Fazenda et al., (2010), long hyphal tips contribute to biomass increment as observed in Figure 4.7.

Sluggish EPS and ENS production trends were noted in D1 to D9, which was attributed to initial stress resulting from the introduction of GASB in liquid media and the adaptation of culture to changed growing conditions (Supramani et al., 2019; Yang et al., 1998). According to Wagner et al., (2004), EPS and ENS production are low during 1st generation growth (D1-D9) but suddenly accelerated at D11 onwards. Pellet inoculum is referred to collectively as 1st generation pellet, is fitted with short hyphal tips protruding, increasing in length and width to form starburst pellets from D5 to D9. Rapid EPS production (D11-D13) is ascribed to the liberation of 2nd generation pellets by a detachment of long hyphal protuberance from starburst pellet on D9 as reported by Wan-Mohtar et al., (2016) for *G. lucidum*. The red arrow on D11 indicate detachment of ovoid-shaped pellet (2nd generation) which produce a feather-like morphology (Wagner et al., 2004; Wan-Mohtar, et al., 2016a). Meanwhile, it indicates a decrease in biomass

due to smaller and less dense core pellets released into the surrounding. Smaller pellets (2nd generation pellets) require more nutrients for growth hence contributes to an increase in EPS (Fazenda et al., 2010; Wagner et al., 2004).

Broth viscosity spiked on D13 onwards, which is due to high cell concentration, change in microbial morphology and accumulation of EPS that alters the characteristic of media (Fazenda et al., 2010). The increase in cell number on D13 illustrates that pellets have completely shaved off protruding hyphal tips on D11 onwards and form less dense pellets with short hyphal tips (D13). This has affected the, decrease in biomass but an increase in EPS and ENS attributed to the “active” growth of liberated pellets. The pellet fragmentation (D13-D17) due to the liberation of pellets affects the size distribution and density of biomass hence contributes to the decreasing trend of biomass demonstrated in this research. Full pellet break-up observed on D17 with fully shaved-off feathers, and small protruding hyphal growth was observed in D19 (Wagner et al., 2004; Wan-Mohtar, et al., 2016a).

A similar growth pattern was demonstrated during D19 to D27 before the liberation of 3rd generation pellet occurs. Biomass increased during this time interval with increasing compact to core pellets. Since the liberation of secondary pellets, the EPS trend fluctuated slightly (D23) with an increasing concentration on D35. Fluctuation (D23) of pellet morphology is due to surge number of ready-to-detach pellets contributing to the weight of biomass growth (D23-D25). Next on D27, a faster decrease in biomass resulted in the initiation of pellet fragmentation liberating lesser dense pellets (3rd generation-yellow arrow). As growth progressed (D27-D35), the protuberance of hyphal filaments was not actively illustrated as previously compared releasing significant 3rd generation pellets. Pellet morphology appeared to be globular, less dense, and hollower compared to initial growth stages (1st and 2nd -generation

pellets) hence attributed to the biomass concentration drop. Long protruding hyphal tips (D27) became shorter after detachment (D29) and still display the ability to grow further with no proximity to the initiation of autolysis compared to similar findings done on *G. lucidum* by Wan-Mohtar et al., (2016) and Supramani et al., (2019).

Universiti Malaya

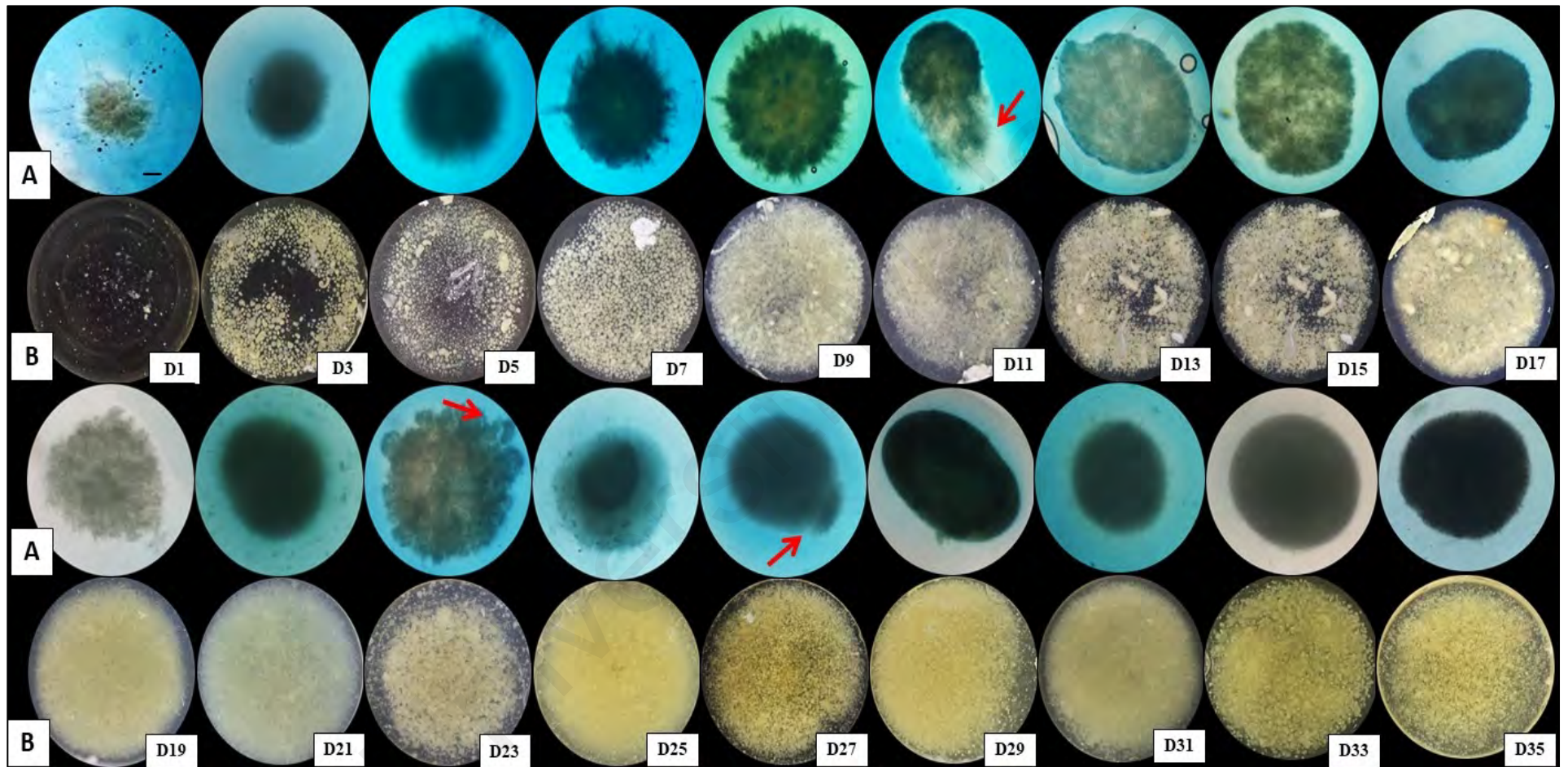


Figure 4.12: Microscopic (A) and macroscopic (B) variations in mycelia during batch-fermentation of wild-Serbian *G. applanatum* strain BGS6Ap at temperature 25°C. Details pellet detachments from protruding hyphal tips is in red arrow. Images (A) and (B) were taken at 4-fold magnification and bar = 100µm.

GASB was subjected to a temperature of 25°C, Figure 4.12 and, shows the 1st generation growth from D1 to D11. Biomass increased following the fungal growth (lag phase from D1 to D7, log phase from D7 to D9 and stationary phase from D9 to D15). It has been demonstrated that GASB slow-growing behavior was unable to undergo the death phase with high biomass on D17. Morphologically, pellets showed short protruding hyphal filaments (D1-D9) that elongated until the liberation of 2nd generation pellets (D11-yellow arrow). Next, the pellets grew in width, size and concentration of biomass increased gradually with densely packed pellets resulting in the pattern of biomass trend in D1 to D15. Meanwhile, a noticeable drop in cell concentration (D17) probably because the pellet fragmented completely after the liberation of the 2nd generation pellet. Pellet was shaved off with no visible protruding hyphae which could be further bolstered by constant agitation rate, therefore, resulting in shorter hyphal tips.

Clumping of GASB, as well as its instinctive tendency for entanglement, causes liquid media to be highly viscous (D17-D21). Clumping is associated with the increase in EPS concentration by mucilage observed surrounding the media (Fazenda et al., 2010). Biomass demonstrates increasing growth at this stage producing the highest cell concentration during 2nd generation growth (D29). At this moment biomass reached the highest quantity as a result of the presence of several parent pellets (2nd generation) associated with the release of the 3rd generation pellets as previously illustrated by Wagner et al., 2004; Wan-Mohtar et al., 2016a). 2nd generation pellets also produced long hyphal protuberance which was subsequently liberated into liquid media (D23) and many of the 3rd generation pellets round out while still attached to the mother pellet (D27- yellow arrow) which liberated shaved-off pellet (D29) thereby giving predominance of 3rd generation pellets (D31-D35). Therefore, due to pellet fragmentation a significant reduction in biomass (D31), followed by a gradual increase due to functional metabolic processes occurred. On the other hand, ENS production was

the highest at 25°C and same day as biomass (D29) with a similar trend. The density of pellet morphology contributed to the higher biomass and ENS production.

Accelerated EPS production was demonstrated in D3, D15, D21, and D31. EPS increase (D3, D15) shows that temperature is most conducive for GASB as it requires less time to produce bulk EPS. The recorded time interval between each generation's growth is shorter compared to other temperatures. Morphologically (D3, D15, D21, D31), the pellet size is small, smooth, short-protruding hyphal filaments predominant to high EPS production (Fazenda et al., 2010; Supramani et al., 2019). EPS was high between the time interval of pellet fragmentation also stemming from the EPS production trend.

Universiti Malaysia

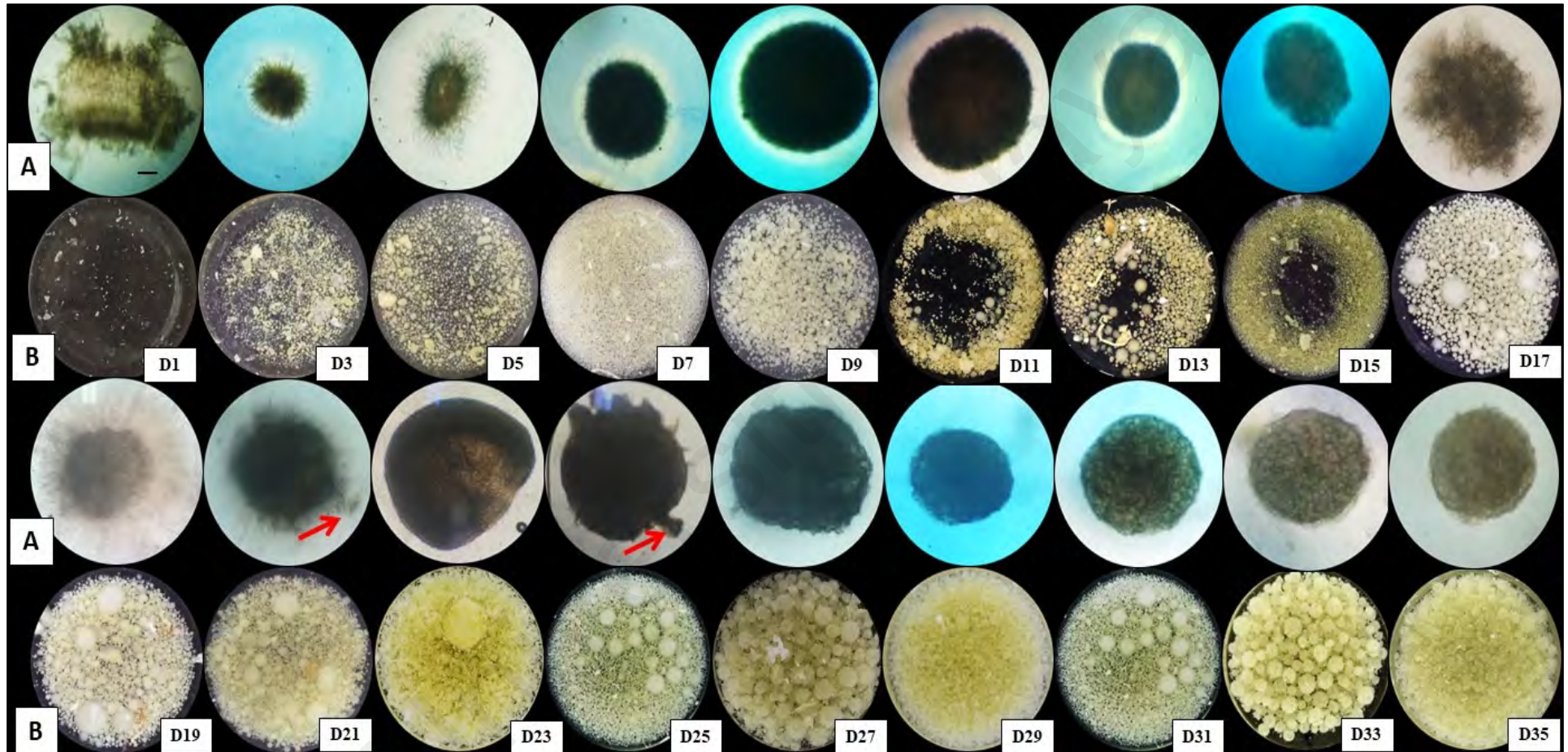


Figure 4.13: Microscopic (A) and macroscopic (B) variations in mycelia during batch-fermentation of wild-Serbian *G. applanatum* strain BGS6Ap at temperature 30°C. Details pellet detachments from protruding hyphal tips is in red arrow. Images (A) and (B) were taken at 4-fold magnification and bar = 100µm.

GASB cultivation at 30°C had a similar cultivation, had a similar growth form as 1st generation pellets (D1- D19) comparatively in Figure 4.11 and 4.12. GASB needed a longer period to adapt to the higher temperature since it originates from a more temperate region. Thus, at 30°C GASB appears as less viable. Biomass, EPS and ENS illustrated a trend of increasing gradual increment before reaching its peak for 1st generation growth. The amount of biomass (D19) was high during the liberation of 2nd generation pellets whereby significant changes in pellet morphology were observed such as fluffy pellets and highly branches hyphal form. These characteristics contributed to apparent viscosity, therefore, corresponding to attributes associated with an increase in mycelial biomass (Fazenda et al., 2010; Wagner et al., 2004; Yang et al., 1998). The quantity of biomass dropped (D21, D31) with significant clumps of mycelia mass forming large pellets as a way of protecting itself from detrimental shear effects, which caused the premature release of 2nd generation pellets, thus resulting in the increase of EPS on the same days. Pellet break-up verified by Wagner, et al., (2004), showed rapid EPS production similarly depicted at this temperature. Meanwhile, large pellet clump (D23) contributed to the increase in EPS.

The 2nd generation pellets released from 1st generation pellet (D17-D25) gave globular shaped hollow pellets and short protruding filaments. Changes in media colour and texture were observed throughout the GASB growth (D23-D35) at varying phases could be due to accumulation of stress by agitation or initial pH change. The cause of pH change is autolysis because of accumulation of toxic metabolites. As they pile-up the disrupt of the mycelium morphology might occur (Aminuddin et al., 2013; Jiang et al., 2014; Romero-Arenas et al., 2012). Other than that, depletion of nutrients could occur due to high temperature that leads to stress and plays a role in actively producing EPS (highest on D35) as a form of response by cells to protect itself from stress conditions, therefore, providing an environment where mycelia cells have to compete

for nutrients (Acharya, Krishnendu et al., 2005; Supramani et al., 2019; Xu et al., 2015; Yang et al., 1998).

During the 2nd generation, the size of pellets enlarged. They look fluffier but are less dense and hollow, probably because of the high rate of EPS production in comparison with biomass. EPS produces a gelatinous substance that causes media to become highly viscous and adhesion of mycelium to one another hence resulting in clumping to growing flask (Wagner et al., 2004). The gelatinous substance is strongly reactive with 95%, indicating the presence of polysaccharides.

Bioactive Compound	Temperature/Day(D)		
	20°C	25°C	30°C
Biomass (g/L)	3.2307 ± 0.04 (D25)	5.0354 ± 0.07 (D29)	4.6487 ± 0.03 (D25)
EPS (g/L)	1.4633 ± 0.02 (D35)	1.3237 ± 0.03 (D31)	0.9683 ± 0.06 (D21)
ENS (g/L)	0.1510 ± 0.03 (D31)	0.5120 ± 0.06 (D29)	0.4474 ± 0.02 (D29)

Table 4.2: Production of maximum yield of biomass, exopolysaccharide, endopolysaccharide by wild Serbian *G. applanatum* strain BGS6Ap when cultivated on different temperatures.

This study showed that cell metabolism and morphological parameters are in tight connection. Based on this data fermentation conditions and parameters can be optimized for the most efficient biomass, EPS and ENS production. The EPS production was the most efficient at the lowest tested temperature (20). Under this stressful environmental condition, the organism undergoes self-defense mode. To survive GASB mycelium produced gelatinous substance. Lower temperatures (20°C, 25°C) endured pellet break-up until 3rd generation growth but least favourable temperature (30°C) until 2nd generation growth as extra time required for environmental adjustment. According to Wagner et al., (2004), the liberation of 3rd generation pellets results in less synchrony and spread over a broader time interval due to the depletion of essential macro-micronutrients in the growing flask. Other than that, the pattern is disrupted due to depletion of nutrient, constant agitation, distribution of oxygen and change in initial pH (Supramani et al., 2019; Wagner et al., 2003; Wagner et al., 2004; Wan-Mohtar et al., 2016a). The production of biomass and ENS was most favored at 25, supported by fungal growth pattern.

In summary, it was concluded that temperature greatly affects the production of biomass, EPS and ENS, including GASB growth but also had an impact on fungal morphology. Time interval and morphology study was necessary before the optimization study using RSM to comprehend control of GASB growth and physiology in SLF.

4.4 Optimisation of growth parameters (initial pH, glucose concentration, agitation rate, temperature) using response surface methodology on day 10 and day 15 for wild-Serbian *G. applanatum* strain BGS6Ap.

RSM has been used to study the relationship between initial pH, glucose concentration, agitation rate and temperature on the biomass, EPS, and ENS production. The 30 experiments generated using central composite design (CCD) in Design Expert 7.0 software are shown in Table 4.3. The sampling point was taken at two different days (D10, D15) to compare and determine the best sampling day following the time interval study in figure 4.7 conducted on the production of the stated responses. Based on the findings of Supramani, et al., (2019) and Rahayu, et al., (2013) who studied *G. lucidum* and *L. squarrosulus* in connection with RSM, D10 has been chosen as the most optimal day for sampling. D15 was chosen as a sampling point based on the growth curve graph achieved in this study because based on the graph obtained the peak production could be observed between day 9 to day 15 to produce EPS, ENS and biomass.

After D15 the results, fluctuated. GA being a resilient fungus could grow more than 35 days without adding any nutrients to the media. CCD design (30 experiments) evaluated each coefficient for every single model using linear regression analysis to assess the significance of the model coefficient. Quadratic regression analysis using ANOVA was applied, and each significance of each coefficient was stated as *p*-value. The level of significance is vital to determine the strength of the interaction between each independent variable.

Table 4.3: Experimental design matrix using response surface methodology through central composite design with variables and responses for the biomass, exopolysaccharide and endopolysaccharide for day 10 of wild-Serbian *G. applanatum* strain BGS6Ap.

Run No.	Variables				Responses		
	Agitation (rpm)	Temperature (°C)	Initial pH	Glucose (g/L)	Biomass (g/L)	EPS (g/L)	ENS (g/L)
1	200	20	4	50	9.2600	1.5623	0.8600
2	100	30	4	50	6.3660	1.7683	0.9600
3	150	25	6	30	8.8073	0.7530	0.4793
4	200	20	4	10	4.5377	1.3113	0.6283
5	200	25	5	30	6.6600	1.6833	0.7823
6	100	30	4	10	6.0490	1.7747	1.0210
7	100	25	5	30	9.8670	1.9103	0.8100
8	200	20	6	50	13.2490	1.2433	1.1357
9	200	30	4	10	5.9500	0.8437	0.6700
10	200	20	6	10	5.9120	1.3280	0.8300
11	100	20	6	10	8.5913	1.0780	0.7840
12	150	25	5	30	6.2793	1.2023	0.6040
13	150	25	5	50	7.4410	1.8140	0.6700
14	200	30	4	50	2.4800	0.8793	0.8553
15	100	20	4	10	6.7293	3.2900	0.9100
16	150	25	5	30	6.2623	1.2660	0.6793
17	150	30	5	30	2.2540	1.5100	0.5140
18	100	20	4	50	15.8213	1.7000	0.9600
19	150	25	5	30	6.3727	1.2870	0.7057
20	200	30	6	10	4.7400	1.0147	0.8600
21	150	25	4	30	7.5100	1.7843	0.5373
22	100	30	6	10	4.8523	1.5887	0.9200
23	150	20	5	30	7.6500	1.6140	0.5297
24	100	30	6	50	8.0550	2.4140	0.5873
25	100	20	6	50	19.9377	1.3517	0.8600
26	150	25	5	30	6.4413	1.3147	0.7060
27	150	25	5	10	3.8300	1.1143	0.6180
28	150	25	5	30	6.1890	1.2907	0.6840
29	200	30	6	50	3.5800	1.6500	0.8100
30	150	25	5	30	6.3127	2.0843	0.6433

4.4.1 Optimisation of Mycelium Biomass at day 10.

The ANOVA for GASB biomass production is shown in Table 4.4. The predicted coefficient determination demonstrates that 99.95% ($R^2 = 0.9995$) of the variability in the response can be described using this model. The model is significant (p -value < 0.005). The adjusted coefficient determination value (Adj. $R^2 = 0.9990$) that implies the significance of the model was within the reasonable agreement with the predicted R^2 value. The regression model based on the actual factor of biomass can be expressed using Eq 1.

BIOMASS =

$$17.88034 - 0.2820 \times \text{Agitation} + 3.25765 \times \text{Temperature} - 14.49929 \times \text{pH} + 0.72953 \times \text{Glucose} + 2.38716\text{E-}003 \times \text{Agitation} \times \text{Temperature} - 1.52171\text{E-}003 \times \text{Agitation} \times \text{pH} - 1.03304\text{E-}003 \times \text{Agitation} \times \text{Glucose} - 0.13699 \times \text{Temperature} \times \text{pH} - 0.021005 \times \text{Temperature} \times \text{Glucose} + 0.031452 \times \text{pH} \times \text{Glucose} + 7.59227\text{E-}004 \times \text{Agitation}^2 - 0.056537 \times \text{Temperature} + 1.79322 \times \text{pH}^2 - 1.82483\text{E-}003 \times \text{Glucose}^2$$

Eq 1

Table 4.4: Analysis of variance for the experimental results of the central composite design quadratic model for biomass of wild-Serbian *G. applanatum* strain BGS6Ap at day 10.

Source	Sum of squares	DF	Mean Square	F value	Prob > F	
Model	390.21	14	27.87	2186.17	< 0.0001	significant
A-Agitation	49.67	1	49.67	3895.74	< 0.0001	
B-Temperature	124.62	1	124.62	9774.61	< 0.0001	
C-pH	9.42	1	9.42	738.83	< 0.0001	
D-Glucose	68.05	1	68.05	5337.44	< 0.0001	
AB	5.70	1	5.70	446.97	< 0.0001	
AC	0.09	1	0.09	7.26	0.0166*	
AD	17.07	1	17.07	1339.27	< 0.0001	
BC	7.51	1	7.51	588.79	< 0.0001	
BD	70.59	1	70.59	5537.02	< 0.0001	
CD	6.33	1	6.33	496.58	< 0.0001	
A ²	9.33	1	9.33	732.13	< 0.0001	
B ²	5.18	1	5.18	405.99	< 0.0001	
C ²	8.33	1	8.33	653.48	< 0.0001	
D ²	1.38	1	1.38	108.28	< 0.0001	
Residual	0.19	15	0.01			
Lack of Fit	0.15	10	0.02	1.95	0.2389	non-significant
Pure Error	0.04	5	0.01			
Cor Total	390.40	29				
Std. Dev.=0.112913097			R² =0.999510145			
Mean=7.266244444			Adjusted R² =0.999052948			

* Significant value

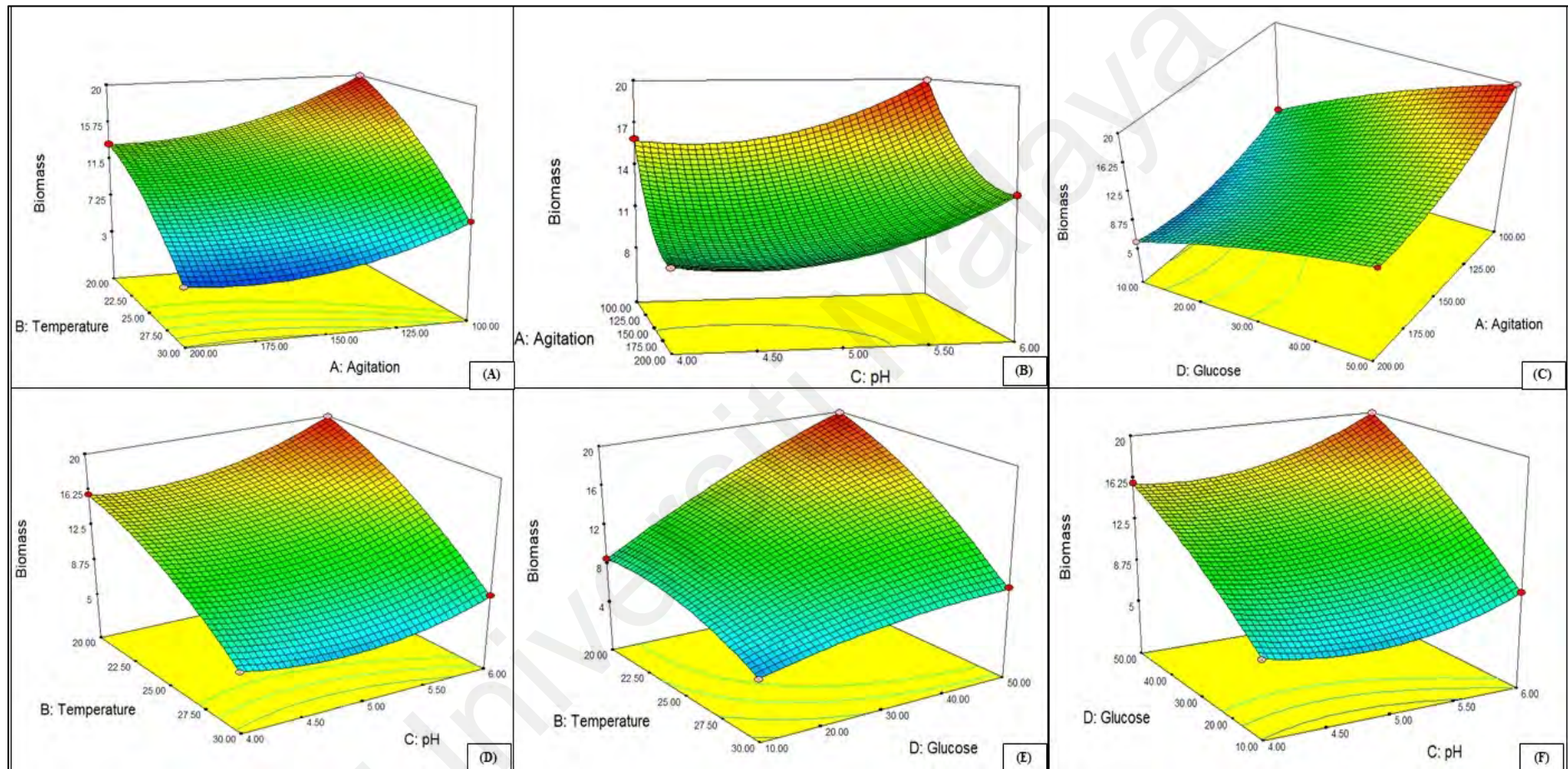


Figure 4.14: Response surface profile (3D plot) of biomass production from wild-Serbian *G. applanatum* strain BGS6Ap (D10) displaying the interaction between (A) temperature and agitation, (B) agitation and pH, (C) glucose and agitation, (D) temperature and pH, (E) temperature and glucose and (F) glucose and pH.

The model showed that agitation (A), temperature (B), initial pH (C) and glucose (D) exhibit a significantly strong effect ($p < 0.0001$) on the production of mycelial biomass. Quadratic terms (AB, AD, BC, BD, CD, AA, BB, CC, DD) exhibit a strong significant effect ($p < 0.0001$) towards the yield of biomass. However, the adverse impact, expressed by the quadratic term AC, of the combined effect of agitation and glucose because agitation affects the enzymatic hydrolysis of glucose by GASB (Kadic et al., 2014; Xu et al., 2008). Other than that, pellet fragmentation affected the size distribution hence glucose consumption also differs (Wagner et al., 2004). Three - dimensional plots (3D) (Figure 4.14) show the combined effect of all parameters (A, B, C, D) with only one combined parameter exhibiting negative impact (AC) within the experimental range. The remaining models show the optimum level of relationship corresponding to the yield of biomass. Figure 4.14 shows that the high glucose concentration which is the sole carbon source provider plays a vital role in the production of biomass followed by lower temperature that contributes to the high yield of biomass. Agitation at all rates shows high productivity of biomass and pH (alkaline) plays a less significant role in the production of biomass. The maximum mycelium biomass has been achieved at glucose concentration (50 g/L), temperature (20°C), 100 rpm, pH 5.99.

4.4.2 Optimisation of exopolysaccharide production at day 10

Table 4.5. represents the ANOVA data for GASB's EPS production. The predicted coefficient determination demonstrates that 70.74% ($R^2 = 0.7074$) of the variability in the response can be described using this model. The model is significant (p -value < 0.05). The adjusted coefficient determination value (Adj. $R^2 = 0.4344$) that implies the significance of the model was within the reasonable agreement with the predicted R^2 value. The regression model based on the actual factor of biomass can be expressed using Eq 2.

EPS =

$$\begin{aligned} &12.89448 - 0.054152 \times \text{Agitation} - 0.41288 \times \text{Temperature} + 0.022425 \times \text{pH} - 0.092169 \\ &\times \text{Glucose} - 2.95817\text{E} - 004 \times \text{Agitation} \times \text{Temperature} + 3.42500\text{E} -003 \times \text{Agitation} \times \\ &\text{pH} + 8.34125\text{E} - 005 \times \text{Agitation} \times \text{Glucose} + 0.053301 \times \text{Temperature} \times \text{pH} + \\ &1.65000\text{E} - 003 \times \text{Temperature} \times \text{Glucose} + 9.24771\text{E} - 003 \times \text{pH} \times \text{Glucose} + \\ &1.19882\text{E} - 004 \times \text{Agitation}^2 + 2.59490\text{E} -0 03 \times \text{Temperature}^2 - 0.22846 \times \text{pH}^2 - \\ &8.24020\text{E} - 005 \times \text{Glucose}^2 \end{aligned} \text{ Eq 2}$$

Table 4.5: Analysis of variance for the experimental results of the central composite design quadratic model for exopolysaccharide production from wild-Serbian *G. applanatum* strain BGS6Ap at day 10.

Source	Sum of squares	DF	Mean Square	F value	Prob > F	
Model	5.1980	14	0.3713	2.5911	0.0388	significant
A-Agitation	1.5959	1	1.5959	11.1373	0.0045*	
B-Temperature	0.0595	1	0.0595	0.4155	0.5289	
C-pH	0.3452	1	0.3452	2.4090	0.1415	
D-Glucose	0.0600	1	0.0600	0.4190	0.5272	
AB	0.0875	1	0.0875	0.6107	0.4467	
AC	0.4692	1	0.4692	3.2746	0.0904	
AD	0.1113	1	0.1113	0.7769	0.3920	
BC	1.1364	1	1.1364	7.9305	0.0130*	
BD	0.4356	1	0.4356	3.0399	0.1017	
CD	0.5473	1	0.5473	3.8196	0.0696	
A ²	0.2327	1	0.2327	1.6241	0.2219	
B ²	0.0109	1	0.0109	0.0761	0.7864	
C ²	0.1352	1	0.1352	0.9437	0.3467	
D ²	0.0028	1	0.0028	0.0196	0.8904	
Residual	2.1494	15	0.1433			
Lack of Fit	1.5924	10	0.1592	1.4295	0.3637	not significant
Pure Error	0.5570	5	0.1114			
Cor Total	7.3474	29				
Std. Dev.=	0.3785	R² =		0.7074		
Mean=	1.5142	Adjusted R² =		0.4344		

* Significant value

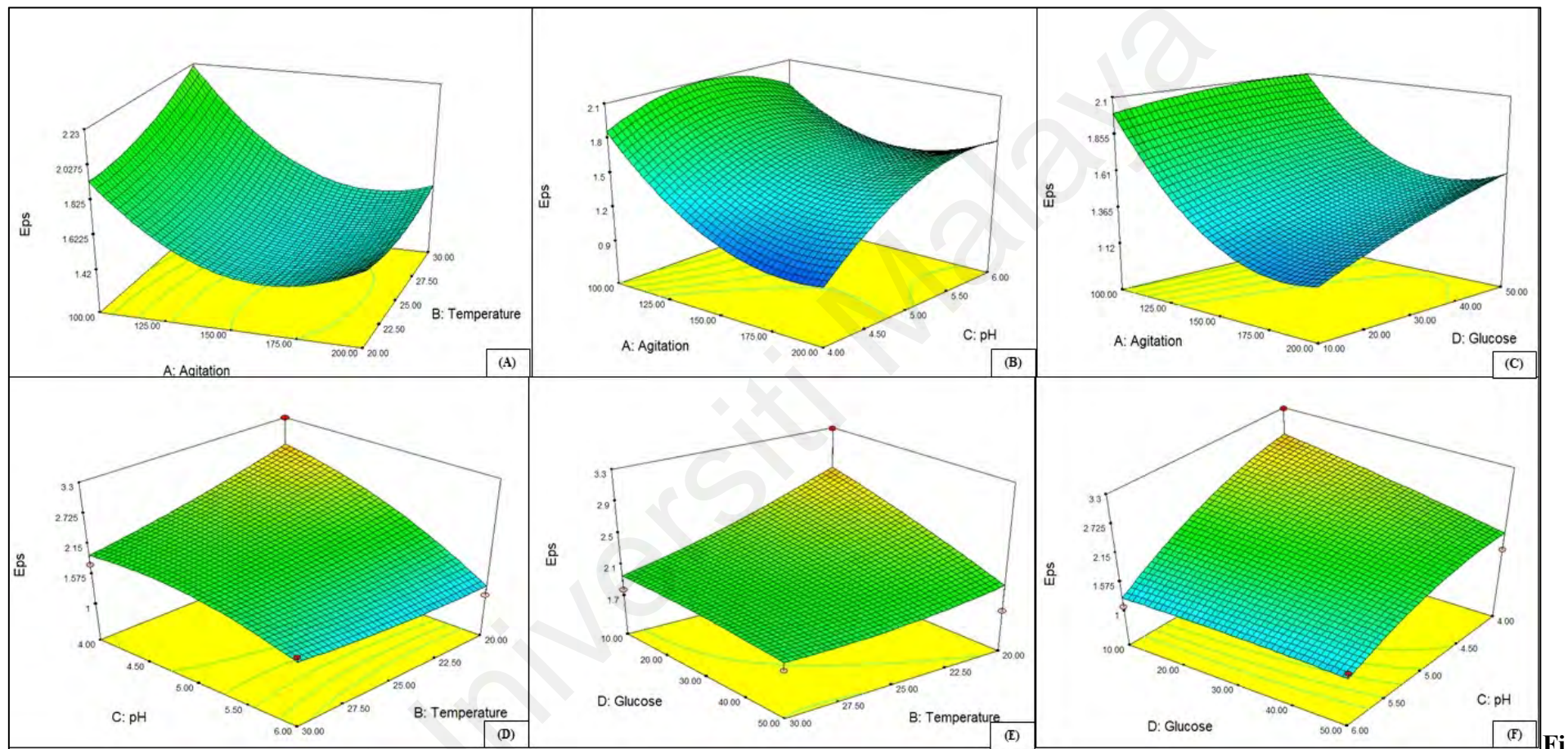


Figure 4.15: Response surface profile (3D plot) of exopolysaccharide production of wild-Serbian *G. applanatum* strain BGS6Ap (D10) displaying the interaction between (A) temperature and agitation, (B) agitation and pH, (C) glucose and agitation, (D) temperature and pH, (E) temperature and glucose and (F) glucose and pH.

The model represented in Table 4.5. showed that agitation (A) and quadratic terms (BC) show a significant effect ($p < 0.05$) towards the yield of EPS. However, adverse effects were shown (B, C, D) and remaining quadratic terms (AB, AC, AD, BD, B^2 , C^2 , D^2). Figure 4.15 shows the merged effect of agitation (A), temperature (B), initial pH (C) and glucose (D) in response surface profiles, also known as three-dimensional (3D) plots. Figure 4.15 shows that agitation plays a vital role in distributing nutrient and carbon source in the media hence 100 rpm being the best agitation rate as it distributes moderately without causing much shear effect.

Other than that, as observed in the model's quadratic terms (BC, CD), a lower pH seems to be more appropriate to produce EPS. Besides, the combined effect of temperature and pH (BC) is attributed to the yield of EPS, also proving that GASB grows well at lower temperature. Low glucose concentration was required to yield high EPS productivity. The maximum quantity of mycelium biomass was achieved at glucose concentration (10 g/L), temperature (20°C), 100 rpm, pH 4.00.

4.4.3 Optimisation of endopolysaccharide production at day 10

The ANOVA data for GASB ENS production are shown in Table 4.6. The predicted coefficient determination demonstrates that 89.89% ($R^2 = 0.8989$) of the variability in the response can be described using this model. The model is significant (p -value < 0.05). The adjusted coefficient determination value (Adj. $R^2 = 0.8045$) that implies the significance of the model was within the reasonable agreement with the predicted R^2 value. The regression model based on the actual factor of biomass expressed using Eq 3.

ENS =

$$\begin{aligned} &0.59963 - 0.037356 \times \text{Agitation} + 0.13481 \times \text{Temperature} + 0.47859 \times \text{pH} + 5.81066\text{E} - \\ &004 \times \text{Glucose} - 5.82500\text{E} - 005 \times \text{Agitation} \times \text{Temperature} + 1.65217\text{E} - 003 \times \\ &\text{Agitation} \times \text{pH} + 5.87750\text{E} - 005 \times \text{Agitation} \times \text{Glucose} - 7.25500\text{E} - 003 \times \text{Temperature} \\ &\times \text{pH} - 5.76083\text{E} - 004 \times \text{Temperature} \times \text{Glucose} - 1.27188\text{E} - 003 \times \text{pH} \times \text{Glucose} + \\ &9.45501\text{E} - 005 \times \text{Agitation}^2 - 1.51699\text{E} - 003 \times \text{Temperature}^2 - 0.051442 \times \text{pH}^2 + \\ &2.10563\text{E} - 004 \times \text{Glucose}^2 \end{aligned} \text{Eq 3}$$

Table 4.6: Analysis of variance for the experimental results of the central composite design quadratic model for endopolysaccharide production by wild-Serbian *G. applanatum* strain BGS6Ap at day 10.

Source	Sum of squares	DF	Mean Square	F value	Prob > F	
Model	0.69	14	0.05	9.525	< 0.0001	significant
A-Agitation	0.01	1	0.01	1.556	0.2314	
B-Temperature	0.01	1	0.01	0.966	0.3412	
C-pH	0.00	1	0.00	0.197	0.6632	
D-Glucose	0.01	1	0.01	2.242	0.1550	
AB	0.00	1	0.00	0.656	0.4308	
AC	0.11	1	0.11	21.096	0.0004*	
AD	0.06	1	0.06	10.679	0.0052*	
BC	0.02	1	0.02	4.068	0.0620	
BD	0.05	1	0.05	10.259	0.0059*	
CD	0.01	1	0.01	2.000	0.1777	
A ²	0.14	1	0.14	27.969	< 0.0001	
B ²	0.00	1	0.00	0.720	0.4095	
C ²	0.01	1	0.01	1.325	0.2678	
D ²	0.02	1	0.02	3.551	0.0790	
Residual	0.08	15	0.01			
Lack of Fit	0.07	10	0.01	4.403	0.0578	not significant
Pure Error	0.01	5	0.00			
Cor Total	0.77	29				
Std. Dev.=	0.0719	R² =	0.8989			
Mean=	0.7538	Adjusted R² =	0.8045			

* Significant value

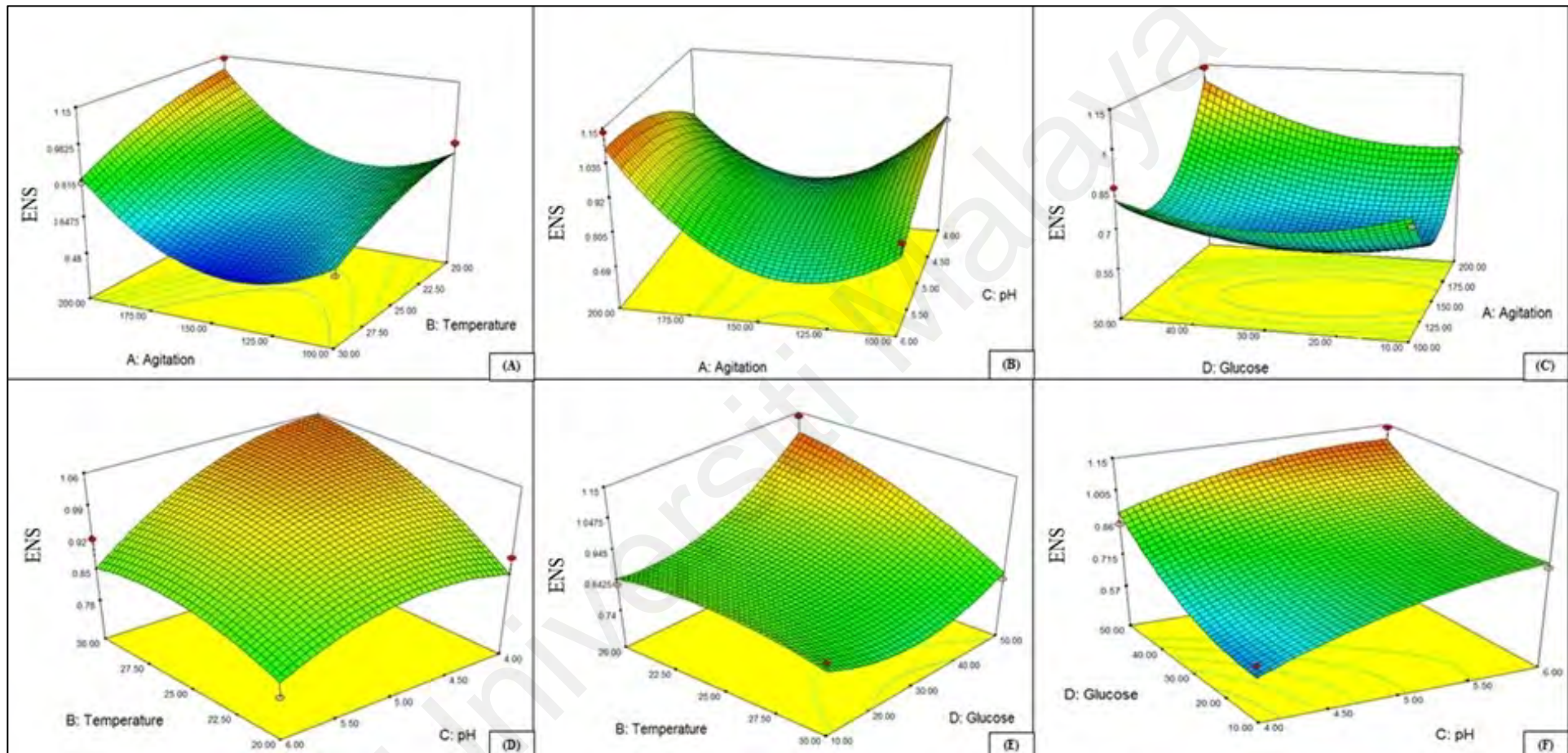


Figure 4.16: Response surface profile (3D plot) of endopolysaccharide production from GASB (D10) displaying the interaction between (A) temperature and agitation, (B) agitation and pH, (C) glucose and agitation, (D) temperature and pH, (E) temperature and glucose and (F) glucose and pH.

The model (Table 4.6) showed that agitation (A), temperature (B), initial pH (C) and glucose (D) express a significantly negative effect individually against ENS production while the impact in combined quadratic terms was significant (A^2 , AC AD, BD) $p < 0.005$. The remaining quadratic terms (AB, BC, CD, B^2 , C^2 , D^2) exhibit negative effects on ENS production. Figure 4.16 shows the merged effect of agitation (A), temperature (B), initial pH (C) and glucose (D) in response surface profiles, also known as 3D plots. Figure 4.15 shows that agitation plays a critical role whereby agitation at all rates affected high ENS production. Glucose plays a crucial role in yielding ENS with the combined effect of agitation and temperature. All the models demonstrate that lower distribution of temperatures harvests higher ENS output. Increasing pH value indicates better efficiency of ENS production. The maximum mycelium biomass was achieved at glucose concentration (50 g/L), temperature (20°C), 200 rpm, pH 5.96.

4.4.4 Validation of the optimised media composition day 10

Table 4.7 illustrates the optimized media compositions produced to validate the biomass, EPS and ENS production statistical model. The validation experiments were conducted using 250 mL shake flasks under controlled conditions. The predictive ability of the model was verified using Eqs 1,2 and 3. The biomass production under optimized condition was 19.93 g L⁻¹, EPS production was 2.78 g L⁻¹ and ENS 1.09 g L⁻¹ under optimized condition. The validation results demonstrated that the model is valid for biomass, EPS and ENS production by GASB.

Table 4.7: Validation of the model with the optimised media composition in 250 mL shake flasks at day 10

Run	Variables				Response		
	Temperature (°C)	pH	Glucose (g/L)	Agitation (rpm)	Biomass (g/L)	EPS (g/L)	ENS (g/L)
Biomass	20	5.99	50	100	19.93	-	-
EPS	20	4.04	10	100	-	2.78	-
ENS	20	5.87	49.99	200	-	-	0.91
Biomass + EPS	20	4.04	42.45	100	14.51	2.12	-
Biomass + ENS	20	4.04	49.99	100	15.69	-	0.97
EPS + ENS	22.72	4.08	10	100	-	2.50	0.96
Biomass + EPS + ENS	20	4.04	50	100	15.74	2.04	0.97

Table 4.8: Experimental design matrix using response surface methodology through central composite design with variables and responses for the biomass, exopolysaccharide and endopolysaccharide for day 15 of wild-Serbian *G. applanatum* strain BGS6Ap.

Run No.	Variables				Responses		
	Agitation (rpm)	Temperature (°C)	Initial pH	Glucose (g/L)	Biomass (g/L)	EPS (g/L)	ENS (g/L)
1	200	25	5	30	6.7697	1.4393	0.3140
2	100	30	4	10	5.7753	1.8450	1.2300
3	150	25	5	30	14.1513	2.5800	1.0827
4	100	20	6	50	5.0350	1.5167	0.6550
5	100	20	4	50	8.0267	1.8090	0.9700
6	100	30	4	50	5.2870	1.5123	1.2253
7	200	30	6	50	5.1107	0.6597	0.2400
8	150	25	5	50	8.6817	2.4230	3.8200
9	100	30	6	10	5.0820	1.4573	1.6593
10	100	20	4	10	3.4433	2.6460	0.7400
11	200	20	6	10	14.5190	1.1747	1.6383
12	200	20	4	10	3.5450	2.0285	0.9373
13	150	25	5	30	19.6290	2.5607	1.2300
14	150	30	5	30	3.4153	0.7283	0.3440
15	200	30	6	10	8.8507	1.2607	1.4700

16	150	25	6	30	11.5500	2.8797	0.3600
17	200	20	4	50	5.3700	1.6460	0.5077
18	150	25	5	30	18.1510	1.7523	1.1063
19	150	20	5	30	8.8507	2.1373	0.1900
20	150	25	5	10	11.5300	1.3573	4.4100
21	200	20	6	50	4.3733	2.2743	0.4423
22	150	25	5	30	15.6953	2.8713	1.0377
23	100	25	5	30	7.4003	1.2697	0.4900
24	150	25	5	30	15.6847	3.0407	1.1513
25	100	30	6	50	3.9647	0.9833	0.6800
26	150	25	4	30	8.0897	2.8300	0.1600
27	200	30	4	50	4.5073	1.3660	0.3800
28	150	25	5	30	15.5867	2.8820	1.1407
29	200	30	4	10	4.5860	1.7243	0.9890
30	100	20	6	10	13.4610	1.1887	1.1543

4.4.5 Optimisation of mycelia biomass growth production at day 15

The ANOVA for GASB biomass production are shown in Table 4.9. The predicted coefficient determination demonstrates that 71.07% ($R^2 = 0.7107$) of the variability in the response can be described using this model. The model is significant (p -value < 0.05). The adjusted coefficient determination value (Adj. $R^2 = 0.4406$) that implies the significance of the model is within the reasonable agreement with the predicted R^2 value. The regression model based on the actual factor of biomass can be expressed using Eq 4.

BIOMASS =

$$\begin{aligned} & -141.93060 + 0.28538 \times \text{Agitation} + 8.34843 \times \text{Temperature} + 9.77150 \times \text{pH} + 0.36243 \\ & \times \text{Glucose} + 1.27609\text{E} - 003 \times \text{Agitation} \times \text{Temperature} + 0.012294 \times \text{Agitation} \times \text{pH} - \\ & 4.18190\text{E} - 004 \times \text{Agitation} \times \text{Glucose} - 0.17689 \times \text{Temperature} \times \text{pH} + 4.21190\text{E} - 003 \\ & \times \text{Temperature} \times \text{Glucose} - 0.091470 \times \text{pH} \times \text{Glucose} - 1.22010\text{E} - 003 \times \text{Agitation}^2 - \\ & 0.16009 \times \text{Temperature}^2 - 0.31540 \times \text{pH} - 7.35292\text{E} - 005 \times \text{Glucose}^2 \end{aligned}$$

Eq 4

Table 4.9: Analysis of variance for the experimental results of the central composite design quadratic model for biomass production by wild-Serbian *G. applanatum* strain BGS6Ap at day 15.

Source	Sum of squares	DF	Mean Square	F value	Prob > F	
Model	490.49	14	35.03	2.6317	0.0365	significant
A-Agitation	0.00	1	0.00	0.0001	0.9921	
B-Temperature	22.32	1	22.32	1.6768	0.2149	
C-pH	30.20	1	30.20	2.2687	0.1528	
D-Glucose	23.20	1	23.20	1.7428	0.2066	
AB	1.63	1	1.63	0.1223	0.7314	
AC	6.05	1	6.05	0.4541	0.5106	
AD	2.80	1	2.80	0.2102	0.6532	
BC	12.52	1	12.52	0.9401	0.3476	
BD	2.84	1	2.84	0.2132	0.6509	
CD	53.55	1	53.55	4.0223	0.0633	
A ²	24.11	1	24.11	1.8108	0.1984	
B ²	41.50	1	41.50	3.1174	0.0978	
C ²	0.26	1	0.26	0.0194	0.8912	
D ²	0.00	1	0.00	0.0002	0.9898	
Residual	199.69	15	13.31			
Lack of Fit	179.51	10	17.95	4.4483	0.0566	not significant
Pure Error	20.18	5	4.04			
Cor Total	690.18	29				
Std. Dev.=	3.6486	R² =	0.7107			
Mean=	8.8707	Adjusted R² =	0.4406			

*Significant

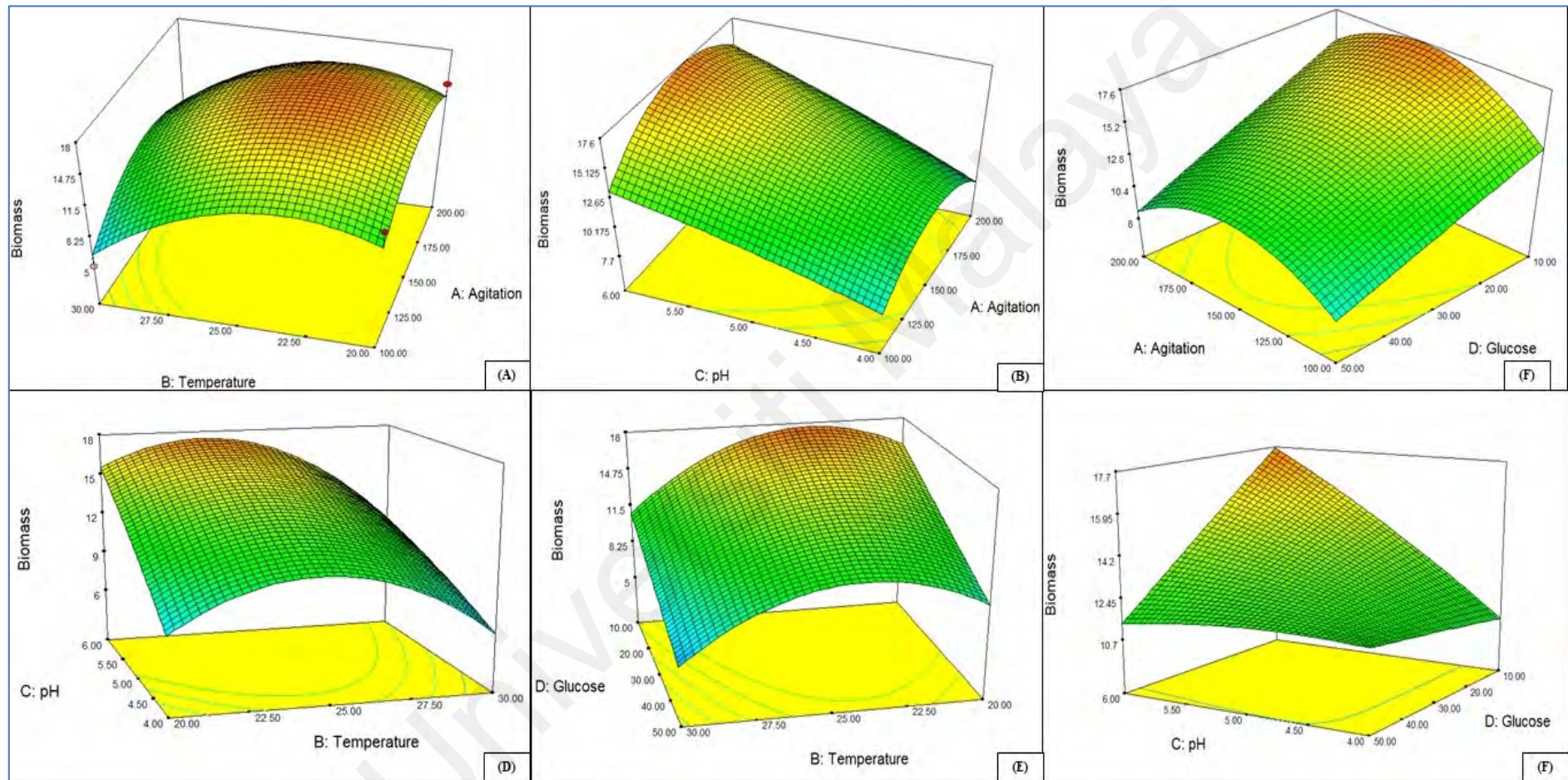


Figure 4.17: Response surface profile (3D plot) of biomass production from wild-Serbian *G. applanatum* strain BGS6Ap (D15) displaying the interaction between (A) temperature and agitation, (B) agitation and pH, (C) glucose and agitation, (D) temperature and pH, (E) temperature and glucose and (F) glucose and pH.

The model (Table 4.9), agitation (A), temperature (B), initial pH (C) and glucose (D) exhibited negative effect on the production of biomass on D15 followed by the quadratic terms (AB, AC, AD, BC, BD, CD, A², B², C², D²) However, the three - dimensional plots (3D) (Figure 4.17) showed that the combined effect of quadratic terms (CD, B²) has some positive effect towards the yield of biomass. Therefore, during the later stages of mycelia growth when nutrients depleted (pH and glucose) are essential for the continued existence of GASB. The model shows a significant change in biomass growth if the temperature drops below 25 °C. At this stage of mycelia growth, higher rpm was required to yield better biomass output. The maximum biomass was achieved at glucose concentration (10 g/L), temperature (23.52°C), 157.64 rpm, pH 6.

4.4.6 Optimisation of exopolysaccharide production at day 15

The ANOVA for GASB EPS production are shown in Table 4.9. The predicted coefficient determination demonstrates that 69.41% ($R^2 = 0.6941$) of the variability in the response can be described using this model. The model is significant (p -value < 0.05). The adjusted coefficient determination value (Adj. $R^2 = 0.4087$) that implies the significance of the model was within the reasonable agreement with the predicted R^2 value. The regression model based on the actual factor of exopolysaccharide can be expressed using Eq 5.

EPS =

$$\begin{aligned} &+ 1.53323 + 0.081900 \times \text{Agitation} + 1.32606 \times \text{Temperature} - 8.31748 \times \text{pH} + 0.013569 \\ &\times \text{Glucose} - 1.87625\text{E} - 004 \times \text{Agitation} \times \text{Temperature} + 1.58854\text{E} - 003 \times \text{Agitation} \times \\ &\text{pH} + 6.70938\text{E} - 005 \times \text{Agitation} \times \text{Glucose} - 1.39375\text{E} - 003 \times \text{Temperature} \times \text{pH} - \\ &1.23385\text{E} - 003 \times \text{Temperature} \times \text{Glucose} + 7.07240\text{E} - 003 \times \text{pH} \times \text{Glucose} - \\ &2.92974\text{E} - 004 \times \text{Agitation}^2 - 0.026164 \times \text{Temperature}^2 + 0.76790 \times \text{pH}^2 - 4.91923\text{E} - \\ &004 \times \text{Glucose}^2 \end{aligned} \quad \text{Eq 5}$$

Table 4.10: Analysis of variance for the experimental results of the central composite design quadratic model for EPS production by wild-Serbian *G. applanatum* strain BGS6Ap at day 15.

Source	Sum of squares	DF	Mean Square	F value	Prob > F	
Model	9.67	14	0.69	2.4316	0.0494	significant
A-Agitation	0.02	1	0.02	0.0838	0.7762	
B-Temperature	1.33	1	1.33	4.6645	0.0474*	
C-pH	0.89	1	0.89	3.1476	0.0963	
D-Glucose	0.01	1	0.01	0.0474	0.8306	
AB	0.04	1	0.04	0.1239	0.7297	
AC	0.10	1	0.10	0.3553	0.5600	
AD	0.07	1	0.07	0.2535	0.6219	
BC	0.00	1	0.00	0.0027	0.9590	
BD	0.24	1	0.24	0.8573	0.3691	
CD	0.32	1	0.32	1.1267	0.3053	
A ²	1.39	1	1.39	4.8920	0.0429*	
B ²	1.11	1	1.11	3.9016	0.0669	
C ²	1.53	1	1.53	5.3772	0.0349*	
D ²	0.10	1	0.10	0.3531	0.5612	
Residual	4.26	15	0.28			
Lack of Fit	3.20	10	0.32	1.4979	0.3431	not significant
Pure Error	1.07	5	0.21			
Cor Total	13.93	29				
Std. Dev.=	0.5330	R² =	0.6941			
Mean=	1.8615	Adjusted R² =	0.4087			

* Significant value

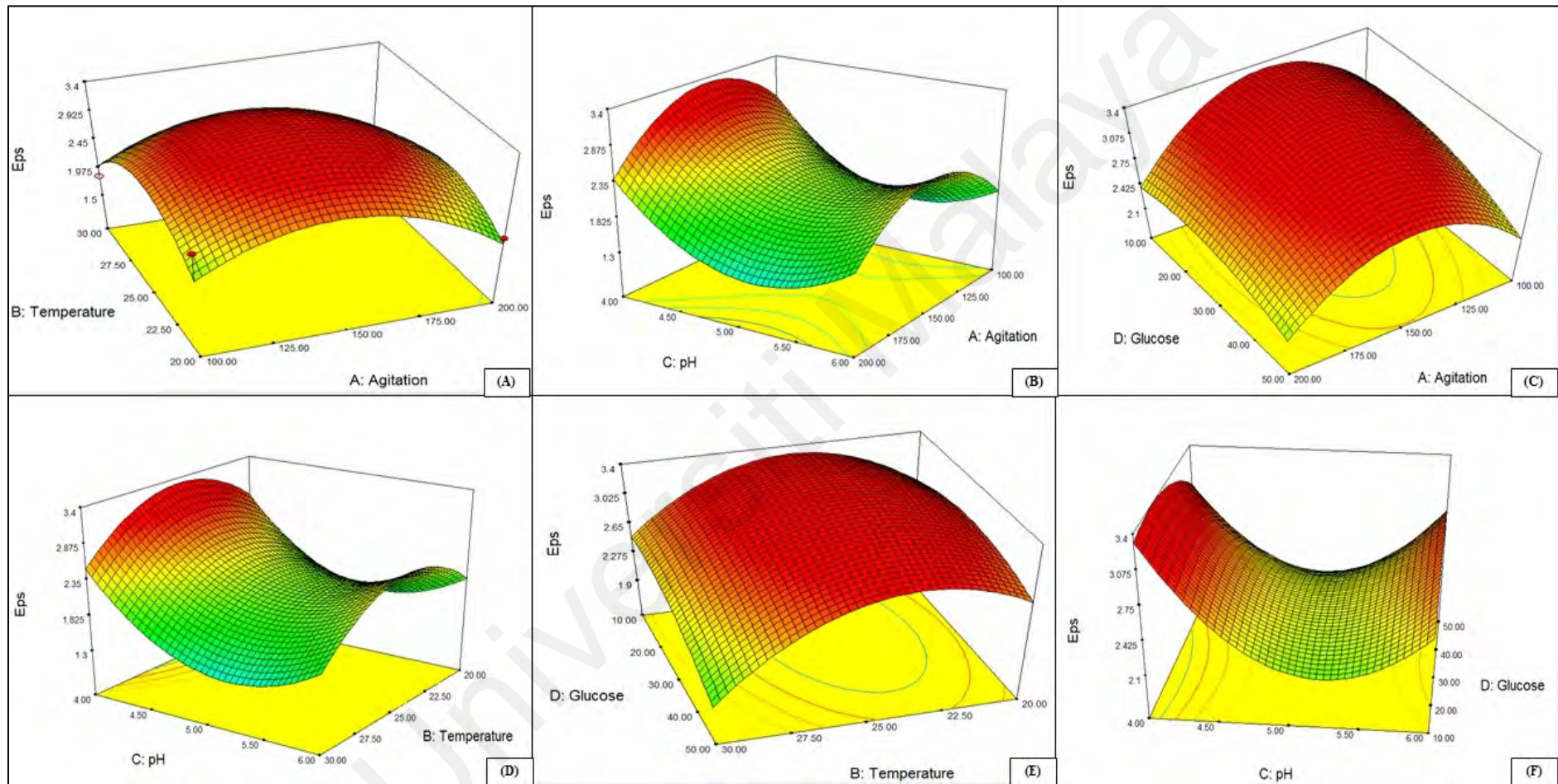


Figure 4.18: Response surface profile (3D plot) of exopolysaccharide production by wild-Serbian *G. applanatum* strain BGS6Ap (D15) displaying the interaction between (A) temperature and agitation, (B) agitation and pH, (C) glucose and agitation, (D) temperature and pH, (E) temperature and glucose and (F) glucose and pH.

The model (Table 4.10), shows that temperature (B), initial pH (C) followed by quadratic terms (A^2 , B^2 , C^2) have a positive effect on the production of EPS on D15 while (A, D, AB, AC, AD, BC, BD, CD, D^2) negatively impacted EPS production. Three - dimensional plots (3D) (Figure 4.18) show that slightly higher temperature, acidic pH value, optimum glucose concentration and higher agitation produced the most EPS comparison with D10. Hence prove that EPS is produced at high concentration when mycelium is placed under a stressful condition with higher rpm that contributes to shear stress followed by higher temperature that is not beneficial. The maximum EPS has been achieved at glucose concentration (29.30g/L), temperature (24.28°C), 135.95 rpm, pH 4.

4.4.7 Optimisation of endopolysaccharide production at day 15

The ANOVA for GASB ENS production are shown in Table 4.9. The predicted coefficient determination demonstrates that 99.17% ($R^2 = 0.9917$) of the variability in the response can be described using this model. The model is significant (p -value < 0.05). The adjusted coefficient determination value (Adj. $R^2 = 0.9840$) that implies the significance of the model was within the reasonable agreement with the predicted R^2 value. The regression model based on the actual factor of ENS can be expressed using Eq 6.

ENS =

$$\begin{aligned} & -58.11283 + 0.11817 \times \text{Agitation} + 2.25422 \times \text{Temperature} + 11.04462 \times \text{pH} - 0.34870 \\ & \times \text{Glucose} - 4.30517\text{E} - 004 \times \text{Agitation} \times \text{Temperature} + 1.24167\text{E} - 003 \times \text{Agitation} \times \\ & \text{pH} - 1.38208\text{E} - 004 \times \text{Agitation} \times \text{Glucose} - 6.37417\text{E} - 003 \times \text{Temperature} \times \text{pH} - \\ & 5.80042\text{E} - 004 \times \text{Temperature} \times \text{Glucose} - 9.66042\text{E} - 003 \times \text{pH} \times \text{Glucose} - 3.71890\text{E} \\ & - 004 \times \text{Agitation}^2 - 0.042589 \times \text{Temperature}^2 - 1.07173 \times \text{pH}^2 + 6.95818\text{E} - 003 \times \\ & \text{Glucose}^2 \end{aligned} \quad \text{Eq 6}$$

Table 4.11: Analysis of variance for the experimental results of the central composite design quadratic model for endopolysaccharide production by wild-Serbian *G. applanatum* strain BGS6Ap at day 15

Source	Sum of squares	DF	Mean Square	F value	Prob > F	
Model	25.31	14	1.81	128.279	< 0.0001	significant
A-Agitation	0.20	1	0.20	14.009	0.0020*	
B-Temperature	0.05	1	0.05	3.806	0.0700	
C-pH	0.07	1	0.07	5.303	0.0360*	
D-Glucose	1.57	1	1.57	111.047	< 0.0001	
AB	0.19	1	0.19	13.149	0.0025*	
AC	0.06	1	0.06	4.375	0.0539*	
AD	0.31	1	0.31	21.683	0.0003*	
BC	0.02	1	0.02	1.153	0.2999	
BD	0.05	1	0.05	3.819	0.0696	
CD	0.60	1	0.60	42.374	< 0.0001	
A ²	2.24	1	2.24	158.888	< 0.0001	
B ²	2.94	1	2.94	208.380	< 0.0001	
C ²	2.98	1	2.98	211.129	< 0.0001	
D ²	20.07	1	20.07	1423.941	< 0.0001	
Residual	0.21	15	0.01			
Lack of Fit	0.19	10	0.02	4.366	0.0587	not significant
Pure Error	0.02	5	0.00			
Cor Total	25.53	29				
Std. Dev.=	0.1187	R² =	0.9917			
Mean=	1.0585	Adjusted R² =	0.9840			

* Significant value

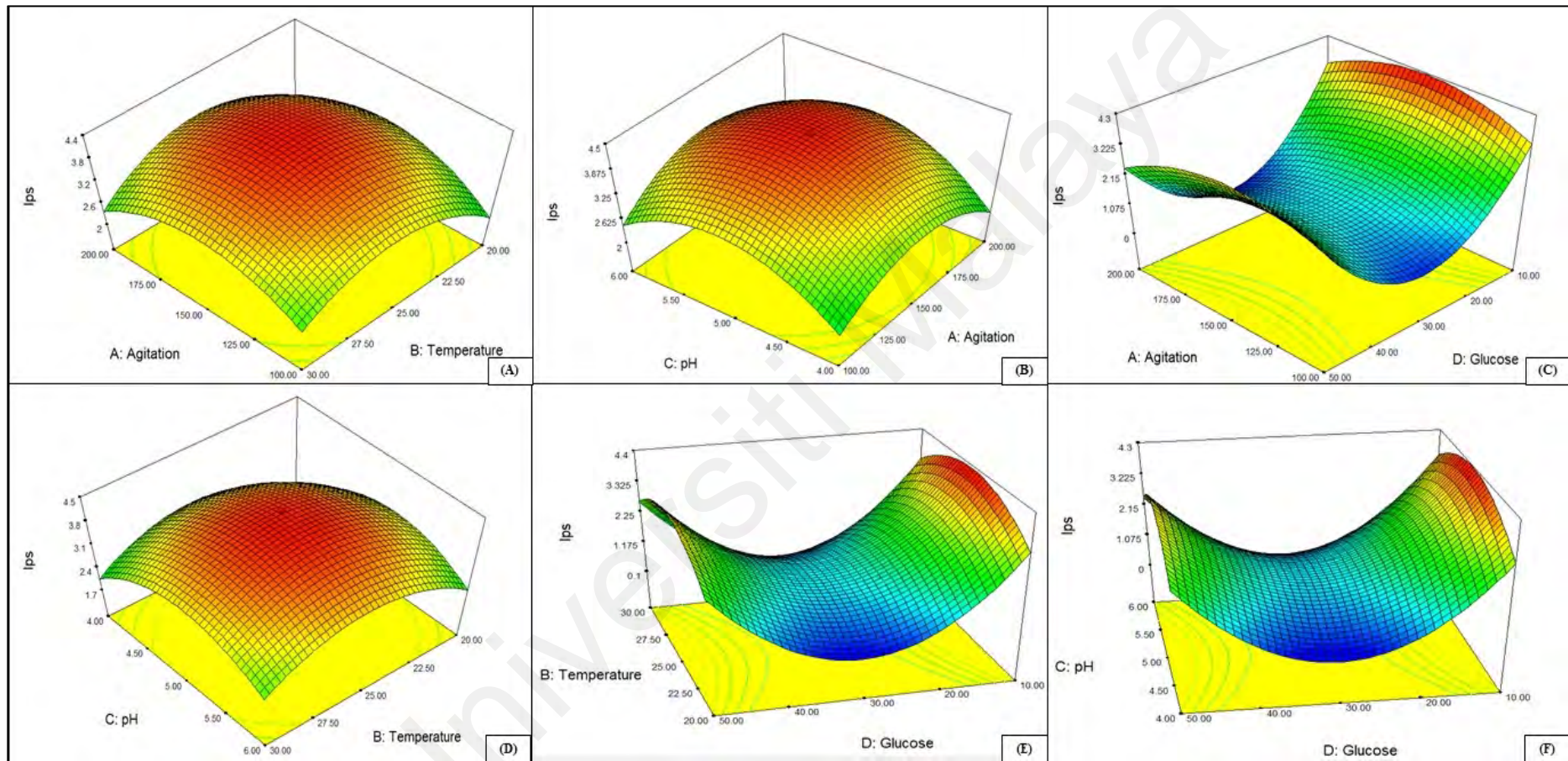


Figure 4.19: Response surface profile (3D plot) of endopolysaccharide production by wild-Serbian *G. applanatum* strain BGS6Ap (D15) displaying the interaction between (A) temperature and agitation, (B) agitation and pH, (C) glucose and agitation, (D) temperature and pH, (E) temperature and glucose and (F) glucose and pH.

The model (Table 4.11), glucose (D) followed by the quadratic terms (AD, CD, A², B², C², D²) showed a significantly strong effect ($p < 0.0001$) on the production of ENS. A (agitation), C (pH) and quadratic terms (AB, AC) showed a significant effect at $p < 0.05$ on the yield of ENS. However, the negative impacts were expressed by temperature (B) and glucose (D) in addition to quadratic terms (BC, BD). However, the three-dimensional plots (3D) (Figure 4.19) showed that the more combined quadratic terms has some positive effect on ENS production. The maximum mycelium biomass was achieved at glucose concentration (10 g/L), temperature (25.25°C), 150.99rpm, pH 5.12. The model shows a significant impact of biomass growth as the temperature increases approximately 25°C. At this stage of mycelia growth, higher rpm is required to yield better ENS output.

4.4.8 Validation of the optimised media composition (day 15)

Table 4.12 illustrates the optimised media compositions produced to validate the biomass, EPS and ENS production statistical model. The validation experiments conducted using 250 mL shake flasks under controlled conditions. The predictive ability of the model was verified using Eqs 4,5 and 6. The biomass production under optimised conditions was 17.66 g L⁻¹, EPS production was 3.33 g L⁻¹ and ENS 4.33 g L⁻¹ under optimised condition. The validation results demonstrated that the model is valid for biomass, EPS and ENS production of GASB.

Table 4.12: Validation of the model with the optimised media composition in 250 mL shake flasks at day 15

Run	Variables				Response		
	Temperature (°C)	pH	Glucose (g/L)	Agitation (rpm)	Biomass (g/L)	EPS (g/L)	ENS (g/L)
Biomass	23.52	6	10	157.64	17.66	-	-
EPS	24.28	4.01	29.3	135.95	-	3.33	-
ENS	25.25	5.12	10	150.99	-	-	4.33
Biomass + EPS	23.95	6	14.2	152.78	16.96	2.69	-
Biomass + ENS	24.43	5.55	10	154	16.24	-	4.10
EPS + ENS	24.97	4.16	10	146.79	-	3.04	3.33
Biomass + EPS + ENS	24.38	6	10	152.96	17.51	2.59	3.47

4.4.9 Comparison with other literature

Table 4.13: Comparison of *Ganoderma sp.* statistical optimisation using submerged-liquid fermentation with the literature.

Physical form	Species	Origin	Optimization approach	Mode	Initial pH	Glucose concentration (g/L)	Temperature (°C)	Agitation (rpm)	Biomass (g/L)	EPS (g/L)	ENS (g/L)	Reference
	<i>Ganoderma applanatum</i> strain BGS6Ap	Serbia	Response Surface Methodology	Shake Flask	6	10	24	150	17.51	2.59	3.47	This study
	<i>Ganoderma lucidum</i> strain BGF4A1	Serbia	Response Surface Methodology	Shake Flask	5.26	50	30	-	3.12	1.96	-	(Hassan et al., 2019)
	<i>Ganoderma lucidum</i> strain QRS 5120	Malaysia	Response Surface Methodology	Shake Flask	4	26.5	-	100	5.19	2.64	1.52	(Supramani et al., 2019)
-	<i>Ganoderma lucidum</i>	Taiwan	Taguchi Orthogonal Array	Shake Flask	6.5	12.1	34	160	18.70	0.42	-	(Chang et al., 2006)
-	<i>Ganoderma lucidum</i> strain CAU 5501	China	Orthogonal Matrix	Shake Flask	-	50	30	150	7.24	1.72	-	(Yuan et al., 2012)

(-) = not available. EPS = Exopolysaccharide, ENS= Intracellular polysaccharide

The comparison of optimization methods for biomass, EPS and ENS production of *Ganoderma sp.* in various literature shown in Table 4.12 and three studies including this study utilized RSM as tool for optimization. The initial studies applied Taguchi's orthogonal array and orthogonal matrix however, all previous studies only showed optimisation of *G. lucidum* with different strains. None of these studies examined the optimization of *G. applanatum* mycelium production. The maximum biomass obtained by GASB was relatively high in comparison to other *Ganoderma sp.* based on similar temperate regions like China. Serbia and China are both four-season weather (temperate climate) countries exhibiting a similar amount of biomass production (Chang et al., 2006; Rašeta, M. et al., 2016; Stojković et al., 2014). Hence proving that temperature plays a significant role in biomass production with the implemented technique of Taguchi's orthogonal array. Chang et al., (2006) stated that Taguchi's method implicated the identification of appropriate control variables obtained optimum result and used an orthogonal matrix that generates a set of experiments. The adverse impact of this technique requires prior knowledge before experimenting and it is a two-factor interaction system (Stone et al., 1994). Orthogonal matrix, is a method used to optimise media conditions by a set of experimental values and responses obtained from multiple OFAAT studies to find suitable range (Yuan et al., 2012). Yuan et al., (2012) and Chang et al., (2006) stated that biomass and polysaccharide production remarkably improved by cultivation of mycelium in optimal media with subsequent optimal operating conditions. *G. lucidum* strain BGF4A1 followed the optimal temperature condition of 30°C despite originating from Europe showed that species and strain play a role depending on the effects of its respective variables. The optimized key factors stated in this research, are the most recent using RSM on glucose concentration, agitation rate, pH and temperature in the improvement of biomass, EPS and ENS by cultivating mycelium in SLF.

4.5 Characterisation of exo-endopolysaccharides from the mycelium of wild-Serbian *G. applanatum* strain BGS6Ap using Fourier-transform infrared spectroscopy (FTIR) and nuclear magnetic resonance spectroscopy (NMR)

4.5.1 Fourier-transform infrared spectroscopy (FTIR)

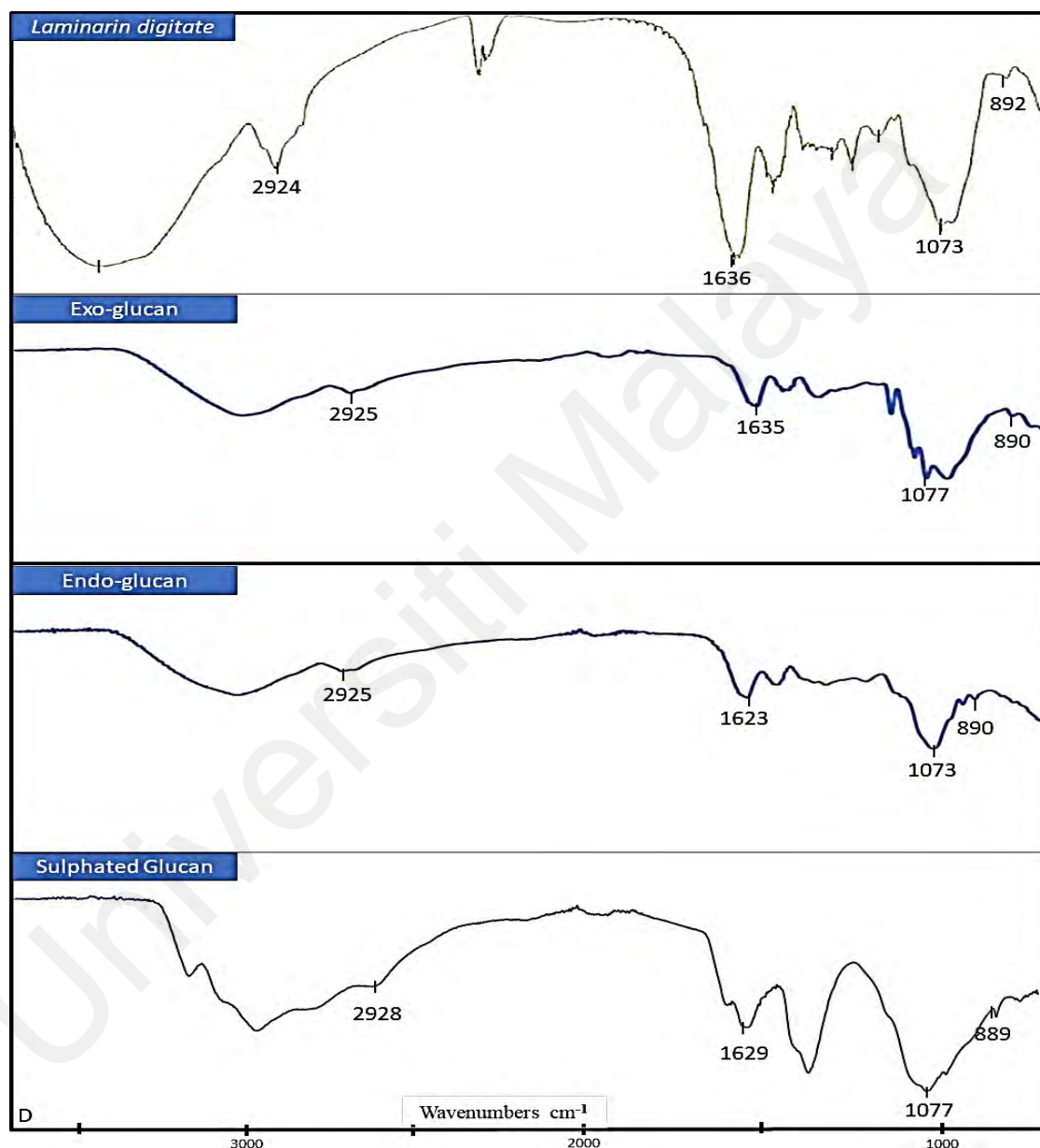


Figure 4.20: Comparison of β -glucan IR spectra. A: *Laminarin digitate*; B: exo-glucan; C: endo-glucan; D: sulfated-glucan derived from batch fermentation of wild-Serbian *G. applanatum* strain BGS6Ap.

FTIR spectroscopy in Fig 4.20 provides the data to identify the organic group of β -glucan from GASB in order to assess structure, linkage, and characteristics of polysaccharides. The EPS, ENS and GS shows absorptions of polysaccharides at a broad-stretched peak from 3000 cm^{-1} to 4500 cm^{-1} that indicate the O-H group in the sugar residue caused by vibrations. The weak peak was observed at 2924 cm^{-1} , 2925 cm^{-1} , 2925 cm^{-1} , and 2928 cm^{-1} and was linked along with the stretching vibrations of C-H in the sugar ring. C=O vibration was illustrated between 1625 cm^{-1} – 1640 cm^{-1} . The absorbance at 1073 cm^{-1} - 1077 cm^{-1} shows the presence of C-O-C and -OH which indicates the presence of β -glucan in formation of pyran structure with the presence of 5 carbon atoms and two sets of the double bond with one oxygen molecule (Liu et al., 2014; Osinska-Jaroszuk et al., 2014) Absorbance at 892 cm^{-1} , 890 cm^{-1} , 890 cm^{-1} and 889 cm^{-1} illustrated the confirmation of α -linked glycosyl (Osinska-Jaroszuk et al., 2014; Wan-Mohtar et al., 2016b). Thus, these structural confirmations resemble the stretching vibration of bands which ensures the presence of glucan efficiently synthesized from GASB.

4.5.2 Nuclear magnetic resonance (NMR)

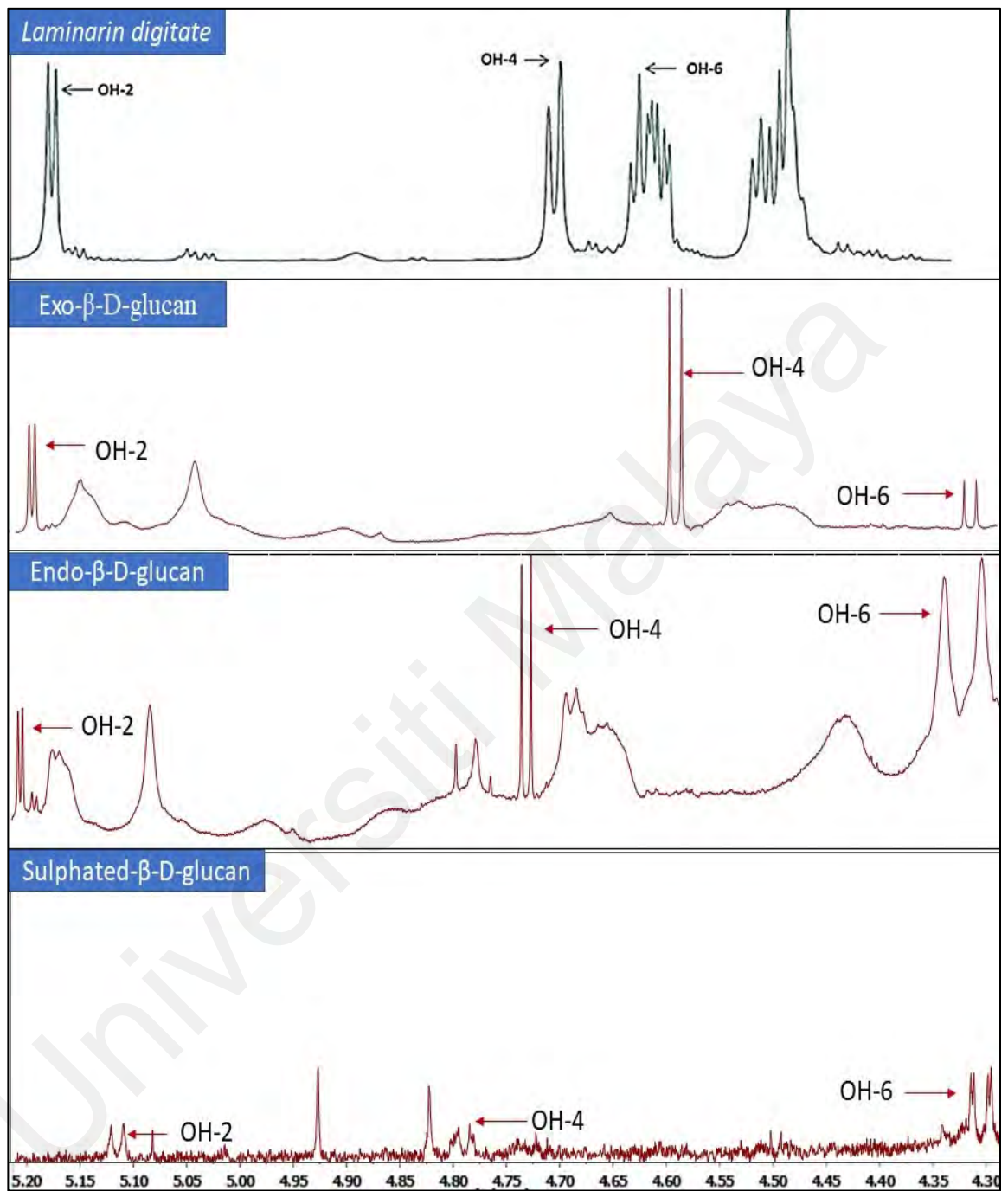


Fig 4.21: Comparison of β-glucan ¹H NMR spectra of β-D-glucan derived from batch cultures of wild-Serbian *G. applanatum* strain BGS6Ap and *Laminaria digitate* standard in D₂O-*d*₆.

H-NMR spectroscopy was used as a characterization and classification technique to confirm the presence of β -glucans to verify the structure of glucose monomers joined by β -1,3-glycosidic and β -1,6-glycosidic bonds in polysaccharides (Lundquist et al., 1992). H-NMR spectroscopic analysis of GASB mycelium was performed at 80° C in D₂O-*d*₆ solvent as observed in Fig 4.21 to compare and confirm the presence and structure of β -glucan in EPS, ENS and GS with laminarin (standard β -1,3-D-glucan). The spectrum of δ 4.3 - 5.2 ppm that indicates the presence of β -glucan and were assigned OH-2, OH-4, and OH-6 which was similar to laminarin which implies that the glycosidic bond in all the compounds is β -type (Wan-Mohtar et al. 2016a). The spectrum in Fig 4.21 (2,3,4) indicates the presence of glycosidic bonds when compared with the anomeric regions for all three compounds with laminarin similar to the reported study by Liu et al., (2014) and Supramani et al., (2019).

CHAPTER 5: CONCLUSION

In summary, this work focused on the molecular and morphological identification of the BGS6Ap wild-Serbian *Ganoderma applanatum* strain, in addition to optimizing the cultivation condition for elevated biomass, EPS and ENS production in SLF. GASB's morphology analysis (macroscopic and microscopic) conducted at different temperatures using batch fermentation and OFAAT was performed to fully understand mycelium growth based on its original location towards EPS and ENS production.

Response surface methodology (statistical software), based on the growth curve and morphological analysis whereby the relevant ranges were selected, was used to optimize media conditions to generate biomass, EPS and ENS. RSM offers a variable architecture that needs to be checked, and the responses for each variable were measured using ANOVA for each response to detect important impacts. (Value $p <$). With the aid of extensive research on morphology pellets, this optimized condition managed to drastically improve the production of ENS and biomass. Utilizing RSM to optimize GASB 's media composition resulted in overall biomass 19.93 g L⁻¹ (day 10), EPS output was 3.33 g L⁻¹ (day 15), and ENS 4.33 g L⁻¹ (day 15), under optimised conditions.

Finally, the compounds extracted from GASB mycelium batch fermentation were studied using FTIR and NMR showing the presence of β -glucan in the form of β -D-glycosidic bond compared to standard laminarin. In conclusion, GASB's optimization of the production of biomass, EPS, and ENS will support the exploration of other local *Ganoderma* sp. strains as a potential carrier of large-scale production of EPS.

In the search for bioactive compounds from *Ganoderma applanatum*, majority of the past research were done using extracts from fruiting body and less studies on extracts using liquid cultivated mycelium. Based on this study, several bioactive compounds were discovered in the mycelium of GASB as well as the benefits of using liquid fermentation over solid substrate cultivation. The ability to manipulate the cultivation medium to optimize GASB mycelium growth at a shorter period with lesser contamination. Hence, this research was necessary to study the physiology production of bioactive compounds such as polysaccharides optimization and upscaling in liquid substrate bioreactors which could eventually be produced as a supplement or herbal medicine for future diseases.

REFERENCES

- Acharya, K., Yonzone, P., Rai, M., & Rupa, A. (2005). Antioxidant and nitric oxide synthase activation properties of *Ganoderma applanatum*. *Indian Journal of Experimental Biology*, 43(10), 926-929.
- Adaskaveg, J. E., & Gilbertson, R. L. (1986). Cultural studies and genetics of sexuality of *Ganoderma lucidum* and *G. tsugae* in relation to the taxonomy of the *Ganoderma lucidum* complex. *Mycologia*, 78(5), 694-705.
- Adl, S. M., Simpson, A. G. B., Lane, C. E., Lukes, J., Bass, D., Bowser, S. S., . . . Spiegel, F. W. (2012). The Revised Classification of Eukaryotes. *Journal of Eukaryotic Microbiology*, 59(5), 429-493.
- Adotey, G., Quarcoo, A., Holliday, J., Fofie, S., & Saaka, B. (2011). Effect of immunomodulating and antiviral agent of medicinal mushrooms (immune assist 24/7 TM) on CD4+ T-lymphocyte counts of HIV-infected patients. *International Journal of Medicinal Mushrooms*, 13(2) 109-113.
- Ahmad, R., Al-Shorgani, N. K. N., Hamid, A. A., Yusoff, W. M. W., & Daud, F. (2013a). Optimization of medium components using response surface methodology (RSM) for mycelium biomass and exopolysaccharide production by *Lentinus squarrosulus*. *Advances in Bioscience and Biotechnology*, 4(12), 1079-1085.
- Ahmad, R., Alias, S. M. U., Hamid, A. A., Yusoff, W. M. W., & Daud, F. (2015). Production and Antiproliferative activity of Various Crude Extract from *Lentinus squarrosulus* mycelium. *Scholars Academic Journal of Biosciences*, 3(4), 377-385.
- Aminuddin, H., Khan, A. M., & Madzlan, K. (2013). Effects of pH on mycelial growth and amino acid composition of *Lentinula edodes* in submerged cultures. *Journal of Tropical Agriculture and Food Science*, 41(1), 63-70.
- Banerjee, S., & Sarkar, A. (1959). Spore-forms in sporophores of *Ganoderma lucidum* (Leyss.) Karst. Paper presented at the *Proceedings of the Indian Academy of Sciences-Section*, 49(2), 94-98.
- Bayne-Jones, S., & Rhee, H. S. (1929). Bacterial calorimetry II. Relationship of heat production to phases of growth of bacteria. *Journal of bacteriology*, 17(2), 123-140.

- Benkeblia, N. (2015). *Ganoderma lucidum* polysaccharides and Terpenoids: profile and health benefits. *International Journal of Food Science and Nutrition*, 1, 1-6.
- Bezerra, M. A., Santelli, R. E., Oliveira, E. P., Villar, L. S., & Escaleira, L. A. (2008). Response surface methodology (RSM) as a tool for optimization in analytical chemistry. *Talanta*, 76(5), 965-977.
- Buchanan, R. (1918). Life phases in a bacterial culture. *The Journal of Infectious Diseases*, 109-125.
- Chang, M.-Y., Tsai, G.-J., & Houg, J.-Y. (2006). Optimization of the medium composition for the submerged culture of *Ganoderma lucidum* by Taguchi array design and steepest ascent method. *Enzyme and Microbial Technology*, 38(3-4), 407-414.
- Cheng, P.-G., Phan, C.-W., Sabaratnam, V., Abdullah, N., Abdulla, M. A., & Kuppusamy, U. R. (2013). Polysaccharides-rich extract of *Ganoderma lucidum* (MA Curtis: Fr.) P. Karst accelerates wound healing in streptozotocin-induced diabetic rats. *Evidence-Based Complementary and Alternative Medicine*.
- Fazenda, M. L., Harvey, L. M., & McNeil, B. (2010). Effects of dissolved oxygen on fungal morphology and process rheology during fed-batch processing of *Ganoderma lucidum*. *Journal of Microbiology Biotechnology*, 20(4), 844-851.
- Gottlieb, A. M., & Wright, J. E. (1999). Taxonomy of *Ganoderma* from southern South America: subgenus *Ganoderma*. *Mycological Research*, 103(6), 661-673.
- Gougouli, M., & Koutsoumanis, K. P. (2013). Relation between germination and mycelium growth of individual fungal spores. *International Journal of Food Microbiology*, 161(3), 231-239.
- Hennicke, F., Cheikh-Ali, Z., Liebisch, T., Maciá-Vicente, J. G., Bode, H. B., & Piepenbring, M. (2016). Distinguishing commercially grown *Ganoderma lucidum* from *Ganoderma lingzhi* from Europe and East Asia on the basis of morphology, molecular phylogeny, and triterpenic acid profiles. *Phytochemistry*, 127, 29-37.
- Jeong, Y. T., Yang, B. K., Jeong, S. C., Kim, S. M., & Song, C. H. (2008). *Ganoderma applanatum*: a promising mushroom for antitumor and immunomodulating activity. *Phytotherapy Research: An International Journal Devoted to Pharmacological and Toxicological Evaluation of Natural Product Derivatives*, 22(5), 614-619.

- Jiang, W., Zhao, J., Wang, Z., & Yang, S.-T. (2014). Stable high-titer n-butanol production from sucrose and sugarcane juice by *Clostridium acetobutylicum* JB200 in repeated batch fermentations. *Bioresourcetechnology*, 163, 172-179.
- Jo, W.-S., Hossain, M. A., & Park, S.-C. (2014). Toxicological profiles of poisonous, edible, and medicinal mushrooms. *Mycobiology*, 42(3), 215-220.
- Kadić, A., Palmqvist, B., & Lidén, G. (2014). Effects of agitation on particle-size distribution and enzymatic hydrolysis of pretreated spruce and giant reed. *Biotechnology for Biofuels*, 7(1), 1-10.
- Kahm, M., Hasenbrink, G., Lichtenberg-Fraté, H., Ludwig, J., & Kschischo, M. (2010). Grofit: fitting biological growth curves. *Nature Precedings*, 1(4), 121-135.
- Khuri, A. I., & Mukhopadhyay, S. (2010). Response surface methodology. *Wiley Interdisciplinary Reviews: Computational Statistics*, 2(2), 128-149.
- Liao, B., Chen, X., Han, J., Dan, Y., Wang, L., Jiao, W., . . . Chen, S. (2015). Identification of commercial *Ganoderma (Lingzhi)* species by ITS2 sequences. *Chinese medicine*, 10(1), 22.
- Moradali, M.-F., Mostafavi, H., Hejaroude, G.-A., Tehrani, A. S., Abbasi, M., & Ghods, S. (2006). Investigation of potential antibacterial properties of methanol extracts from fungus *Ganoderma applanatum*. *Chemotherapy*, 52(5), 241-244.
- Nie, S., Zhang, H., Li, W., & Xie, M. (2013). Current development of polysaccharides from *Ganoderma*: isolation, structure and bioactivities. *Bioactive Carbohydrates and Dietary Fibre*, 1(1), 10-20.
- Niemelä, T., & Miettinen, O. (2008). The identity of *Ganoderma applanatum* (Basidiomycota). *Taxon*, 57(3), 963-966.
- Obratov-Petković, D., Popović, I., Belanović, S., & Kadović, R. (2006). Ecobiological study of medicinal plants in some regions of Serbia. *Plant Soil Environmental*, 52(10), 459-467.
- Ogbe, A., Ditse, U., Echeonwu, I., Ajodoh, K., Atawodi, S., & Abdu, P. (2009). Potential of a wild medicinal mushroom, *Ganoderma sp.*, as feed supplement in chicken diet: effect on performance and health of pullets. *International Journal of Poultry Science*, 8(11), 1052-1057.

- Pamment, N., Hall, R., & Barford, J. (1978). Mathematical modeling of lag phases in microbial growth. *Biotechnology and Bioengineering*, 20(3), 349-381.
- Papinutti, L. (2010). Effects of nutrients, pH and water potential on exopolysaccharides production by a fungal strain belonging to *Ganoderma lucidum* complex. *Bioresource Technology*, 101(6), 1941-1946.
- Parnmen, S., Sikaphan, S., Leudang, S., Boonpratuang, T., Rangsiruji, A., & Naksuwankul, K. (2016). Molecular identification of poisonous mushrooms using nuclear ITS region and peptide toxins: a retrospective study on fatal cases in Thailand. *The Journal of Toxicological Sciences*, 41(1), 65-76.
- Pegler, D. (1996). Hyphal analysis of Basidiomata. *Mycological Research*, 100(2), 129-142.
- Pegler, D. N., & Young, T. (1973). Basidiospore form in the British species of *Ganoderma* Karst. *Kew Bulletin*, 28(3), 351-364.
- Phillips, R. (1981). Mushrooms and Other Fungi of Great Britain & Europe: The Most Comprehensively Illustrated Book on the Subject this Century. *Italy: Pan Books*.
- Prichard, L., & Barwick, V. (2003). Preparation of calibration curves: A guide to best practice. *Report No. TR LGC/VAM/2003/032, LGC Group, Ltd., Teddington, Middlesex, UK*.
- Rašeta, M., Karaman, M., Jakšić, M., Šibul, F., Kebert, M., Novaković, A., & Popović, M. (2016). Mineral composition, antioxidant and cytotoxic biopotentials of wild-growing *Ganoderma* sp. (Serbia): *G. lucidum* (Curtis) P. Karst vs. *G. applanatum* (Pers.) Pat. *International Journal of Food Science & Technology*, 51(12), 2583-2590.
- Rašeta, M. J., Vrbaški, S. N., Bošković, E. V., Popović, M. R., Mimica-Dukić, N. M., & Karaman, M. A. (2017). Comparison of antioxidant capacities of two *Ganoderma lucidum* strains of different geographical origins. *Zbornik Matice srpske za prirodne nauke* 133(2), 209-219.
- Romero-Arenas, O., Huato, M., Treviño, I., Lezama, J., García, A., & Arellano, A. (2012). Effect of pH on growth of the mycelium of *Trichoderma viride* and *Pleurotus ostreatus* in solid cultivation mediums. *African Journal of Agricultural Research*, 7(34), 4724-4730.
- Rosemary Kinge, T., Apiseh Apalah, N., Mue Nji, T., Neh Acha, A., & Mathias Mih, A. (2017). Species richness and traditional knowledge of macrofungi (mushrooms)

in the Awing forest reserve and communities, northwest region, Cameroon. *Journal of Mycology*, 2017,2(1), 1-9.

- Smania Jr, A., Monache, F. D., Smania, E. d. F. A., & Cuneo, R. S. (1999). Antibacterial activity of steroidal compounds isolated from *Ganoderma applanatum* (Pers.) Pat.(Aphyllorphomycetideae) fruit body. *International Journal of Medicinal Mushrooms*, 1(4), 332-338.
- Stojković, D. S., Barros, L., Calhella, R. C., Glamočlija, J., Ćirić, A., Van Griensven, L. J., . . . Ferreira, I. C. (2014). A detailed comparative study between chemical and bioactive properties of *Ganoderma lucidum* from different origins. *International Journal of Food Sciences and Nutrition*, 65(1), 42-47.
- Stone, R., & Veevers, A. (1994). The Taguchi influence on designed experiments. *Journal of Chemometrics*, 8(2), 103-110.
- Subramaniam, R., & Vimala, R. (2012). Solid state and submerged fermentation for the production of bioactive substances: a comparative study. *International Journal of Science Nature*, 3(3), 480-486.
- Sun, X., Zhao, C., Pan, W., Wang, J., & Wang, W. (2015). Carboxylate groups play a major role in antitumor activity of *Ganoderma applanatum* polysaccharide. *Carbohydrate Polymers*, 123, 283-287.
- Supramani, S., Jailani, N., Ramarao, K., Zain, N. A. M., Klaus, A., Ahmad, R., & Wan, W. A. A. Q. I. (2019). Pellet diameter and morphology of European *Ganoderma pfeifferi* in a repeated-batch fermentation for exopolysaccharide production. *Biocatalysis and Agricultural Biotechnology*, 19(2), #101118.
- Synytsya, A., Míčková, K., Synytsya, A., Jablonský, I., Spěvák, J., Erban, V., . . . Čopíková, J. (2009). Glucans from fruit bodies of cultivated mushrooms *Pleurotus ostreatus* and *Pleurotus eryngii*: Structure and potential prebiotic activity. *Carbohydrate Polymers*, 76(4), 548-556.
- Ubaidillah, N., Hafizah, N., Abdullah, N., & Sabaratnam, V. (2015). Isolation of the intracellular and extracellular polysaccharides of *Ganoderma neojaponicum* (Imazeki) and characterization of their immunomodulatory properties. *Electronic Journal of Biotechnology*, 18(3), 188-195.
- Usuldin, S. R. A., Mahmud, N., Ilham, Z., Ikram, N. K. K., Ahmad, R., & Wan, W. A. A. Q. I. (2020). In-depth spectral characterization of antioxidative (1, 3)- β -D-glucan from the mycelium of an identified tiger milk mushroom *Lignosus*

rhinocerus strain ABI in a stirred-tank bioreactor. *Biocatalysis and Agricultural Biotechnology*, 23, #101455.

- Utomo, C., Werner, S., Niepold, F., & Deising, H. (2005). Identification of *Ganoderma*, the causal agent of basal stem rot disease in oil palm using a molecular method. *Mycopathologia*, 159(1), 159-170.
- Valverde, M. E., Hernández-Pérez, T., & Paredes-López, O. (2015). Edible mushrooms: improving human health and promoting quality life. *International Journal of Microbiology*, 2015.
- Wagner, R., Mitchell, D. A., Lanzi Sasaki, G., Lopes de Almeida Amazonas, M. A., & Berovič, M. (2003). Current techniques for the cultivation of *Ganoderma lucidum* for the production of biomass, ganoderic acid and polysaccharides. *Food Technology and Biotechnology*, 41(4), 371-382.
- Wagner, R., Mitchell, D. A., Sasaki, G. L., & de Almeida Amazonas, M. A. L. (2004). Links between morphology and physiology of *Ganoderma lucidum* in submerged culture for the production of exopolysaccharide. *Journal of Biotechnology*, 114(1-2), 153-164.
- Wan-Mohtar, W. A. A. Q., Young, L., Abbott, G. M., Clements, C., Harvey, L. M., & McNeil, B. (2016b). Antimicrobial Properties and Cytotoxicity of Sulfated (1, 3)- β -D-Glucan from the Mycelium of the Mushroom *Ganoderma lucidum*. *Journal of Microbiology and Biotechnology*, 26(6), 999-1010.
- Wan, W. A. A. Q. I., Ab Kadir, S., & Saari, N. (2016a). The morphology of *Ganoderma lucidum* mycelium in a repeated-batch fermentation for exopolysaccharide production. *Biotechnology Reports*, 11, 2-11.
- Wan, W. A. A. Q. I., Latif, N. A., Harvey, L. M., & McNeil, B. (2016). Production of exopolysaccharide by *Ganoderma lucidum* in a repeated-batch fermentation. *Biocatalysis and Agricultural Biotechnology*, 6, 91-101.
- Wan, W. A. A. Q. I., Malek, R. A., Harvey, L. M., & McNeil, B. (2016a). Exopolysaccharide production by *Ganoderma lucidum* immobilised on polyurethane foam in a repeated-batch fermentation. *Biocatalysis and Agricultural Biotechnology*, 8, 24-31.
- Wan, W. A. A. Q. I., Viegelmann, C., Klaus, A., & Lim, S. A. H. (2017). Antifungal-demelanizing properties and RAW264. 7 macrophages stimulation of glucan

sulfate from the mycelium of the mushroom *Ganoderma lucidum*. *Food Science and Biotechnology*, 26(1), 159-165.

- Wang, X. C., Shao, J. J., & Liu, C. (2016). The complete mitochondrial genome of the medicinal fungus *Ganoderma applanatum* (Polyporales, Basidiomycota). *Mitochondrial DNA Part A*, 27(4), 2813-2814.
- Xu, J.-W., Ji, S.-L., Li, H.-J., Zhou, J.-S., Duan, Y.-Q., Dang, L.-Z., & Mo, M.-H. (2015). Increased polysaccharide production and biosynthetic gene expressions in a submerged culture of *Ganoderma lucidum* by the overexpression of the homologous α -phosphoglucosyltransferase gene. *Bioprocess and Biosystems Engineering*, 38(2), 399-405.
- Xu, P., Ding, Z.-Y., Qian, Z., Zhao, C.-X., & Zhang, K.-C. (2008). Improved production of mycelial biomass and ganoderic acid by submerged culture of *Ganoderma lucidum* SB97 using complex media. *Enzyme and Microbial Technology*, 42(4), 325-331.
- Yang, F.-C., Hsieh, C., & Chen, H.-M. (2003). Use of stillage grain from a rice-spirit distillery in the solid state fermentation of *Ganoderma lucidum*. *Process Biochemistry*, 39(1), 21-26.
- Yang, F.-C., & Liao, C.-B. (1998). The influence of environmental conditions on polysaccharide formation by *Ganoderma lucidum* in submerged cultures. *Process Biochemistry*, 33(5), 547-553.
- Yuan, B., Chi, X., & Zhang, R. (2012). Optimization of exopolysaccharides production from a novel strain of *Ganoderma lucidum* CAU5501 in submerged culture. *Brazilian Journal of Microbiology*, 43(2), 490-497.
- Zhang, H., Li, W.-J., Nie, S.-P., Chen, Y., Wang, Y.-X., & Xie, M.-Y. (2012). Structural characterisation of a novel bioactive polysaccharide from *Ganoderma atrum*. *Carbohydrate Polymers*, 88(3), 1047-1054.
- Zhang, Y., Geng, W., Shen, Y., Wang, Y., & Dai, Y.-C. (2014). Edible mushroom cultivation for food security and rural development in China: bio-innovation, technological dissemination and marketing. *Sustainability*, 6(5), 2961-2973.
- Zhang, Z. C., Shen, W. L., Liu, D., & Li, J. S. (2011). Enhanced production of mycelial biomass and ganoderic acid in submerged culture of *Ganoderma applanatum* ACCC-52297 elicited by feeding rutin. *African Journal of Microbiology Research*, 5(21), 3452-3461.

Zhou, S., Guan, S., Duan, Z., Han, X., Zhang, X., Fan, W., . . . Liu, H. (2018). Molecular cloning, codon-optimised gene expression, and bioactivity assessment of two novel fungal immunomodulatory proteins from *Ganoderma applanatum* in *Pichia*. *Applied Microbiology and Biotechnology*, 102(13), 5483-5494.

Zwietering, M., Jongenburger, I., Rombouts, F., & Van't Riet, K. (1990). Modeling of the bacterial growth curve. *Applied Environmental of Microbiology*, 56(6), 1875-1881.

Universiti Malaya